# Deciphering Regulatory Mechanisms of the Met Receptor Tyrosine Kinase

by

Bruce Hao Huang

A thesis submitted to McGill University in partial fulfillment of the requirements of the degree of Doctor of Philosophy



Department of Biochemistry
McGill University
Montreal (QC) Canada

June 2023
First Date Published
Aug. 15th, 2024

# ABSTRACT

The Met Receptor Tyrosine Kinase (RTK) is frequently selected for mutations that result in loss of exon 14, within the intracellular juxtamembrane (JM) domain, in cancers of lung and brain origin. In this work, I have explored the mechanisms through which loss of exon 14 in the Met RTK (MetΔex14) enhances phosphorylation of a key tyrosine residue (Y1349) in the carboxyl-tail (C-tail) required for downstream signalling to lower concentrations of ligand, Hepatocyte Growth Factor (HGF). I discovered in the WT Met RTK, that the formation of an anti-parallel dimer occurs within an α-helical structure in the carboxyl terminal portion of the juxtamembrane domain (JM-C) and through structure function analyses determined that is essential for ligand induced tyrosine phosphorylation of Met Y1349. Existing crystallography structures indicate that Y1349 is initially cis-docked onto the C-lobe of the Met kinase domain. In this arrangement this Met activation dimer is not conducive to phosphorylating Y1349. Modelling predicted that a ligand induced tetramer of the Met RTK may occur and this could facilitate access of Y1349 to phosphorylation. I established that MetΔex14 was able to form a tetramer under low dosage of HGF, supporting the enhanced Met signaling observed downstream from MetΔex14 in an HGF-dependent manner. Small Angle X-ray Scattering (SAXS) revealed that an isolated exon 14 peptide is predominantly unstructured. Although a structure prediction algorithm, AlphaFold, predicted that exon 14 may be capable of forming a tetrameric β-sandwich structure exhibiting dihedral symmetry. Using Phos-tag and Immunoprecipitation- Mass Spectrometry (IP-MS) techniques, I found that exon 14 in Met displays basal levels of phosphorylation. Specifically, these were identified as Threonine 977. Collectively my data suggest that exon 14 may act as a regulatory element and/or

rate-determining 'rheostat' in HGF-induced multimeric Met kinase assembly and activation.

To identify regulators of Met RTK surface protein levels I utilized a Kinome/FDA-approved drug targeted CRISPR screen. My observations point to negative Met regulators being linked with the cell cycle. This is particularly evident when Protein Phosphatase 2A (PP2A) and Checkpoint kinase 1 (Chk1) were disrupted, leading to a decrease in Met protein levels on the cell surface. An inverse relationship between Met and Cyclin B1 protein levels was also observed in different cancer cohorts.

Overall, my research enhances our understanding of the role of exon 14 skipping in Met signaling and highlights the potential for Met-targeted strategies in cancer treatment.

# RÉSUMÉ

Le récepteur tyrosine kinase (RTK) du récepteur Met est fréquemment choisi pour des mutations qui entraînent la perte de l'exon 14, au sein du domaine intracellulaire juxtamembranaire (JM), dans les cancers d'origine pulmonaire et cérébrale. Dans ce travail, j'ai exploré les mécanismes par lesquels la perte de l'exon 14 dans le récepteur Met RTK (MetΔex14) renforce la phosphorylation d'un résidu clé de tyrosine (Y1349) dans la queue carboxyle (C-tail) nécessaire à la signalisation aval vers des concentrations plus faibles du ligand, le facteur de croissance hépatocytaire (HGF). J'ai découvert dans le récepteur Met RTK de type sauvage que la formation d'un dimère antiparallèle se produit dans une structure α-hélicoïdale dans la partie terminale carboxyle du domaine juxtamembranaire (JM-C) et grâce à des analyses de structure fonctionnelle, j'ai déterminé que c'est essentiel pour la phosphorylation de la tyrosine induite par le ligand de Met Y1349. Les structures de cristallographie existantes indiquent que Y1349 est initialement en position cis-dockée sur le lobe C du domaine kinase de Met. Dans cet agencement, ce dimère d'activation de Met n'est pas propice à la phosphorylation de Y1349. La modélisation a prédit qu'un tétramère induit par le ligand du récepteur Met RTK pourrait se former et cela pourrait faciliter l'accès de Y1349 à la phosphorylation. J'ai établi que MetΔex14 était capable de former un tétramère sous faible dosage de HGF, ce qui soutient la signalisation accrue de Met observée en aval de MetΔex14 de manière dépendante de HGF. La diffusion des rayons X à petit angle (SAXS) a révélé qu'un peptide d'exon 14 isolé est principalement non structuré. Bien qu'un algorithme de prédiction de structure, AlphaFold, ait prédit qu'un tétramère de type β-sandwich pouvait se former avec une symétrie diédrale. En utilisant des techniques Phos-

tag et Immunoprécipitation-Spectrométrie de masse (IP-MS), j'ai constaté que l'exon 14 de Met présente des niveaux basaux de phosphorylation. Plus précisément, il s'agissait de la thréonine 977. Collectivement, mes données suggèrent que l'exon 14 pourrait agir comme un élément régulateur et/ou un 'rhéostat' déterminant le taux dans l'assemblage et l'activation multimerique du kinase Met induits par HGF. Pour identifier les régulateurs des niveaux de protéines de surface du récepteur Met RTK, j'ai utilisé un criblage CRISPR ciblant la kinome/les médicaments approuvés par la FDA. Mes observations indiquent que les régulateurs négatifs de Met sont liés au cycle cellulaire. Cela est particulièrement évident lorsque la protéine phosphatase 2A (PP2A) et la kinase de point de contrôle 1 (Chk1) sont perturbées, ce qui entraîne une diminution des niveaux de protéines de Met à la surface cellulaire. Une relation inverse entre les niveaux de protéines de Met et de la cycline B1 a également été observée dans différentes cohortes de cancers.

Dans l'ensemble, mes recherches améliorent notre compréhension du rôle du saut d'exon 14 dans la signalisation de Met et mettent en évidence le potentiel des stratégies ciblant Met dans le traitement du cancer.

# ACKNOWLEDGEMENTS

This research has been made possible due to the generous support from Défi Canderel, Dr. Victor S. Lui, alongside awards granted by the Goodman Cancer Research Institute and the Department of Biochemistry, to whom I extend my profound gratitude.

I would like to thank my thesis supervisor, Dr. Morag Park, I am immensely grateful for the time and effort you have invested in mentoring. Throughout this research endeavor, you have demonstrated an unwavering commitment to excellence, fostering an environment of intellectual growth and academic rigor.

My acknowledgement extends to my esteemed Research Advisory Committee, comprising Dr. Sidong Huang, Dr. William Muller, Dr. Bhushan Nagar, and Dr. Connie Krawczyk. I am indeed fortunate to have had the opportunity to learn and grow under their remarkable guidance and mentorship.

I also wish to express my gratitude towards all former members of the Park lab, Dr. Jennifer Knight and Dr. Danielle De Verteuil who welcomed me into the lab, as well as Dr. Paul Savage, Dr. Crista Thomson, Dr. Vanessa Sung, Dr. Colin Ratcliffe, Dr. Tina Grusso, Amrita Shergill, Dr. Yaakov Stern, Dr. Gabe Brewer, Dr. Paula Coelho, Dr. Coni Martinez, Dr. Geneviève Deblois, Danlin Zeng, Michael Shwartz, Camby Chor, Valentina Munoz Ramoz, and Monica Naujokas. Each of you has uniquely enriched my experience in the lab and helped shape my academic journey through stimulating scientific discussions, shared moments of joy, steadfast support, and invaluable friendships.

Special thanks are due to Anie Monast, who has shared her expertise in handling mice, thereby instilling in me a confidence in animal work. Virginie Pilon deserves a heartfelt

thanks not only for her exemplary partnership in mouse experiments but also for the friendship and camaraderie she has offered throughout our time in the lab.

My appreciation extends to Dr. Dongmei Zuo for sharing her expertise in imaging experiments, and Dr. Hong Zhao for her insightful guidance in conducting qPCRs.

I am also sincerely grateful to Dr. Jean-Francois Trempe, Dr. Zhong Yao, Dr. Igor Stagliar, and Dr. Peng Wang for their invaluable contributions to this thesis and the meaningful impact they have made on my scientific journey.

I would like to extend my gratitude to Isabella Pecora for your invaluable assistance during the experiments conducted for this thesis. Your dedication and willingness to lend a helping hand have been instrumental in the successful completion of this research.

My appreciation extends to Dr. Abdulhameed Ghabkari for the thought-provoking discussions about philosophy and religious ideas, Dr. Hellen Kuasne for consistently spreading positivity, and Marina Fukano for being a beacon of inspiration in the lab.

I am grateful to Dr. Anne-Marie Fortier for her constant support and hard work, Dr. Stephanie Duhamel for infusing light-hearted moments into our lab work, Promita Gosh for her amicability, Annika Pedersen for consistently uplifting the lab atmosphere, and Sandrine Busque for sharing her knowledge at her young age.

I would like to express my heartfelt gratitude to my wife, Kathleen Belisle, for her unwavering love and unwavering support.

Lastly, I want to dedicate a special thank you to my beloved little angel, Krystal Huang. You are my pillars of strength. It is because of you that I find the strength to persevere and continue fighting.

# PREFACE

This thesis is written in the traditional format, which is divided into six chapters:

**Chapter 1: Literature Review**

**Chapter 2: Structural Basis of Met Exon 14 Skipping in Cancers**

**Chapter 3: A Pooled Kinome/Druggable CRISPR Screen Identifies Cell Cycle Control of the Met RTK**

**Chapter 4: General Discussion**

**Chapter 5: Materials and Methods**

**Chapter 6: Bibliography**

# CONTRIBUTION TO ORIGINAL KNOWLEDGE

In the second chapter of my work, I elucidated the molecular mechanisms of Met exon 14 skipping in JM-N, also provided insights into the structural basis of Met activation through an antiparallel α-helical JM-C dimer.

In the third chapter of my work, I undertook a CRISPR screen to explore regulators of Met protein levels, a pursuit that has led to significant discoveries. Additionally, I successfully optimized the Phos-tag technique to examine Met phosphorylation, overcoming the previous hurdles encountered when analyzing high molecular weight proteins. For the first time, I discovered that Met is internalized in the M phase, a process that remained uncharacterized until now. Furthermore, I discerned that the exon 14 region undergoes phosphorylation when the cells are arrested at M phase.

Together, my research has contributed to a more comprehensive understanding of Met regulation in cancers.

# PUBLICATIONS ARISING FROM THIS THESIS

Chapters 2 and 3 contain material presented in the following article:

Huang, B. H., Croteau, N., Cyr, N., Golenar, T., Pecora, I., Coelho, P., Trempe, J.-F., & Park, M. Structural Basis of Met Exon 14 Skipping in Cancers. (In preparation)

Huang, B. H., Morin, G., Yao, Z., Wang, P., Pecora, I., Zuo, D., Coelho, P., Sonenberg, N., Stagljar, I., Huang, S., & Park, M. A Pooled Kinome/Druggable CRISPR Screen Identifies Cell Cycle Control of the Met RTK. (In preparation)

# CONTRIBUTION OF AUTHORS

Morin, G. aided in the processing of CRISPR screen next-generation sequencing data. Pecora, I. western blot crosslinking. Coelho, P. and Zuo, D. provided assistance with confocal microscopy and immunofluorescent data analysis. Yao, Z. conducted MaMTH assay, Wang, P. conducted the co-immunoprecipitation experiments with PP2A. Trempe, J.-F. assisted with SAXS and IP-MS. Golenar, T., conducted 3D migration experiments. Park, M. supervised the research and co-wrote the manuscript. Huang, B. H. designed and performed the research and co-wrote the manuscript.

# ADDITIONAL PUBLICATIONS

Rajadurai CV, Havrylov S, Coelho PP, Ratcliffe CD, Zaoui K, Huang BH, Monast A, Chughtai N, Sangwan V, Gertler FB, Siegel PM. 5′-Inositol phosphatase SHIP2 recruits

Mena to stabilize invadopodia for cancer cell invasion. Journal of Cell Biology. 2016 Sep 12;214(6):719-34.

Al-Ghabkari, A., Huang, B., & Park, M. The Role of Aberrant Met Receptor Tyrosine (MET) Kinase Signaling in Glioblastoma: Targeted Therapy and Future Directions. (Review article, submitted to *Cells*)

Wang, P., Li, Z., Kim, S.-H., Huang, H., Choi, J.-H., Xu, H., Yang, C., Snape, A., Bermudez, S., Boivin, M.-N., Ferry, N., Sood, R., Sharma, V., Ryan, J., Park, M., Karamchadani, J., Nagar, B., & Sonenberg, N. PPM1G dephosphorylates eIF4E to reduce selective mRNA translation. (Submitted to *Nature Communications*)

## Table of Contents

# LIST OF FIGURES

# LIST OF TABLES



# LIST OF ABBREVIATIONS

**AAs: Amino Acids**

**ALK: Anaplastic Lymphoma Kinase**

**ALK2: Activin Receptor-Like Kinase 2**

**ANOVA: Analysis of Variance**

**AP-2: Adaptor Protein 2**

**APC: Allophycocyanin**

**ATP: Adenosine Triphosphate**

**BMPR2: Bone Morphogenetic Protein Receptor, Type II**

**C: carboxyl terminus**

**Cbl: Casitas B-Lineage Lymphoma**

**Cas9: CRISPR-associated protein 9**

**CCVs: Clathrin-coated vesicles (CCVs)**

**CDK: Cyclin-Dependent Kinase**

**CDK1: Cyclin-Dependent Kinase 1**

**CDK2: Cyclin-Dependent Kinase 2**

**Cbl: Casitas B-Lineage Lymphoma**

**CRISPR: Clustered Regularly Interspaced Short Palindromic Repeats**

**Cryo-EM: Cryogenic Electron Microscopy**

**CUPs: Cancers of Unknown Primary origin**

**DFG: Asp-Phe-Gly (residues in the activation loop of kinases)**

**DSP: Dithiobis (succinimidyl propionate), a crosslinker used in protein studies**

**EGF: Epidermal Growth Factor**

**EGFR: Epidermal Growth Factor Receptor**

**EMT: Epithelial-to-Mesenchymal Transition**

**ERBB: Erythroblastic Leukemia Viral Oncogene Homolog**

**ERK: Extracellular Signal-Regulated Kinase**

**ESCRT: Endosomal Sorting Complexes Required for Transport**

**FACS: Fluorescence Activated Cell Sorting**

**FDA: Food and Drug Administration**

**FGFR: Fibroblast Growth Factor Receptor**

**FLT1: Fms-related tyrosine kinase 1 (also known as VEGFR1)**

**FRET: Förster Resonance Energy Transfer**

**Gab1: Grb2-Associated Binder 1**

**GDNF: Glial cell line-Derived Neurotrophic Factor**

**GPCRs: G-protein Coupled Receptors**

**GGA3: Golgi-Associated, Gamma Adaptin Ear-Containing, ARF-Binding Protein 3**

**HCC: Hepatocellular Carcinoma**

**HER2: Human Epidermal growth factor Receptor 2**

**HER3: Human Epidermal growth factor Receptor 3**

**HGF: Hepatocyte Growth Factor**

**IgG: Immunoglobulin G**

**IP-MS: Immunoprecipitation-Mass Spectrometry**

**JM: Juxtamembrane**

**kDa: Kilodalton, a unit of molecular mass**

**KIT: KIT Receptor Tyrosine Kinase (also known as CD117 or Mast/Stem Cell Growth Factor Receptor)**

**lDDT-Cα: Local Distance Difference Test for C-alpha atoms**

**MAGeCK: Model-based Analysis of Genome-wide CRISPR-Cas9 Knockout**

**MaMTH: Mammalian Membrane Two-Hybrid**

**MAPK: Mitogen-Activated Protein Kinase**

**Met: Hepatocyte growth factor receptor**

**MMPs: Matrix Metalloproteinases**

**MOI: Multiplicity of Infection, the average number of virus particles infecting a cell**

**M phase: mitotic phase**

**MuSK: Muscle-Specific Kinase**

**N: Amino terminus**

**NGF: Nerve Growth Factor**

**NGS: Next Generation Sequencing, a high-throughput method to sequence DNA**

**NMR: Nuclear Magnetic Resonance**

**NSCLC: Non-Small Cell Lung Cancer**

**PC12: Rat Pheochromocytoma Cells**

**PDGF: Platelet-Derived Growth Factor**

**PDGFR: Platelet-Derived Growth Factor Receptor**

**PDX: Patient-Derived Xenograft**

**PE: Phycoerythrin**

**PCR: Polymerase Chain Reaction**

**PFA: Paraformaldehyde**

**PIP2: Phosphatidylinositol 4,5-bisphosphate**

**PPP2R2A: Protein Phosphatase 2 Regulatory Subunit B Alpha**

**pLDDT: Per-residue Local Distance Difference Test**

**PP2A: Protein Phosphatase 2A**

**RAS/MAPK: Rat Sarcoma/Mitogen-Activated Protein Kinases**

**RET: Rearranged During Transfection Receptor**

**ROS1: c-Ros oncogene 1 receptor tyrosine kinase**

**RPPA: Reverse Phase Protein Array**

**RTK: Receptor Tyrosine Kinase**

**SAXS: Small Angle X-ray Scattering**

**SDS-PAGE: Sodium Dodecyl Sulfate-Polyacrylamide Gel Electrophoresis**

**SEM: Standard Error of the Mean**

**sgRNA: Single-guide RNA**

**SIMPL: Split Intein-Mediated Protein Ligation**

**SOS: Son of Sevenless**

**STAT3: Signal Transducer And Activator Of Transcription 3**

**TCPA: The Cancer Protein Atlas**

**TCGA: The Cancer Genome Atlas**

**Tris: Tris(hydroxymethyl)aminomethane**

**Trk: Tropomyosin receptor kinase**

**TrkA: Tropomyosin receptor kinase A**

**TGFβ: Transforming Growth Factor Beta**

**Two-Dimensional: 2D**

**Three-Dimensional: 3D**

**WT: Wild Type**

# CHAPTER 1 – LITERATURE REVIEW

## 1.1 General mechanisms of RTK activation

Ligand binding to the extracellular ectodomains of RTK triggers conformational reorganization inducing receptor dimerization and activation of the protein kinase activity in the intracellular domains. Subsequently, the activated kinase domain of each monomer undergoes trans-autophosphorylation of tyrosine residues in the opposing monomer C-terminal domain, JM region, and/or activation loop, further facilitating engagement of signalling complexes and enhancing downstream signaling activation (Figure 1.1).

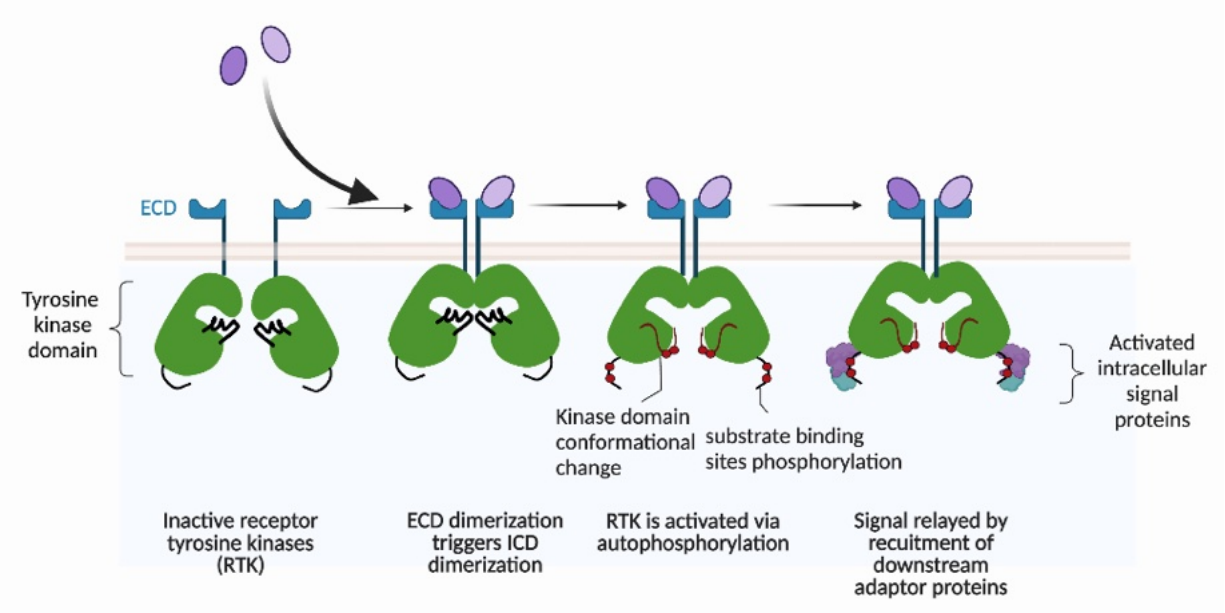


***Figure 1.1 RTK activation by ligand induced dimerization***

Activation of most receptor tyrosine kinases is dependent on ligand binding, which induces conformational changes in the extracellular domain, leading to the formation of a dimer interface in the catalytic domain. Subsequently, this dimerization event triggers the phosphorylation of the kinase activation loop. The phosphorylation enables the binding of ATP and the tyrosine substrate to the catalytic groove, resulting in the transfer of the gamma phosphate from ATP to the tyrosine residue.

In contrast to the majority of RTKs that exist as inactive monomers, the insulin receptor (INSR) and insulin-like growth factor 1 receptor (IGF1R) exhibit a unique characteristic of

constitutive disulfide-linked dimerization (Wybenga-Groot et al., 2001). Investigations have shed light on the existence of inactive pre-dimers and higher oligomeric states in certain RTKs, including EGFR (Nagy et al., 2010; Saffarian et al., 2007), where larger clusters form within the cellular membrane.

## 1.2 RTK extracellular dimerization mechanisms

RTKs can be classified into various subfamilies based on the organization and sequence similarity of their extracellular domains (ECDs). These include the epidermal growth factor receptor (EGFR) family, the fibroblast growth factor receptor (FGFR) family, the vascular endothelial growth factor receptor (VEGFR) family, the platelet-derived growth factor receptor (PDGFR) family, the insulin receptor (IR) family, the tropomyosin receptor kinase (Trk) family, and many others (Lemmon & Schlessinger, 2010). Each RTK subfamily is characterized by distinct ECD architectures and functional domains, which determine their specific ligand-binding properties and activation mechanisms. The diversity of ECD architectures is essential for the ability of RTKs to recognize and respond to a wide range of extracellular signals and regulate diverse cellular processes.

Ligand binding to the ECDs of RTKs is a critical step for receptor activation, as it induces receptor dimerization, which is necessary for the activation of the intracellular kinase domains and the initiation of downstream signaling events. The mechanisms of ligand-induced dimerization and activation of RTKs are highly diverse, ranging from ligand-mediated dimerization to receptor-mediated dimerization, with various intermediate mechanisms in between.

### 1.2.1 Receptor-mediated dimerization

Receptor-mediated dimerization occurs without the ligand making any direct contribution to the dimer interface. Instead, the receptor ECDs make direct contacts with each other, leading to dimerization and activation. This mechanism is observed only in the EGFR family and insulin receptors, where the ligand-induced conformational changes in the ECDs expose a dimerization arm that engages with a complementary interface on the adjacent receptor molecule. The cryo-electron microscopy (cryo-EM) structures of EGFR (Huang et al., 2021), HER2, and HER3 ECDs in their homo/hetro-dimeric forms (Bai et al., 2023; Diwanji et al., 2021) have provided detailed insights into the molecular basis of receptor-mediated dimerization and activation.

### 1.2.2 Ligand-mediated Dimerization

In contrast to receptor-mediated dimerization, ligand-mediated dimerization involves the binding of a bivalent ligand to two receptor molecules, leading to the formation of a dimeric complex and cross-activation. This mechanism is observed in various subfamilies of RTKs such as Axl (Sasaki et al., 2006), Eph (Lisabeth et al., 2013), Flt1 (Wiesmann et al., 1997), KIT (Liu et al., 2007), TrkA (Franco et al., 2020) as well as Met (Emiko Uchikawa et al., 2021).

### 1.2.3 Mixed dimerization mechanisms

Some RTKs exhibit a mixed dimerization mechanism, where both the ligand and the receptor contribute to the dimer interface. For example, the FGFR family employs a combination of ligand- and receptor-mediated interactions for dimerization. The crystal structures of the FGFR ECDs bound to their ligands have revealed a unique symmetric dimer arrangement, where the ligand contributes to the dimer interface through both its N- and C-terminal regions, while the receptor ECDs also make direct contacts with each other (Pellegrini et al., 2000; Stauber et al., 2000).

Indirect activation of receptor tyrosine kinases introduces a distinct paradigm in the mechanisms of RTK activation. The Ret (rearranged during transfection) receptor serves as an exemplar of this phenomenon, as it requires the presence of homodimeric ligands from the glial-derived neurotrophic factor (GDNF) family. However, activation of Ret occurs only subsequent to the binding of these ligands to a GDNF-family receptor-α (GFRα) chain. This ligand-receptor complex facilitates Ret dimerization and subsequent activation (Schlee et al., 2006).

## 1.3 Hepatocyte growth factor

HGF, alternatively known as scatter factor (SF), is a ligand that binds exclusively to Met (Bottaro et al., 1991; Giordano et al., 1989; Naldini, Vigna, et al., 1991). HGF is a unique kringle-containing ligand for Met, a transmembrane receptor. HGF is a heparin-binding protein that stimulates the proliferation, migration, and differentiation of various cellular targets, including hepatocytes, epithelial cells, melanocytes, endothelial, and

hematopoietic cells (Bottaro et al., 1991; Matsumoto & Nakamura, 1996; Weidner et al., 1990).

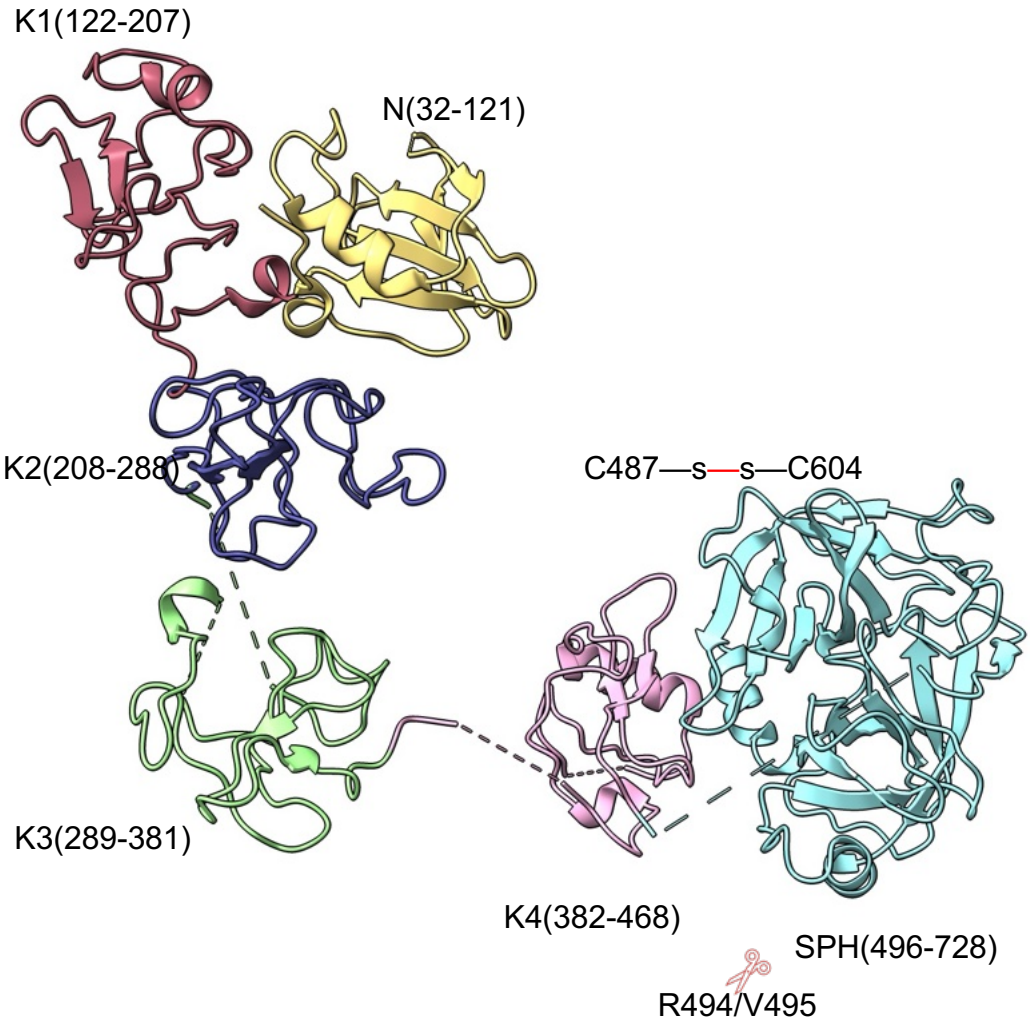


***Figure 1.2 Structure of HGF***

The structural organization of hepatocyte growth factor/scatter factor is composed of distinct domains. The cryo-EM structure HGF using PDB:7MO7. The N-terminal domain represents the amino-terminal region, while K1–K4 denote the kringle domains 1–4. Additionally, the serine proteinase homology domain is abbreviated as SPH. Following proteolytic cleavage at R494/V495, the ligand generates α and β subunits and connects through C487 and C604.

Initially, HGF/SF was identified as two separate molecules, each exhibiting unique biological properties. HGF was first uncovered as a hepatotropic factor instrumental in rat

hepatocyte regeneration (Matsumoto & Nakamura, 1996; Nakamura et al., 1989), while SF was characterized as a growth factor that facilitates the movement and positioning of cells released from fibroblast cells, acting solely on epithelial cells (Stoker et al., 1987; Weidner et al., 1990). Nonetheless, upon thorough analysis, these ligands were found to be indistinguishable based on various parameters, such as growth, motility, and binding affinities (Naldini, Weidner, et al., 1991).

The HGF gene is situated on chromosome 7q21.1 and spans 70 kilobases, containing 18 exons and 17 introns. According to nucleotide sequencing, the gene is expected to produce a 728-amino-acid protein (Nakamura, 1991; Nakamura et al., 1989)..

HGF is synthesized as a precursor, pro-HGF, which must be cleaved. The initial 54 amino acid of the pro-HGF molecule can be partitioned into a signaling sequence and a pro-sequence, with the first 29 amino acids being hydrophobic and characteristic of a signaling sequence. The remaining amino acids constitute the pro-sequence (Montesano et al., 1991; Tashiro et al., 1990). The pro-HGF molecule exhibits approximately 27 to 40% homology with plasminogen (Miyazawa et al., 1989). In-vitro, a trypsin-like protease, Factor XIIa of the blood coagulation system can activate HGF through a cleavage reaction, cleaving the chains at an Arg-Val site, which is vital for its biological activity (Naka et al., 1992; Peek et al., 2002).

The mature HGF molecule forms a heterodimeric molecule consisting of an α-chain (69 kDa) and a β-chain (34 kDa) covalently linked through a disulfide bond (Stamos et al., 2004). The α and β chains contain potential sites for N-linked glycosylation and form an interchain bridge at specific cysteine residues that is homologous with plasminogen. The HGF α chain contains four kringle structures, also present in plasminogen, albeit with five

kringle structures (Nakamura et al., 1989). These kringle structures may be involved in protein-protein interactions, though their precise biological role remains elusive. The first kringle domain of the α-chain is sufficient for receptor binding, although certain residues in the β-chain are essential for HGF's structure, regulation, and activity (Stamos et al., 2004). The N-terminal region (amino acids 32-121) has a 5-strand β-pleated sheet, a 2-strand β-pleated sheet, and an α-helix region, while the first kringle domain (amino acids 122-207) has three disulfide bridges and a 2-strand anti-parallel β-pleated sheet (Gherardi et al., 2003).

The β chain of HGF also demonstrates homology to certain proteases involved in fibrinolysis and blood coagulation like plasminogen within its serine protease domain; however, differences exist in the active site residues of the two molecules, with HGF featuring glutamine and tyrosine residues instead of the histidine and serine residues observed in plasminogen. Therefore HGF lacks serine protease activity (Nakamura & Mizuno, 2010). (Figure 1.2)

The HGF gene encodes multiple mRNA species that produce at least three distinct proteins: the full-length HGF molecule and two truncated isoforms (NK1 and NK2), which contain the N-terminal domain (N) linked in tandem with the first one (K1) or two (K1+K2) kringle domains, respectively. Both NK1 and NK2 directly bind to Met and retain some degree of scatter activity. The NK1 domain's interaction with heparin stabilizes receptor binding, and specific residues within NK1 contribute to receptor activation (Lokker et al., 1992). The components of HGF have varying properties. NK1 retains almost all of the mitogenic potency of full-length HGF, while the N domain retains heparin binding properties and mediates heparin-stimulated ligand oligomerization but has little mitogenic

activity. In contrast, the K1 domain does not bind heparin but can stimulate DNA synthesis and MAP kinase activity in HGF-responsive cells at concentrations of 30 nM or more (Rubin et al., 2001).

The NK2 domain acts as a Met antagonist, inducing cell motility without mitogenesis, but not facilitating Met dimerization due to its monomeric nature, which explains its Met antagonism (Schwall et al., 1996; Tolbert et al., 2010).

## 1.4 Structure-function insights of the Met receptor tyrosine kinase

The Met proto-oncogene receptor, encoded by the *MET* gene located on chromosome 7q31 (Park et al., 1987), is a member of the subclass IV receptor tyrosine kinase gene family. Expressed in both epithelial and endothelial cells, the *MET* gene synthesizes a 150 kDa polypeptide in normal cells, which subsequently undergoes glycosylation, forming a 170 kDa precursor protein (Mondino et al., 1991). This precursor protein is processed at the cell surface into two linked chains, a 50 kDa chain and a 145 kDa chain, which ultimately form the mature heterodimeric Met protein through disulfide bond formation (Stamos et al., 2004).

As a single-pass transmembrane protein, Met displays several key structural features (Gherardi et al., 2012). The extracellular domain of Met facilitates HGF binding (Stamos et al., 2004), while the transmembrane helix and juxtamembrane region precede the tyrosine kinase domain, which shares conserved features with other RTKs. The C-terminal regulatory tail of Met contains a unique bidentate substrate binding sites involved in regulating the downstream signaling cascade (K. A. Furge et al., 2000), enabling Met to play a critical role in regulation of cellular growth and development. (Figure 1.3)

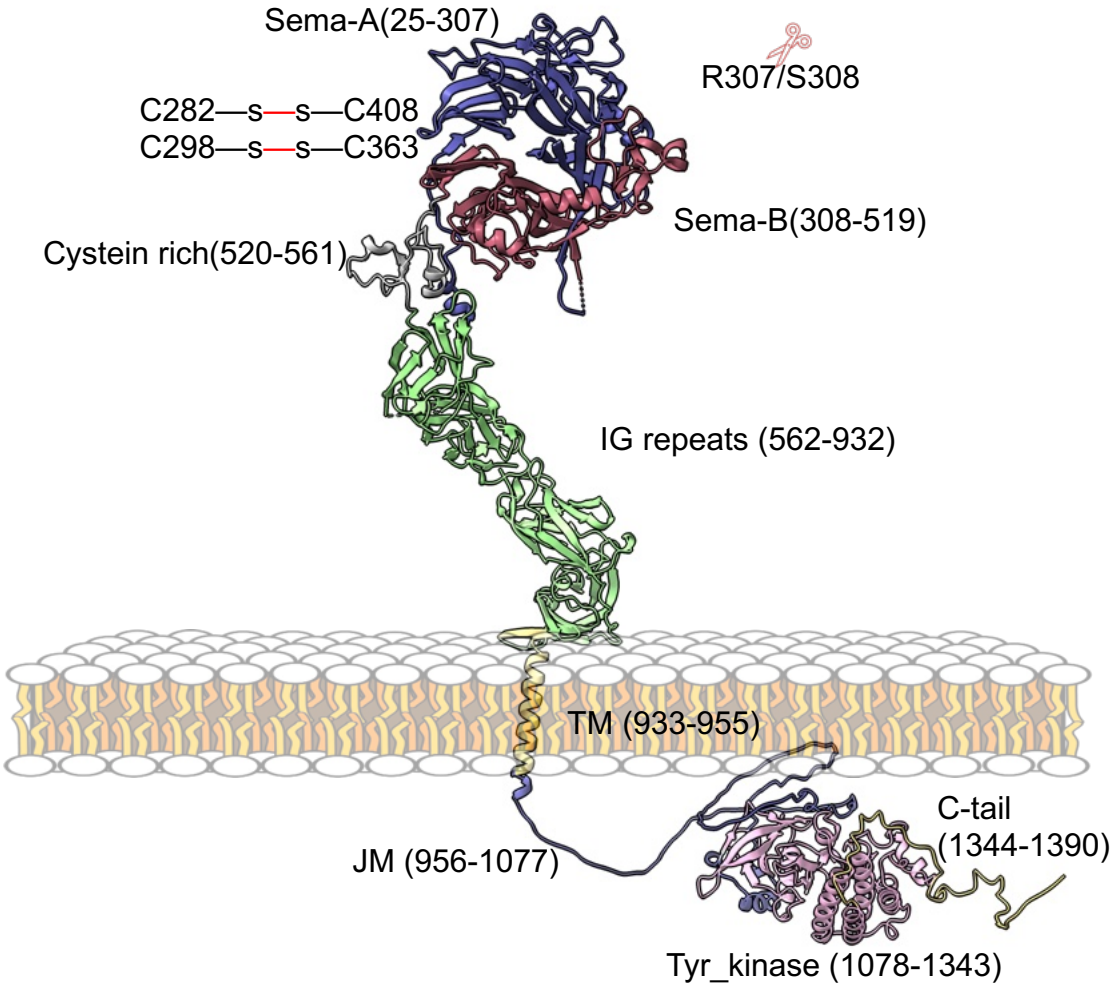


***Figure 1.3 Structure of Met receptor tyrosine kinase***

The structural organization of Met is composed of the SEMA domain, Cysteine-rich domain, Immunoglobulin repeats (Ig-repeats), transmembrane (TM), Juxtamembrane (JM) kinase domain (Tyr_kinase) and C-tail. Following proteolytic cleavage at R307/S308, the receptor generates α and β subunits and re-connected through disulfide bonds through C282-C408 and C298-C363. Three-dimensional model depicting the Met structure was developed by adapting CryoEM structure of Met extracellular domain (PDB:7MO7) and connecting the missing structures through Alphafold ( AF-P97523-F1-model_v4).

### 1.4.1 Extracellular domain of the Met receptor

#### *1.4.1.1 Met activation by HGF*

Met has a unique extracellular domain that consists of a semaphorin (SEMA) domain followed by a PSI domain (Stamos et al., 2004). The SEMA domain is similar to the semaphorin domain of plexins and semaphorins, which are important for axon guidance (Neufeld et al., 2012). In contrast, the PSI domain is related to the identically named domain found in plexins and integrins (de Jong & Dijkstra, 2003; Gherardi et al., 2004; Kozlov et al., 2004). These domains are followed by four immunoglobulin-like domains, with the fourth domain being highly conserved and referred to as the Met-related sequence (MRS) domain (Gherardi et al., 2006).

In physiological settings, the primary method of activating Met is through HGF. The first 212 residues of the Met receptor SEMA domain play a critical role in binding with the HGF/SF ligand (Stamos et al., 2004). While the details of this binding process have only recently begun to emerge, it is clear that the SEMA domain of Met is vital for HGF/SF-mediated activation (Gherardi et al., 2006).

An examination of the structure of the Met ectodomain initially revealed a complex composed of the Met SEMA and PSI domains along with the HGF/SF β-chain (Stamos et al., 2004). Binding of the HGF/SF ligand involves certain residues from the region responsible for forming the active site in serine-proteases (Gherardi et al., 2006). For the appropriate Met binding site to be established in the β-chain of the two-chain HGF/SF, the N-terminus produced by proteolysis must be inserted into an activation pocket (Gherardi et al., 2003). Although this new N-terminus does not directly interact with Met,

it does exert an allosteric influence by organizing the "active site" in a manner similar to the activation of serine proteases (Gherardi et al., 2006).

An initial *in vitro* study demonstrated that the HGF β-chain exhibits low-affinity binding to Met, but a secondary high-affinity binding site for Met is located within the NK1 fragment, which consists of the N-terminal hairpin and the first kringle domain(K1) of HGF (Lokker et al., 1992). Additionally, a 2:2 HGF:Met complex in solution could also be structurally identified (Chirgadze et al., 1999; Gherardi et al., 2006; Lietha et al., 2001).

A recent study further revealed the structural basis of HGF-mediated Met activation using cryo-EM. The results showed that HGF activates Met asymmetrically, inducing dimerization and activation. Cryo-EM analysis shows the first HGF (HGF-A) is the primary activator, five of the six HGF domains (N, K1, K2, K3, and SPH) facilitate HGF-Met association. Notably, mutations that disrupt K1-SEMA or SPH-SEMA interaction completely prevent HGF-induced Met activation, while mutations affecting N-SEMA, K2-SEMA, or K3-SEMA interaction only partially preserve activity necessary for Met dimerization and activation, while a second HGF (HGF-B) typically adopts a flexible conformation, with only the SPH domain interacting with the SEMA domain of a second Met (Met-B). HGF-B plays a more ancillary role (E. Uchikawa et al., 2021). (Figure 1.4)

In summary, the cryo-EM-derived HGF:Met complexes provide insight into the structural basis of HGF-mediated Met activation, indicating that HGF activates Met asymmetrically and induces dimerization and activation. HGF and its isoforms have distinct properties, with the K1 and SPH fragment containing the most important binding sites for Met. Heparin and heparan sulfate play a critical role in facilitating Met activation and downstream signaling (E. Uchikawa et al., 2021).

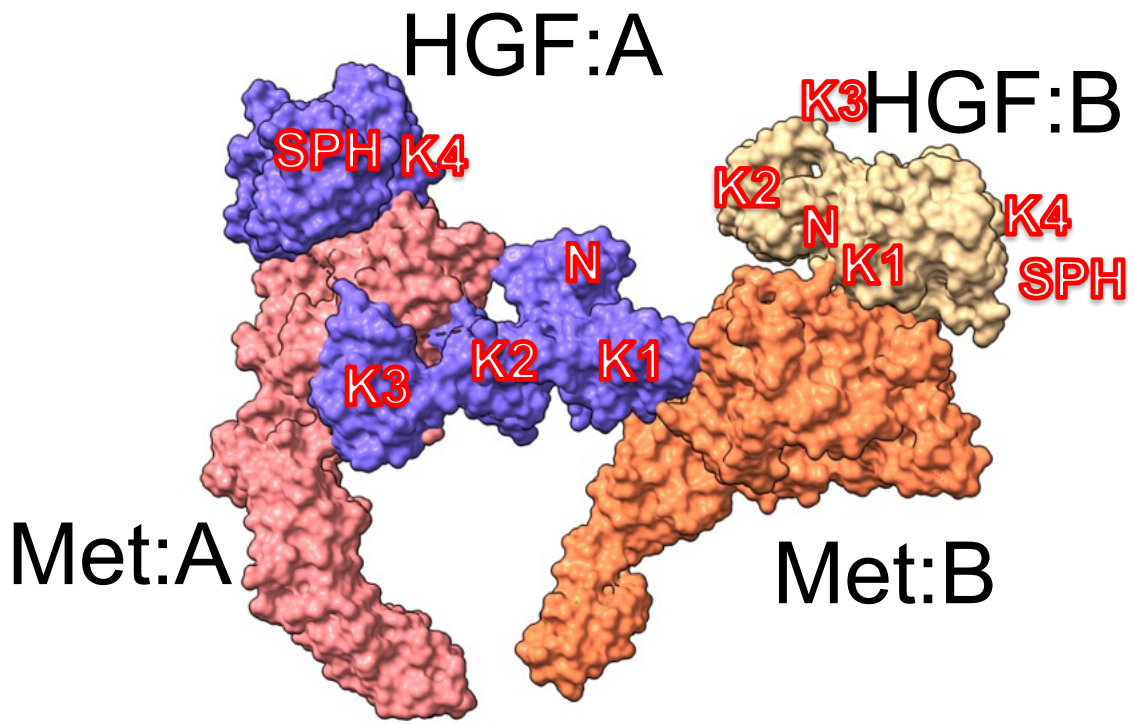


***Figure 1.4 Dimerization mechanisms of Met***

Structure of HGF bound to the extracellular domain of Met (PDB: 7MO7) (Emiko Uchikawa et al., 2021). The cryo-EM structure illustrates the binding mode of HGF and Met, demonstrating that HGF:A binds to the SEMA domain and participates in the Met A:B dimer interface, while HGF:B solely binds to Met:B.

*1.4.1.2 Met regulation by other proteins*

Additional non-canonical ways of Met activation by various proteins have been explored. CD44 and its isoform CD44v6 have been identified as important co-receptors in the activation of Met by HGF. In certain contexts, CD44v6 can play an important role in the context of HGF-induced Met activation and subsequent Ras/MAPK signaling in a wide

array of primary and malignant cells (Orian-Rousseau et al., 2002). The extracellular domain of CD44 was found to enhance Met autophosphorylation, while its cytoplasmic tail forged a connection with downstream signaling events, particularly Ras activation, via the recruitment of an intricate cytoskeletal remodeling apparatus comprised of Ezrin, Radixin and Moesin (ERM) actin cytoskeletal binding proteins and Son of Sevenless (SOS), a guanine nucleotide exchange factor for Ras. A subsequent study by the same group (Orian-Rousseau et al., 2007) reinforced the indispensability of ERM proteins tethered to both CD44v6 and F-actin in the orchestration of HGF-induced Ras activation. CD44v6 can play a critical role in HGF-induced motility and invasion in various types of cancer, including malignant peripheral nerve sheath tumors (Su et al., 2004). Furthermore, direct binding of HGF and vascular endothelial growth factor (VGEF) to CD44v6 highlights its significance in HGF signaling (Volz et al., 2015). These findings suggest that CD44 and its isoforms, particularly CD44v6, are important co-receptors that contribute to the complex interplay between HGF, its co-receptors, and Met signaling in cancer development and progression. Targeting these co-receptors may represent a promising strategy for the development of effective cancer therapies (Lai et al., 2009).

In parallel, the interplay between integrins and the Met receptor also plays a crucial factor in various cellular processes that contribute to cancer progression. α6β4 Integrin serves as an alternative coreceptor for Met, which contributes to HGF-mediated Met activation and provides additional docking sites for Shc and PI3K. This interaction links activated Met to the Ras/MAPK and PI3K pathways, exerting considerable influence over survival, proliferation, and migration (Ahn et al., 2013; Hemler, 2001).

Furthermore, the study by Mitra and colleagues provided insights into the mechanisms underlying the activation of Met in ovarian cancer cells and its impact on cancer invasion and metastasis. They found that fibronectin and α5β1-integrin could activate Met independently, leading to downstream signaling pathways that promote invasion and metastasis. The inhibition of either fibronectin or α5β1-integrin could decrease Met activation and impede cancer cell invasion and metastasis, highlighting their potential as therapeutic targets (Mitra et al., 2011).

In addition to aforementioned-studies, Met could maintain breast cancer cell survival through a kinase-independent interaction with integrin α3β1 (Tesfay et al., 2016).

Taken together, these findings further underscore the complexity of the relationship between integrins and Met and suggest that Met can regulate cell survival through integrin interactions that are not mediated by kinase signaling.

### 1.4.2 Juxtamembrane domain of the Met receptor

One of the unique features of the Met receptor is its juxtamembrane domain, which is the longest among all 58 receptor tyrosine kinases, but remains structurally uncharacterized (Ma, 2015) (Figure 1.5 a & b). This domain is partially encoded by the *MET* exon 14 region in the *MET* gene. *MET exon 14* alterations at RNA splice acceptor or donor sites have been recently described as a distinct mechanism of Met oncogenesis, leading to Met exon 14 skipping (MetΔex14) (P. K. Paik et al., 2015). Two sites are of significance reported in the literature: S985 and Y1003.

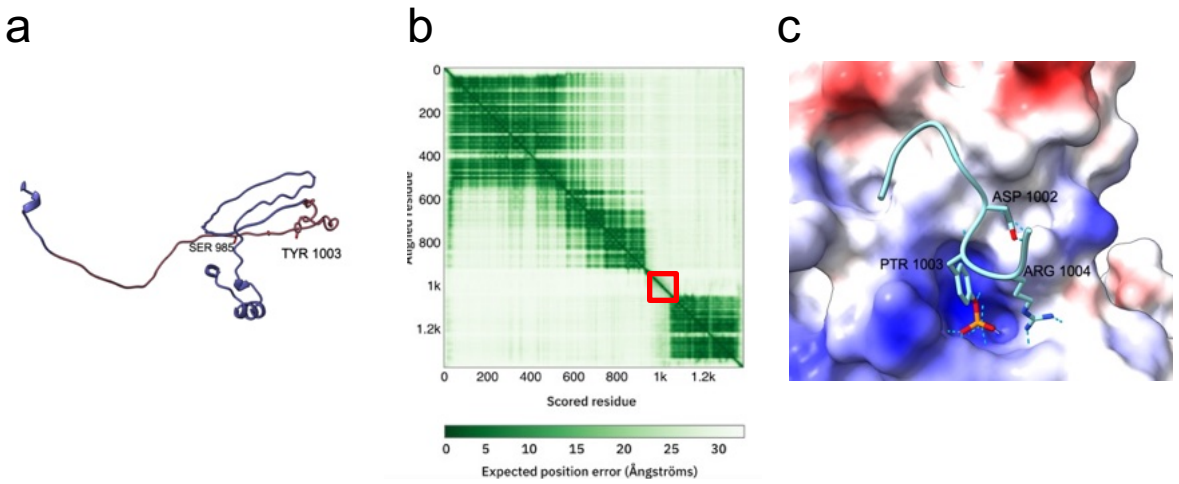


***Figure 1.5 Structural features of Met juxtamembrane domain***

The Met juxtamembrane domain is long compared to other RTKs and is likely disordered. (a) Extended confirmation was predicted by AlphaFold (AF-P97523-F1-model_v4). (b) The AlphaFold predicted alignment error heatmap features a high position error in the juxtamembrane region, indicating a disordered region by the red box (c) Crystal structure of the Met Y1003 region (green) bound to Cbl. PDB: 3BUX. The electrostatic potential surface of Cbl was colored red and blue for negative and positive charges, respectively, while white color represents neutral residues.

Serine 985 phosphorylation site on Met receptor tyrosine kinase has garnered attention for its potential to modulate downstream signaling pathways and cellular responses. Extensive research on this subject has revealed that regulation of S985 by various proteins, including PKC, PP2A, and PKG II, can regulate Met activity in a diverse array of contexts (Hashigasako et al., 2004; Wu et al., 2016). For instance, PKC-mediated phosphorylation of S985 has been shown to reduce the ability to activate Met in response to HGF, whereas dephosphorylation of S985 by PP2A has been found to amplify Met activity (Hashigasako et al., 2004). Additionally, recent studies have demonstrated that PKGII-mediated phosphorylation of S985 can abrogate HGF-triggered cellular activities in gastric cancer cells by decreasing activation of downstream signaling pathways (Wu et al., 2016). Despite promising findings, the underlying molecular mechanisms of S985

phosphorylation-mediated Met regulation remain unclear and warrant further investigation to fully comprehend the implications of this process in physiological and pathological conditions.

Cbl ubiquitin ligase negatively regulates several RTKs by promoting their ubiquitination and subsequent degradation. When Cbl is uncoupled from RTKs, it can lead to enhanced RTK stability and prolonged signalling. Phosphorylation of Y1003 in exon 14 of Met creates a binding site for the tyrosine kinase binding (TKB) domain of Cbl (Figure 1.5 c), which promotes the ubiquitination of Met enhancing its inclusion into multivesicular bodies through ESCRT ubiquitin recognizing proteins and subsequent degradation of Met in the lysosome terminating downstream signaling (Peschard et al., 2001; P. Peschard et al., 2004; Peschard & Park, 2003). Met receptor variant Y1003F, which cannot be phosphorylated at Y1003, escape ubiquitination and exhibit prolonged signalling and oncogenic properties in fibroblast and epithelial cells in the presence of HGF. These mutants are internalized and still undergo endosomal trafficking but are inefficiently targeted for degradation, resulting in sustained stability and activation of the Met Y1003F mutant and downstream signals, such as the MAPK pathway. Cbl-dependent ubiquitination is critical for targeting the Met receptor to the lysosomal sorting machinery and turning off Met signaling through protein degradation, although it is not required for Met internalization.

In addition to loss of Y1003, the loss of the E3 ligase Cbl in gastric cancer is associated with increased Met expression and activation (Lai et al., 2012) and Met endocytosis plays a direct role in promoting tumorigenesis by facilitating Met activation and downstream signaling (Joffre et al., 2011).

Overall, these provide valuable insights into the understanding of Met regulation and by S985 and Y1003 phosphorylation as well as raise the importance of exon 14 skipping in the juxtamembrane region.

### 1.4.3 Kinase domain of the Met receptor

The kinase domain of the Met receptor exhibits a bi-lobal architecture observed in many other kinases. Its structure has been solved by crystallography which has provided insights into the conformational changes and interactions that regulate the activity of the human Met kinase and acts as a template for designing inhibitors that target this kinase. The Met kinase domain shares 44% sequence identity with the kinase domains of insulin receptor (IR) kinase and 41% fibroblast growth factor (FGF) receptor kinase (Bolanos-Garcia, 2005). However, the crystal structure of Met kinase demonstrates specific characteristics that distinguish it, such as the absence of a functionally relevant salt bridge and a unique $3_{10}$ helix adjacent to the core Met kinase domain (Bolanos-Garcia, 2005). Additionally, the orientation of the Met N-terminal juxtamembrane region formed an extension into an α-helix, which seems to be part of the structural elements involved in kinase activation.

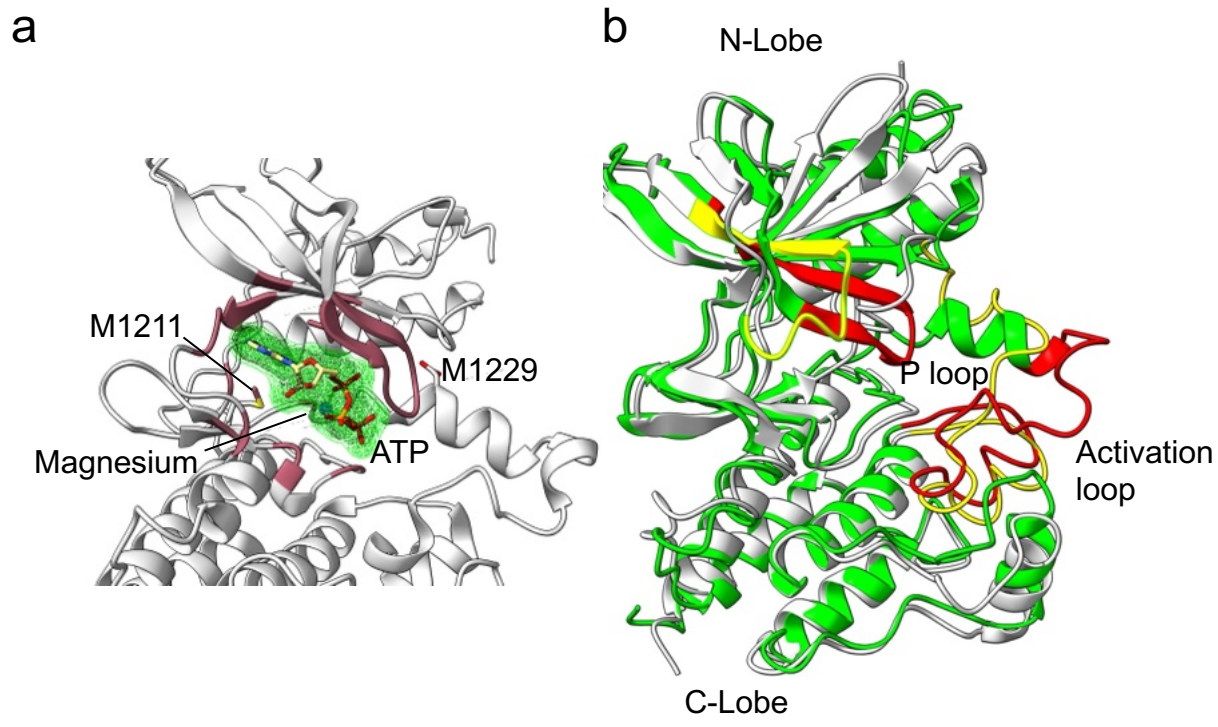


***Figure 1.6 Structural features of Met kinase domain***

(a) The crystal structure of the Met receptor tyrosine kinase domain in complex with ATP (PDB: 3DKC) reveals that amino acids contacting ATP are colored in red, Magnesium is colored in blue.
(b) Structure comparison of the Met receptor tyrosine kinase domain between the active state (PDB: 3Q6U, shown in green) and the inactive state (PDB: 2G15, shown in gray). In the active state (3Q6U), an extended activation loop is observed, along with an ordered P-loop (colored red). In contrast, the inactive state (2G15) exhibits a closed activation loop and a disordered P-loop (colored yellow).

The activation of Met through HGF binding results in the phosphorylation of specific tyrosine residues within the kinase domain, such as Y1234 and Y1235 in the activation loop. This phosphorylation leads to the stabilization of an open conformation that enables ATP-binding (Gherardi et al., 2012).

In the active form, the ATP molecule is the source of phosphate being transferred to the tyrosine substrates. The adenine ring position between V1092 and M1211 plays a crucial role in determining separation of the kinase lobes in the active form (Schiering et al.,

2003). The A-loop also plays a crucial role in substrate recognition and catalysis, the intricate details of the A-loop of Met are critical for its enzymatic activity, as its disengaged state enables the binding of a peptide substrate. The conformation of the A-loop in this state exposes pY1230 to solvent, while pY1234 and pY1235 stabilize it through a network of interactions. Tri-phosphorylation of the A-loop does not seem critical for Met enzymatic activity (Miller et al., 2001) as the non-phosphorylated tyrosine residues from the A-loop also play a role in stabilizing the A-loop through interactions with neighboring residues. However, several mutations within PRC (papillary renal carcinomas) contribute to stabilizing the active conformation of the A-loop, with D1228N/H mutations being particularly important (Bardelli et al., 1998). In addition, the crystal structure of Met kinase suggests that phosphorylation of Y1194 might also contribute to the establishment of the active conformation by contacting the pivot point of the C-terminal α-helix (Bolanos-Garcia, 2005) (Figure 1.6 a).

In the inhibited form, the ATP- and peptide-substrate-binding sites of the unphosphorylated wild-type Met are obstructed by the A-loop (Miller et al., 2001) (Figure 1.6 b). The A-loop is stabilized by several interactions, including phosphorylation of tyrosine residues, interactions with other protein domains, and interactions with the peptide substrate.

The detailed understanding of the kinase domain's structure has provided valuable insight for designing inhibitors. Various inhibitors have been developed to target the Met kinase, such as SU11274, which differentially affects the kinase activity and subsequent signaling of various mutant forms of Met (Berthou et al., 2004; Ma et al., 2005). The basis for the sensitivity or resistance to SU11274 in terms of the position of these mutations has been

discussed (Berthou et al., 2004; Zimmer et al., 2010). Additional mechanisms participate in the regulation of the activity of the Met kinase domain, such as the binding of scaffolding and adaptor proteins that modulate signal transduction (Gherardi et al., 2012; Organ & Tsao, 2011). The development of new inhibitors has been facilitated by the detailed understanding of the Met kinase domain structure and activation mechanisms.

### 1.4.4 Carboxy-terminus of the Met receptor

The activation of the Met receptor by HGF, which triggers the formation of homodimers is considered to enable trans-phosphorylation of tyrosine residues within the carboxy terminal tail of Met. This phosphorylation event creates a docking site for adaptor proteins, which subsequently activate downstream signaling pathways (detailed in section 1.5).
Phosphorylation of tyrosine residues Y1349 and Y1356 in the C-terminal tail of Met allows for the binding of intracellular signal transducers (Fixman et al., 1996; Fournier et al., 1996; Ponzetto et al., 1993; Zhu, Naujokas, Fixman, et al., 1994), These transducers dock onto the tyrosine phosphorylated sequence using SH2, MBD, and PTB domains.
SH2 domains are found in 121 proteins within the human proteome and are typically composed of around 100 amino acid modules (Liu et al., 2012a). These domains contain a positively charged binding pocket with an FLVR amino acid motif, including a critical arginine residue that binds to the negatively charged phosphotyrosine on their interacting proteins. The specificity of binding is usually determined by the residues +1 to +6 downstream from the phosphotyrosine, although non-canonical binding mechanisms have also been reported (Kaneko et al., 2010; Liu et al., 2012b). For instance, Cbl can recognize residues at both the carboxy and amino terminal of pTyr through two known

motifs, (N/D)XpY(S/T)XXP and DpYR, which have been identified in Met RTK (P. Peschard et al., 2004; Wagner et al., 2013) (Figure 1.7 a).

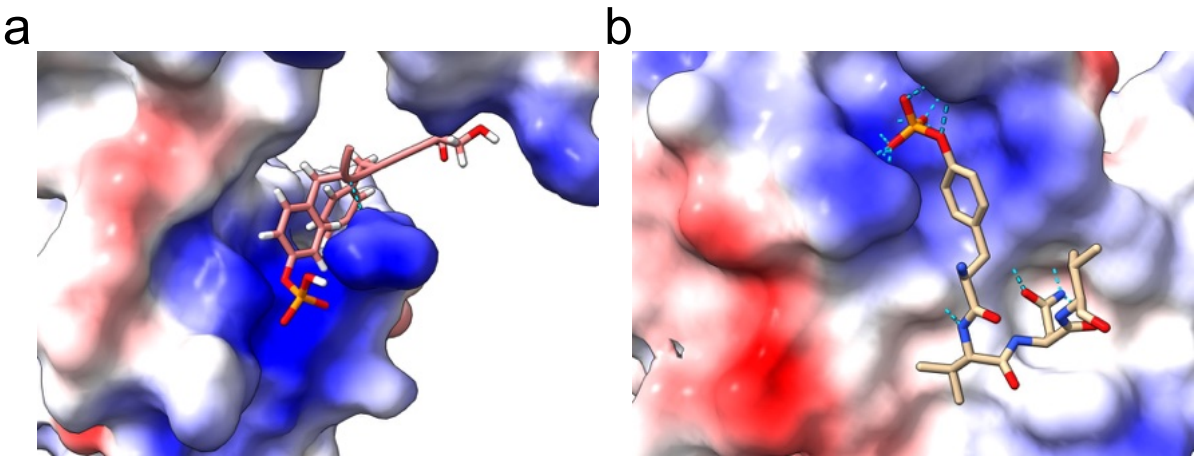


***Figure 1.7 Structural differences of PTB and SH2 domain***

(a) PDB: 1SHC Shc PTB domain complexed with a TrkA receptor phosphopeptide, (nmr, minimized average structure).
(b) PDB: 1TZE Grb2 SH2 domain complexed with a pYVNV substrate. Electrostatic potential surface of Shc and Grb2 is colored red and blue for negative and positive charges, respectively, and white color represents neutral residues.

PTB domains, on the other hand, are structurally unrelated to SH2 domains and are found in 60 proteins within the human proteome (Kaneko et al., 2012). These domains consist of approximately 160 amino acid modules that can bind their substrates in a pTyr-dependent or -independent manner to the NPxpY motif (Forman-Kay & Pawson, 1999). In the pTyr-dependent mechanism, the binding pocket is basic and positively charged, with key arginine and lysine residues that participate in hydrogen bonding with the negatively charged phosphate group in pTyr. In the pTyr-independent binding, although the tyrosine residue is required, the binding pocket is less basic and shallow, forming hydrogen bonds with unphosphorylated tyrosine in the NPxY motif (Wagner et al., 2013) (Figure 1.7 b).

In the inactive state, the non-phosphorylated residues $Y^{1349}$VHV adopts an extended conformation similar to phosphopeptides bound to typical SH2 domains (Schiering et al., 2003) (Figure 1.7 a).

The residues $N^{1353}$ATY forms a type I β-turn, similar to the structure found in Shc-PTB domain-binding peptides (NPXY) (Bolanos-Garcia, 2005). NMR structure analysis of the PTB domain of a Shc-peptide complex reveals a type I β-turn structure at the C-terminal region of a β-strand (Trüb et al., 1995). Although the conformation of this β-turn is strikingly similar to Met $N^{1353}$ATY β-turn, docking the PTB domain with Met would be predicted to result in clashes with the kinase C lobe, suggesting $N^{1353}$ATY is unlikely to be important for recruiting downstream effector proteins.

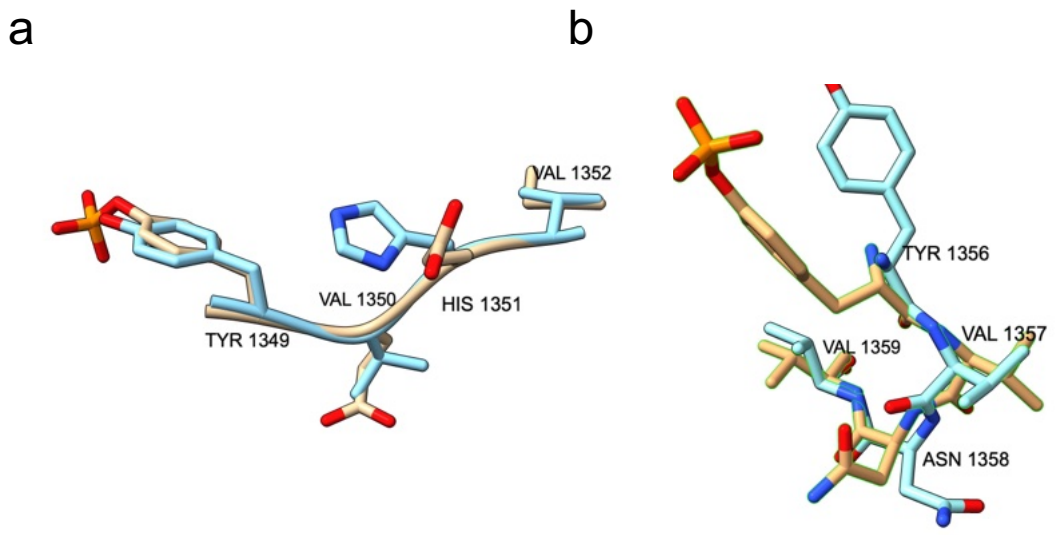


***Figure 1.8 Structural features of Met carboxy-terminal tail***

(a) Lck kinase SH2 domain substrate pYEEI (brown) superimposed with Met-$Y^{1349}$VHV (green).
(b) Grb2 SH2 domain substrate pYVNV (brown) superimposed with Met-$N^{1353}$ATY (green).

In contrast, the Grb2 SH2 domain binds specifically to the phosphorylated $Y^{1356}$VNV motif and forms hydrogen bonds with the asparagine residue in the SH2 domain. The $Y^{1356}$VNV motif forms a type II β-turn, which differs from the type I β-turn found in phosphopeptides that bind to Grb2 (Schiering et al., 2003) (Figure 1.8 b). Type I and Type II β-turns are related through a 180-degree flip of the central peptide unit (Chou & Fasman, 1977; Gunasekaran et al., 1998). Despite some conformational differences in residues Y1356, V1357, and N1358, a rotamer conformational change allows the N1358 side chain to occupy the position in the Grb2 complex. This allows the SH2 domain of Grb2 to dock with Met by superimposing residues 1356–1359 without significant steric clashes with the C-lobe of Met kinase (Bolanos-Garcia, 2005).

## 1.5 Met downstream signalling cascade

Met signaling is activated in response to HGF binding, predominantly triggers recruitment of Grb2 (Maina et al., 1996; Ponzetto et al., 1996; Schaeper et al., 2000), the p85 subunit of phosphoinositide 3-kinase (PI3K) (Bardelli et al., 1999; Maroun et al., 2003), Grb2-associated protein 1 (Gab1) (Fixman et al., 1996; Fixman et al., 1997; Maroun et al., 1999; Sachs et al., 2000; Weidner et al., 1996), and the Grb2-associated ubiquitin ligase Cbl (Peschard et al., 2001) (Figure 1.9).

Gab1 is of particular importance in Met signaling as it is the primary scaffold protein recruited to Met through its interaction with Grb2 SH3 domains (Maroun et al., 1999). In addition, Gab1 possesses a unique Met-binding domain (Lock et al., 2003; Weidner et al., 1996), enabling it to engage with residues upstream of Y1349 providing a bimodal engagement with the Met C-tail.

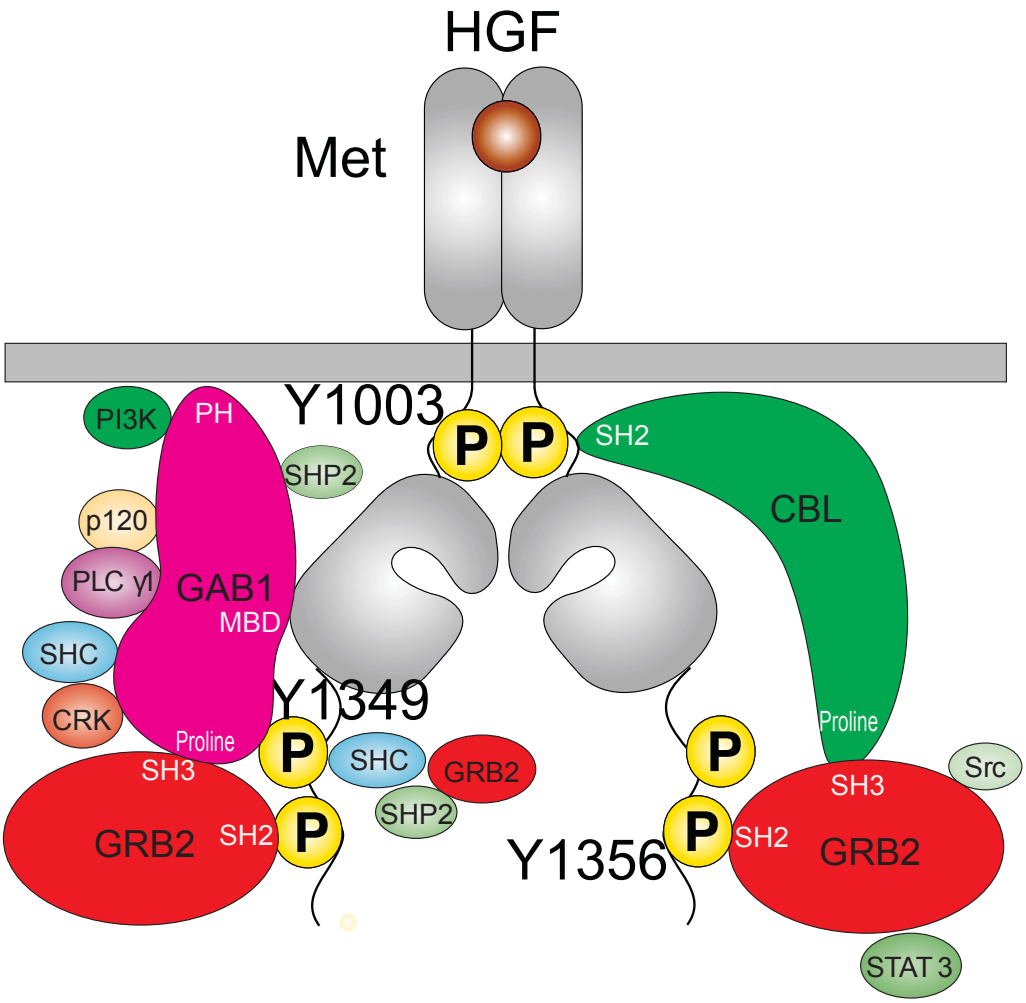


***Figure 1.9 Met signaling interactions among various components of the pathway***

In the context of Met signaling, adaptor proteins such as Gab1 provide a crucial scaffold for Met. Gab1 exhibits both direct and indirect interactions with Met, mediated through its association with Grb2. Upon Met-dependent tyrosine phosphorylation, Gab1 facilitates the recruitment of Src-homology-2 domain-containing transforming protein (Shc), PI3K, SHP2, and phospholipase Cγ1 (PLCγ1) by providing additional binding sites. These proteins associate with Met and serve as secondary messengers for recruiting signal transducers, thereby enhancing signaling outputs. Cbl can directly bind to Met through Y1003 or indirectly through Grb2, thereby limiting the signal duration upon Met activation.

Upon Met activation, following recruitment to Met, Gab1 is phosphorylated on multiple tyrosine residues and promotes the recruitment of additional signaling molecules through

SH2 domain interactions. These include the p85 subunit of PI3K (Bardelli et al., 1999), Src homology 2 domain-containing phosphatase 2 (SHP2) (Maroun et al., 2000; Schaeper et al., 2000), phospholipase C gamma (PLCγ) (Okano et al., 1993), CT10 regulator of kinase (Crk) adaptor protein (Garcia-Guzman et al., 1999; Lamorte et al., 2000) and p21-activated kinase 4 (PAK4) (Paliouras et al., 2009) to the Met signaling complex.

In addition, recruitment of Grb2 to phosphorylated tyrosine Y1356 in Met leads to the recruitment of the SOS, a Ras guanine nucleotide exchange factor, which activates the Ras/Raf/MEK/ERK signaling pathway. This pathway ultimately promotes cell proliferation, differentiation, and survival (Birchmeier et al., 2003; Kyle A Furge et al., 2000). Furthermore, the recruitment of the p85 subunit of PI3K to Gab1 activates the mammalian target of rapamycin complex 1 (mTORC1) through its downstream effector, promoting cell growth and survival. PLCγ recruitment activates RAC1, inducing actin-based protrusions necessary for cell migration and filopodia formation (Zhang et al., 2018). PAK4 recruitment helps regulate the actin cytoskeleton through the WAVE regulatory complex activation (Chen et al., 2014). Gab1 also recruits SHP2 tyrosine phosphatase to inactivate Ras negative regulators (Dance et al., 2008; Montagner et al., 2005). Other activated pathways include STAT3 (Kermorgant & Parker, 2008; Lai et al., 2014; Zhang et al., 2002), JNK (Lamorte et al., 2000; Rodrigues et al., 1997) and p38 MAPKs (Recio & Merlino, 2002). The complex interplay between these signaling proteins and pathways forms a sophisticated regulatory network that coordinates cell processes induced by HGF-Met signaling. Proper recruitment of signaling proteins to Met is vital, as dysregulation can lead to abnormal cellular functions and diseases.

## 1.6 Met upstream regulation

Met signal regulation is a multifaceted process, involving a variety of mechanisms that act on different stages of the pathway. Abnormal Met levels, which have been implicated in cancer, can arise from numerous defects, including transcript-level misregulation through gene amplification or oncogene-enhanced transcription (explained in detail in Section 1.6), activation of hypoxia-inducible factor 1 (HIF-1) transcription factor (Glück et al., 2018; Xu et al., 2010), down-regulation of Met-targeting miRNAs (Duan et al., 2010; El Bezawy et al., 2017; Reid et al., 2012), and stabilization by heat-shock protein 90 (HSP90) (Jiao et al., 2011; Lee et al., 2021; Yallowitz et al., 2018).

Various mechanisms have been identified to negatively regulate Met signaling. Cbl ubiquitin ligases, for example, mediate the ubiquitination of activated Met, targeting it for lysosomal and proteasomal degradation (Peschard et al., 2001; Pascal Peschard et al., 2004; Peschard & Park, 2003). Additionally, several phosphatases, including receptor protein tyrosine phosphatase β (RPTPβ (Zeng et al., 2014)), PTP1B (Sangwan et al., 2011), and SHIP (Koch et al., 2005), negatively regulate Met signaling by dephosphorylating activated Met or downstream signaling molecules, such as phosphatidylinositol 3,4,5-trisphosphate (PIP3) (Zhang et al., 2018). Phosphatases are vital biological molecules that deactivate tyrosine kinases through dephosphorylation. Protein-tyrosine-phosphatase (PTP) 1B and T-cell phosphatase (TCPTP) are two phosphatases implicated in the negative regulation of Met, targeting its main phosphorylation sites Y1234 and Y1235. PTB-1B is a non-receptor tyrosine phosphatase, interacting with multiple RTKs, while TCPTP is structurally similar but exhibits different

specificities. After HGF-induced activation, both PTB-1B and TCPTP co-localize with Met and dephosphorylate its major autophosphorylation site (Sangwan et al., 2008).

Furthermore, the Met receptor tyrosine kinase is negatively regulated by several Met-binding proteins, such as suppressor of cytokine signaling 1 (SOCS1), a member of the SOCS family. SOCS1 negatively regulates Met signaling by recruiting the ubiquitin ligase complex containing the von Hippel-Lindau tumor suppressor protein (pVHL) to activated Met, thereby increasing Met ubiquitination and degradation (Gui et al., 2015; Santharam et al., 2021).

Understanding these diverse mechanisms that regulate Met signaling is crucial for developing targeted therapeutic strategies in diseases where Met signaling plays a critical role.

### 1.6.1 Ligand dependent regulation

#### *1.6.1.1 Endocytosis*

The internalization of Met is regulated by the scaffold function of Cbl (Mohapatra et al., 2013). Clathrin-coated vesicles (CCVs) fuse with sorting endosomes, forming multivesicular bodies (MVBs) that direct proteins toward lysosomal degradation or recycling to the cell membrane (Pryor & Luzio, 2009). Met activation and ubiquitination are required for recruitment by the HRS/STAM complex, which forms the endosomal sorting complex for transport (ESCRT) and initiates the recruitment of other ESCRT complexes to the sorting endosome. This process regulates the formation of MVBs (Abella et al., 2005).

Late MVBs are targeted to the lysosome, where the endocytosed Met receptor is degraded (Tanaka et al., 2008). Alternatively, proteasome activity can also contribute to Met degradation, as ligand-induced Met degradation is decreased by proteasomal inhibitors (Hammond et al., 2003; Hammond et al., 2001; Jeffers et al., 1997). In addition to degradation, the endocytic machinery also sorts Met receptors for recycling. When activated by HGF, Met engages with Golgi-Associated, Gamma Adaptin Ear-Containing, ARF-Binding Protein 3 (GGA3) microdomains in early endosomes dependent via Crk, allowing for recycling from the Rab4-positive endosome to the plasma membrane. Without GGA3, Met recycling is hindered, leading to increased degradation and reduced signaling downstream (Parachoniak et al., 2011). (Figure 1.10)

Efficient recycling is crucial for precise regulation of Met signaling and cellular responses, including cell migration. Thus, understanding the molecular mechanisms underlying ligand-dependent regulation of Met signaling is essential for developing targeted therapeutic approaches in various diseases where Met signaling plays a critical role.

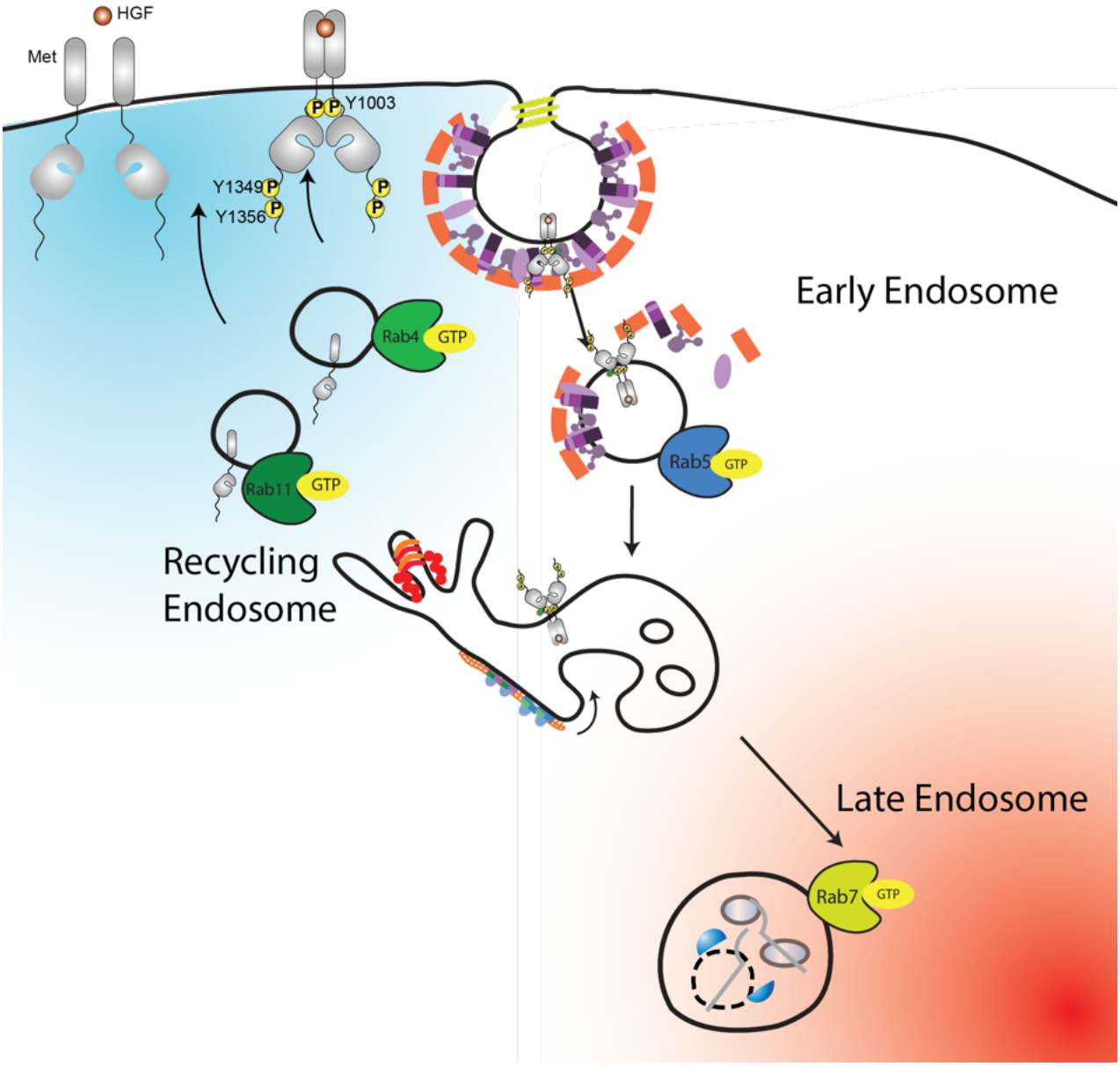


***Figure 1.10 Met trafficking through internalization and recycling***

Following HGF binding, Met enters clathrin coated pits and is internalized into early endosomes Early endosomes have the capacity to fuse with one another as they traverse along microtubules, eventually converge in the perinuclear region of the cell and become late endosomes and mature with multivesicular bodies (MVB). In late endosomes ubiquitinated cargo are recognized by ESCRT proteins promoting membrane invagination and internalisations into MVB. Non-ubiquitinated Met can undergo sorting towards recycling endosomes, facilitating the return Met to the cell surface.

*1.6.1.2 Autophagy*

Autophagy and endocytosis are two vital cellular processes that are crucial for detecting and adapting to extracellular stimuli. Met is regulated by both pathways. The hATG8 family member LC3C is particularly important in this regard, as it selectively interacts with a Met complex upon HGF stimulation and internalization, leading to autophagic degradation. Notably, this regulation is highly specific and does not affect EGFR responses and stability (Emily S Bell et al., 2019; Coelho et al., 2022). Under nutrient deprivation, Met is directed to an autophagic compartment rather than the canonical endosomal pathways activated by ligand binding. Met was also found to localize to nascent autophagosomes and show significant enrichment and colocalization with LC3B (Barrow-McGee et al., 2016). This observation underscores the selective and tightly regulated nature of autophagic targeting of Met.

The LC3C-mediated regulation of Met trafficking and biological responses is integrated into a larger signaling network that modulates cell motility and adaptation to starvation. These processes are critical for wound healing, organ regeneration, and other physiological activities in which Met/HGF signaling is essential (Bell et al., 2020).

In renal cell carcinoma (RCC), LC3C levels are often decreased due to VHL loss, which is common in hypoxic tumor regions (Bastola et al., 2013; Mikhaylova et al., 2012). The loss of LC3C-mediated autophagic regulation of Met in these areas could contribute to the aggressive cancer phenotypes associated with high Met levels, promoting invasiveness and metastatic progression. Furthermore, given that hypoxic cells rely on autophagy for survival and therapy resistance, this may represent a prevalent condition

in which pro-tumorigenic autophagy is increased. Understanding these complex interactions between autophagy, Met regulation, and hypoxia will be crucial for the development of targeted therapeutic strategies (Simpson & Gammoh, 2020).

### 1.6.2 Ligand independent regulation

Met can be regulated in a ligand-independent manner through various mechanisms. One such mechanism is caspase cleavage during apoptosis, wherein cysteine-dependent aspartate-directed proteases cleave Met at specific motifs (Foveau et al., 2007; Lefebvre et al., 2013; Tulasne et al., 2004). This process generates a membrane-anchored N-terminal fragment and a cytoplasmic C-terminal fragment that are unresponsive to ligand stimulation. Consequently, the full-length Met receptor abundance decreases, potentially inhibiting survival responses triggered by HGF. The caspase cleavage of Met during apoptosis bears resemblance to dependence receptors, which induce cell death in the absence of ligand, relying on ligand for cell survival (Montagne et al., 2015). These findings suggest that Met cleavage may play essential roles in regulating the delicate balance between survival and apoptosis, although its physiological relevance in development and cancer remains unclear.

Shedding of the extracellular domain of the Met receptor is facilitated by presenilin-regulated intramembrane proteolysis (PS-RIP). Membrane metalloproteases initiate the shedding process, resulting in a soluble N-terminal fragment (Met-NTF) and a membrane-anchored C-terminal fragment (Met-CTF). The CTF is subsequently cleaved by the γ-secretase complex, and the intracellular domain (Met-ICD) subsequently undergoes degradation by the proteasome. While this process differs from ligand-dependent

degradation, recent evidence suggests shared features between these processes. Inhibition of both proteasomal and lysosomal degradation leads to the accumulation of CTFs, highlighting the complementary nature of these pathways. The degradation of Met CTFs in the lysosome following receptor internalization resembles HGF-triggered degradation (Ancot et al., 2012). Notably, this degradation does not require tyrosine kinase activity, and there have been no observations of ubiquitination of the fragments (Foveau et al., 2009).

The intriguing aspect of caspase cleavage is the generation of active fragments that can promote apoptosis. The membrane-anchored Met extracellular domain acts as a decoy receptor, limiting HGF binding to the full-length Met receptor and reducing the cell survival response during apoptosis (Deheuninck et al., 2008). Conversely, the cytoplasmic Met fragment, when ectopically expressed, intensifies cell death and activates Caspase-3. By inhibiting the generation of the p40 Met fragment, it becomes possible to prevent cell death induced by mild stress (Tulasne et al., 2004). These mechanisms further underline the conversion of the survival receptor into a proapoptotic molecule through caspase cleavage of Met. The physiological significance of a proapoptotic function for Met in development and cancer warrants further investigation, as it may have crucial implications for regulating the balance between cell survival and apoptosis (Lefebvre et al., 2012).

## 1.7 Biological function of Met

The HGF-Met signaling pathway is essential in various biological processes, including embryonic development, organogenesis, organ regeneration, and the regulation of cell motility, division, survival, and differentiation (Birchmeier et al., 2003). HGF, initially

identified as a hepatocyte mitogen, binds to the Met RTK which is expressed in diverse cell types such as epithelial cells, myoblasts, and neuronal precursors (Birchmeier & Gherardi, 1998; Zhang & Vande Woude, 2003). Met signaling is involved in numerous aspects of embryonic development, such as placental development (Clark et al., 1996; Ueno et al., 2013), migration of muscle progenitors (Bladt et al., 1995), sensory nerve development, axonal growth (Maina et al., 1997), and olfactory interneuron migration (Garzotto et al., 2008; Powell et al., 2001). The complex roles of Met in development and tumorigenesis are exemplified by its function as a potent mediator of the morphogenic program branching tubulogenesis (Fournier et al., 1996; Gual et al., 2000), which underlies organogenesis during development and involves epithelial-to-mesenchymal transition (EMT). This process also plays a part in the initiation of Met-mediated metastasis in cancers (detailed in section 1.6) (Lee et al., 2014).

HGF plays a critical role in maintaining normal tissue structure, with its primary production occurring in the liver. During liver regeneration, Kupffer cells increase HGF expression. HGF is also vital for skeletal muscle formation in limbs and diaphragms, as well as muscle progenitor proliferation and motility (Matsumoto & Nakamura, 1996; Nakamura & Mizuno, 2010). In vitro studies have shown that HGF primarily causes epithelial cell scattering and is linked to invasiveness in cancers (Qian et al., 2003; Royal & Park, 1995). HGF is also involved in tubular structure formation in cells grown in three-dimensional collagen matrices and stimulates angiogenesis in endothelial cells, indicating its significance in developmental and homeostatic processes (Fournier et al., 1996) HGF-dependent angiogenesis can interact with and potentially enhance signaling through VEGF receptor

tyrosine kinases (Xin et al., 2001), although HGF and VEGF may have opposing biological effects in some cases (Sulpice et al., 2009).

Genetically modified mice have offered valuable insights into the biological functions of the HGF-Met signaling pathway. Cre recombinase in gene editing has facilitated deeper exploration of HGF-Met signaling pathway in development and adult homeostasis. The co-ordinated deletion of Met in adult liver tissue revealed a significant decrease in liver cell proliferation during wound-induced liver regeneration compared to control mice (Huh et al., 2004). HGF-dependent Met activation has a critical impact on the recruitment of anti-tumor neutrophils to murine tumors, and the removal of Met in epithelial thymic cells disrupts the development of regulatory T cells (Glodde et al., 2017). Mice lacking either Met or HGF experience in utero death due to placental defects (Kolatsi-Joannou et al., 1997), while heterozygous mice display defects in liver, heart, skeletal muscle, and kidney development, as well as reduced wound healing and impaired liver regeneration. The absence of either HGF or Met in whole-body knockout mice leads to early embryonic lethality, reduced cell proliferation, and increased apoptosis in the liver (Huh et al., 2004). Additionally, the migration of myogenic precursor cells to developing limb buds and the invasion of trophoblast cells into the maternal decidua are impeded (Bladt et al., 1995; Kauma et al., 1999; Yang et al., 1996). Experiments using explant tissues from HGF-deficient mice reveal that HGF acts as a chemoattractant for limb bud innervating axons, emphasizing the role of HGF-Met signaling in axon guidance (Caton et al., 2000; Ebens et al., 1996).

## 1.8 Met dysregulation in cancers

Aberrant activation of the Met RTK has been extensively studied in the context of human cancers. Met was first discovered as a transforming oncogene from a chemically treated (MNNG) human osteogenic sarcoma (HOS) cell line using the NIH3T3 cell transfection assay (Cooper et al., 1984), then subsequently cloned using Alu repeats. Since Met was not first discovered as a retrovirally transduced oncogene the suffix c-Met should not be used.

Several molecular mechanisms contribute to Met dysregulation in cancers, including overexpression, gene amplification, chromosomal rearrangements, exon 14 skipping, and activating mutations in the kinase domain. Overexpression of the wild-type Met RTK protein is the most common mechanism of Met-mediated oncogenicity (Lengyel et al., 2005; Sawada et al., 2007). Hypoxia-induced elevated transcription of Met (Chen et al., 2007; Pennacchietti et al., 2003) as well as a hypoxia dependent decrease in LC3C which engages Met with a degradative autophagy pathway elevates Met in tumor hypoxic domains (Emily S. Bell et al., 2019). Moreover, autocrine or paracrine stimulation of Met by HGF has been reported in many cancers, including lung (Drilon et al., 2017; Sadiq & Salgia, 2013; Jürgen Wolf et al., 2020), colorectal (Bardelli et al., 2013; Di Renzo et al., 1995; Umeki et al., 1999), kidney (Marona et al., 2019), liver (Bladt et al., 2014), breast (Lengyel et al., 2005; Tuck et al., 1996), pancreatic (Li et al., 2011), ovary (Sawada et al., 2007) and cancer of unknown primary origin (CUPs) especially in advanced metastatic cancers (Stella et al., 2017). Germline mutations in *MET* have also been identified in

familial renal carcinoma (Schmidt et al., 1997), emphasizing the importance of Met activation in human cancer and the potential for therapeutic intervention.

Met exon14 skipping has been recognized as a critical event in cancer progression and been linked to poor prognosis in various cancers. These alterations are more prevalent in NSCLC, affecting approximately 4% of patients (Heist et al., 2016; Paul K Paik et al., 2015). Importantly, MetΔex14 has also been implicated in the development of resistance to EGFR tyrosine kinase inhibitors (EGFR TKIs) in patients with EGFR-mutant NSCLC (Suzawa, Offin, Schoenfeld, et al., 2019). The Cbl binding site required for Met ubiquitination is located within exon 14 (Peschard et al., 2001).

Furthermore, the oncogenic chromosomal fusion protein TPR-Met, lacks the entire extracellular and transmembrane domain, localized in the cytoplasm, also skips the exon 14 region and lacks the binding site for Cbl ubiquitin ligases. The transformation of cells in-vitro through loss of the Cbl binding site in the oncogenic TPR-Met fusion protein highlights the key role played by Met in cell transformation (Peschard & Park, 2007).

Additionally, *MET* gene fusions with genes that confer dimerization motifs to the Met kinase and the phosphatase gene *PTPRZ1* have been identified in pediatric glioblastomas (Bao et al., 2014) (Figure 1.11).

Recent advances have uncovered more complex roles of Met in cancer. For example, Met present in melanoma-derived exosomes can educate bone marrow progenitor cells towards metastasis (Peinado et al., 2012). High glucose can also activate Met in a ligand-independent manner in hepatocellular carcinoma, consequently increasing tumor burden (Topel et al., 2021). Surprisingly, a role for Met as a potential tumor suppressor has also been uncovered, with Met being essential for the recruitment of anti-tumor neutrophils to

the tumor microenvironment (Glodde et al., 2017). Conversely, Met can also disrupt the response to T cell immunotherapy by promoting an immunosuppressive tumor microenvironment (Spina et al., 2015).

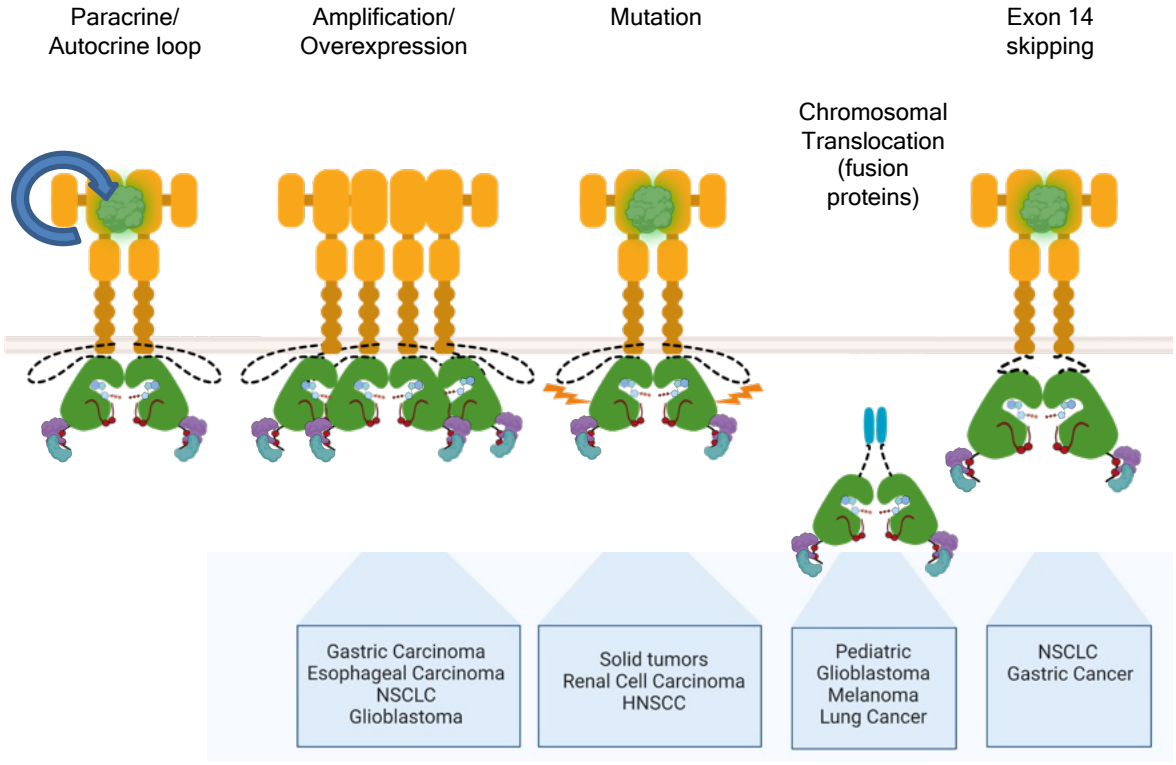


***Figure 1.11 Schematic Mechanisms of Met deregulation in cancers***

Various mechanisms contribute to the upregulation of Met signaling in cancers. Paracrine and autocrine stimulation by HGF leads to aberrant Met activation, *MET* copy number alterations, such as gains, can arise through polysomy or focal amplification, where chromosome 7, where *MET* is located, is inappropriately replicated point mutations in the kinase domain can lead to HGF-independent activation of the Met receptor, while other mutations can occur throughout the molecule, including the SEMA domain containing an HGF-binding site, with most of their functional consequences remaining unknown. Met can undergo fusion events with other proteins, occurring either through intra-chromosomal or inter-chromosomal fusions. A notable example is the TPR-Met fusion, which involves a cytosolic protein leading to constitutive activation of the Met kinase. Additionally, *MET exon 14* splice site alterations result in exon 14 loss, further contributing to Met deregulation in cancer.

Overall, the dysregulation of Met in cancers has been established as a significant driver of cancer progression, metastasis, and therapeutic resistance. The wealth of data obtained from human cancer cell lines, animal models, and human cancer patients has elucidated many ways in which Met activation can contribute to cancer development and progression. These discoveries have not only informed the development of targeted therapies but have also highlighted the complexity of Met signaling and the need for continued research in this area.

## 1.9 Therapeutic targeting of Met in cancer

Small molecule kinase inhibitors targeting Met have attracted substantial attention within the pharmaceutical industry, reflecting their growing importance. The field of Met-targeting therapies has witnessed remarkable progress in recent years, with significant advancements being made.

Type I inhibitors engage in a competitive binding with ATP at the active kinase site of Met. These inhibitors establish hydrogen bond interactions with specific residues, namely P1158, Y1159, and M1160, located in the hinge region of Met. This interaction occurs within an Asp-Phe-Gly (DFG)-in conformation (Schiering et al., 2003).

Crizotinib, a multi-targeted Type I inhibitor originally developed as a Met inhibitor, was found to also inhibit Anaplastic Lymphoma Kinase (ALK) and c-Ros oncogene 1 (ROS) RTKs (Heigener & Reck, 2014, 2018; Ou, 2012). Despite its wide range of targets, Crizotinib was approved for NSCLC based on its efficacy in ALK-rearranged patients (Desai et al., 2016; Ou, 2011; Shaw et al., 2017). Still, Met alterations are included as an on-label indication for the drug.

The FDA's approvals of capmatinib and tepotinib as Type I inhibitors represent significant breakthroughs in the treatment of metastatic non-small cell lung cancer (mNSCLC) with Met exon 14 skipping mutations. Capmatinib is indicated for patients with mNSCLC whose tumors exhibit Met exon 14 skipping, while tepotinib is approved for mNSCLC harboring Met exon 14 skipping alterations. The approvals were based on clinical trials: GEOMETRY mono-1 for capmatinib and VISION for tepotinib. These approvals mark the first targeted therapies specifically approved by the FDA for metastatic NSCLC patients with Met exon 14 skipping mutations (Mathieu et al., 2022).

In contrast, Type II inhibitors adopt an extended conformation and occupy a hydrophobic region adjacent to the ATP binding site, assuming a DFG-out conformation. Notably, cabozantinib is an example of a Type II inhibitor that not only targets Met but also demonstrates activity against VEGF receptor 2 (VEGFR2) (Scott et al., 2018).

Despite the initial optimism surrounding antibody-based therapies targeting HGF/Met, clinical trial results have been mixed. Yet, these therapeutics still hold promise. For instance, YYB-101, an HGF-neutralizing antibody, has shown potential in suppressing Met activation and inhibiting tumor growth in glioblastoma (Kim et al., 2017). Meanwhile, ficlatuzumab is an antibody that targets HGF, which is also implicated in promoting tumor growth and metastasis (D'Arcangelo & Cappuzzo, 2013).

Targeting Met is often trialed as a second- or third-line therapy following chemotherapy and other precision medicine strategies. Met-targeted treatments have also been developed in combination with other treatments, primarily those targeting EGFR in lung cancer (Gelsomino et al., 2014). The success of these therapeutics is not without challenges, as evidenced by the lack of clinical benefit when combining Onartuzumab

(Merchant et al., 2013), an anti-Met antibody, with bevacizumab in a phase II clinical trial involving patients with recurrent glioblastoma. Similarly, two phase III trials involving antibodies targeting Met were halted due to concerns regarding early mortality in patients. Nevertheless, this is an exciting time for research into Met-targeted therapies. Technological advancements and increasing knowledge of molecular oncology continue to spur innovation in the field. For instance, antibody mixtures targeting the Met receptor at multiple sites are currently under preliminary safety and response assessments in humans. If successful, this approach could provide a novel way of overcoming HGF-dependent and -independent modes of Met activation.

***Tabel 1 Targeted drugs for Met/HGF in clinical trials and/or approved***

| Therapy Name | Mechanism of Action | Description | References |
|---|---|---|---|
| crizotinib (Xalkori) | Met/ALK/ROS1 inhibitor | Used for the treatment of ALK-positive NSCLC, it has shown promising activity against MET amplification and exon 14 skipping mutations. | (Heigener & Reck, 2018) |
| cabozantinib (CaboMetyx) | Met/VEGFR2/RET inhibitor | A multi-kinase inhibitor, approved for the treatment of advanced RCC and HCC. Clinical trials are also ongoing for other solid tumors. | (Abou-Alfa et al., 2018; Gebreyohannes et al., 2016; Yakes et al., 2011) |
| tivantinib (ARQ 197) | Met inhibitor | Investigated in clinical trials for several cancers, including NSCLC, HCC, and gastric cancer. | (Kim et al., 2018; Maguire et al., 2021) |

| | | | |
|---|---|---|---|
| savolitinib (AZD6094) | Met inhibitor | Investigated in clinical trials for multiple cancer types, including NSCLC, RCC, and papillary renal cell carcinoma. | (Lu et al., 2020; Sequist et al., 2020) |
| capmatinib (Tabrecta) | Met inhibitor | Approved for the treatment of MET exon 14 skipping mutation-positive NSCLC. Investigated in clinical trials for other solid tumors. | (Mathieu et al., 2022; Jürgen Wolf et al., 2020) |
| glesatinib (MGCD265) | Met/VEGFR1-3/AXL inhibitor | Investigated in clinical trials for the treatment of several cancers, including NSCLC and gastric cancer. | (Cui et al., 2019; Engstrom et al., 2017) |
| merestinib (LY2801653) | Met/ALK/FLT3/ AXL/MST1R inhibitor | Investigated in clinical trials for various cancers, including NSCLC, HCC, and biliary tract cancer. | (He et al., 2019; Konicek et al., 2018) |
| AMG 337 | Met inhibitor | Evaluated in clinical trials for various cancers, including gastric cancer and head and neck squamous cell carcinoma. | (Hong et al., 2019; Van Cutsem et al., 2019) |
| emibetuzumab | Met antibody | A bivalent humanized IgG4 antibody, investigated in clinical trials for various cancers, including NSCLC, HCC, and gastric cancer. | (Camidge et al., 2016; Rosen et al., 2017; Scagliotti et al., 2020) |
| onartuzumab (MetMab) | Met antibody | A monovalent humanized IgG1 antibody, investigated in clinical trials for several cancers, including NSCLC, gastric cancer, and triple-negative breast cancer. | (Merchant et al., 2013) |

| | | | |
|---|---|---|---|
| rilotumumab (AMG 102) | HGF antibody | A human monoclonal antibody that targets HGF, investigated in clinical trials for various cancers, including gastric cancer and glioblastoma. | (Catenacci et al., 2017; Giordano, 2009; Zhu et al., 2014) |
| ficlatuzumab (AV-299) | HGF antibody | A humanized IgG1 monoclonal antibody, investigated in clinical trials for several cancers, including NSCLC and head and neck cancer. | (D'Arcangelo & Cappuzzo, 2013; Mok et al., 2016; Patnaik et al., 2014) |

## 1.10 Rational and unsolved questions

Despite the substantial progress in understanding the functional role of the Met receptor, many questions remain unanswered. The Met receptor is characterized by the longest JM domain among all 58 receptor tyrosine kinases, and the molecular and structural basis of its regulation and activation remains elusive. In particular, the role of the Met exon 14 region, which partially encodes the JM domain, has not been comprehensively studied.

Recent studies have reported that mutations in the *MET* gene leading to exon 14 skipping are prevalent in various types of cancer, such as NSCLC and secondary glioblastoma (sGBM). Although two small molecule inhibitors, tepotinib and capmatinib, have been FDA approved for the treatment of MetΔex14 patients (Mathieu et al., 2022), the precise molecular mechanisms underlying MetΔex14 activation and its role in cancer progression remain poorly understood.

An important unresolved question in the field is the role of the JM domain in modulating Met activation and the molecular consequences of exon 14 skipping. It is not clear whether the loss of the exon 14-encoded region is sufficient for constitutive Met activation,

or if additional factors contribute to enhanced signaling. Furthermore, the structural organization of the JM domain and its potential impact on Met dimerization and downstream signaling are not well understood.

Another aspect warranting further investigation is the role of post-translational modifications, such as phosphorylation, in regulating the activity of the Met receptor. While some phosphorylation sites have been identified in the exon 14 region, their functional significance and the kinases responsible for their phosphorylation have not been fully elucidated.

A better understanding of the molecular mechanisms governing Met activation, particularly in the context of exon 14 skipping, is crucial for the development of more effective therapeutic strategies targeting Met in cancers. Identifying the structural determinants of Met activation and regulation, as well as the functional implications of post-translational modifications, will provide valuable insights into the complex biology of Met signaling and its role in cancer progression. Furthermore, a comprehensive understanding of MetΔex14 regulation and activation will contribute to the rational design of targeted therapies, ultimately improving patient outcomes.

# CHAPTER 2 – STRUCTURAL BASIS OF MET EXON 14 SKIPPING IN CANCERS

The Met receptor tyrosine kinase and its unique ligand HGF play a pivotal role in organ morphogenesis during embryonic development and liver regeneration in adulthood. Met possesses the longest Juxta-membrane domain among all 58 receptor tyrosine kinases, and remains structurally uncharacterized. This domain is partially encoded by exon 14 in *MET* and mutations at splice donor or acceptor motifs in cancer can result in the skipping of exon 14 (MetΔex14) generating an in frame Met RTK protein. These type of mutations are prevalent in various types of cancer and occur in ~4% NSCLC (Jee et al., 2022; Network, 2014) and ~17% of secondary GBM (Hu et al., 2018). MetΔex14 generating mutations are found in early-stage and late-stage NSCLC and are predominantly mutually exclusive with mutations in EGFR or K-Ras found in NSCLC (Bubendorf et al., 2017). In early stage NSCLC MetΔex14 is non amplifies but in late-stage NSCLC MetΔex14 is frequently amplified and can occur as a mechanism of resistance to EGFR therapy (Suzawa, Offin, Lu, et al., 2019). Tepotinib and capmatinib, two small molecule inhibitors, have recently been FDA approved for the treatment of MetΔex14 patients in 2021 and 2022, respectively (Paik et al., 2020; J. Wolf et al., 2020). Despite the effectiveness of those inhibitors for Met kinase patient response is variable highlighting a poor understanding and lack of companion diagnostics reflecting MetΔex14 dependence. The role of MetΔex14 in cancer is still not well understood. In metastatic NSCLC mutations that give rise to exon 14 skipping are found at the highest frequency when compared to mutations that result in substitution of the Cbl binding site at Y1003 within exon 14, or mutations within residues and D1228, Y1230 in the kinase activation loop (Figure 2.1 a).

## 2.1 MetΔex14 activation requires lower level of HGF

In order to understand the role of exon 14 deletion in the activation of the Met receptor tyrosine kinase, we investigated whether deletion of exon 14 alone results in direct activation of Met signaling, bypassing the requirement for its ligand, HGF. To accomplish this, we utilized a naturally occurring MetΔex14 cell line (H596) as well as mutant HeLa and DLD-1 clones generated using CRISPR/Cas9 technology to convert WT Met to MetΔex14.

To examine Met RTK activation and response to ligand we tested various concentrations of HGF on Met tyrosine phosphorylation within the activation loop (Y1234/35) and carboxy terminal substrate tyrosine Y1349 required for substrate engagement. Our results revealed that phosphorylation of Met Y1234/35 in the kinase activation loop and Y1349 in the C-tail were both dependent on HGF in all cell lines tested, indicating that there was no evidence of constitutive activation of MetΔex14 in the absence of HGF. Notably, we observed that a low physiological concentration of HGF (10 U) was sufficient to trigger robust phosphorylation of Y1349 in MetΔex14 cells, resulting in a significant reduction in the potency required for HGF to activate Met signaling (Figure 2.1 b). This observation was also evident in 3D cell invasion assay (Golenar, 2022). These findings are particularly relevant in the clinical setting, as 10U of HGF falls within the upper limit range observed in the plasma of cancer patients (Golenar, 2022).

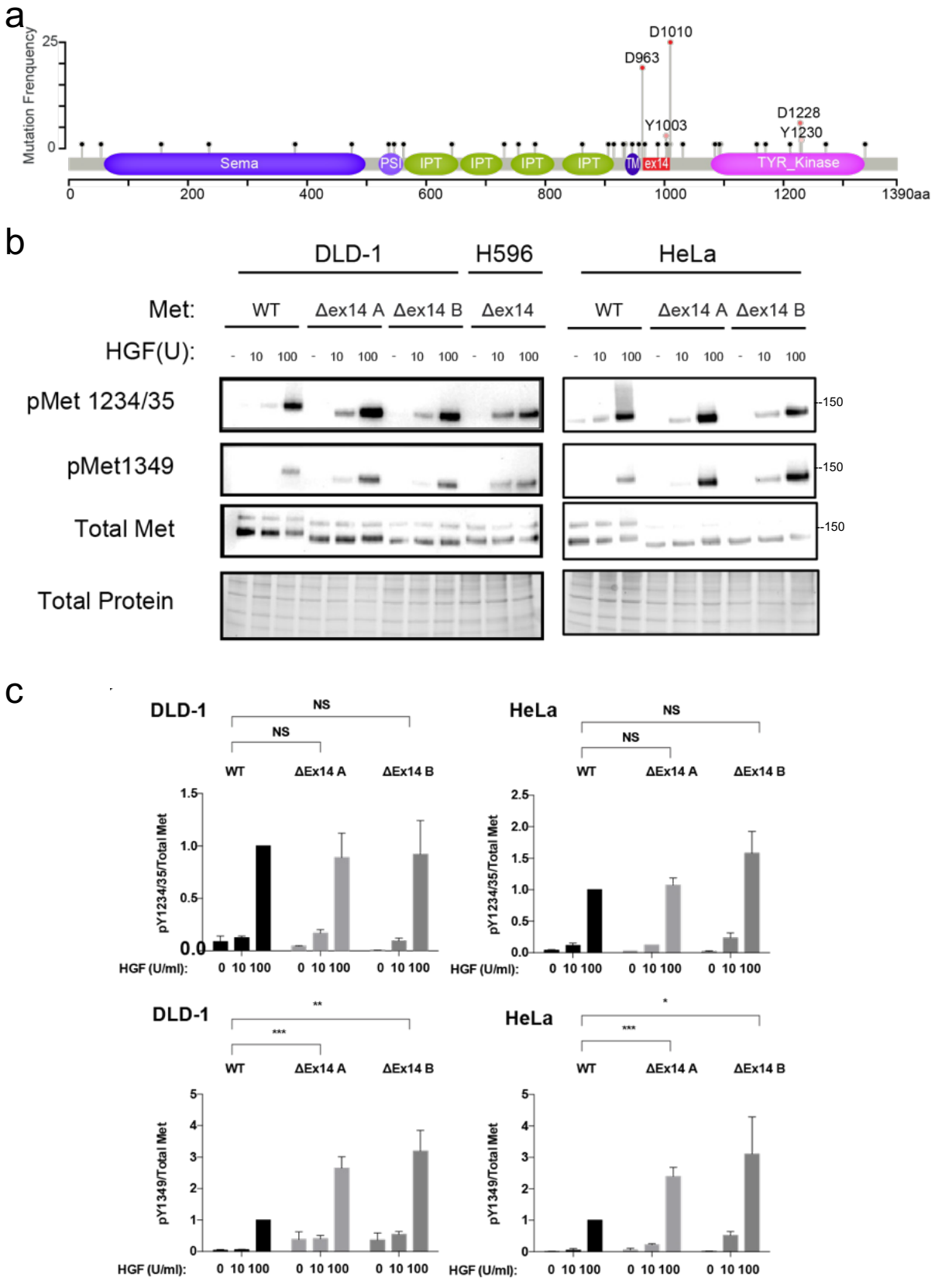
a
Mutation Frenquency
25
0
D1010
D963
Y1003
D1228
Y1230
Sema
PSI
IPT
IPT
IPT
IPT
TM
ex14
TYR_Kinase
0
200
400
600
800
1000
1200
1390aa
b
DLD-1
H596
HeLa
Met:
WT
Δex14 A
Δex14 B
Δex14
WT
Δex14 A
Δex14 B
HGF(U):
- 10 100 - 10 100 - 10 100 - 10 100 - 10 100 - 10 100 - 10 100
pMet 1234/35
pMet1349
Total Met
Total Protein
150
150
150
c
DLD-1
NS
NS
WT
ΔEx14 A
ΔEx14 B
pY1234/35/Total Met
1.5
1.0
0.5
0.0
HGF (U/ml):
0 10 100 0 10 100 0 10 100
HeLa
NS
NS
WT
ΔEx14 A
ΔEx14 B
pY1234/35/Total Met
2.5
2.0
1.5
1.0
0.5
0.0
HGF (U/ml):
0 10 100 0 10 100 0 10 100
DLD-1
**
***
WT
ΔEx14 A
ΔEx14 B
pY1349/Total Met
5
4
3
2
1
0
HGF (U/ml):
0 10 100 0 10 100 0 10 100
HeLa
*
***
WT
ΔEx14 A
ΔEx14 B
pY1349/Total Met
5
4
3
2
1
0
HGF (U/ml):
0 10 100 0 10 100 0 10 100

***Figure 2.1 MET mutations in NSCLC, and effects on signaling***

(a) *MET* mutations in NSCLC: Mutations in the *MET* gene in metastatic non-small cell lung cancer (NSCLC) are designated using mature Met numbering. The most commonly observed mutations involve exon junction skipping at positions D963 and D1010 (Jee et al., 2022).
(b) Met phosphorylation in CRISPR-Cas9 engineered cells and in response to HGF: HeLa and DLD-1 cells were genetically modified using CRISPR-Cas9 technology to endogenously express wild-type (WT) Met, Δex14 clones, and natural Δex14 H596 NSCLC cells. Cells were stimulated with the indicated concentration of HGF for 5 minutes. Subsequently, Met tyrosine phosphorylation levels were assessed using immunoblotting of cell lysates, using antibodies that recognise pY1234/35 (located in the kinase activation loop), pY1349 (located in the C-tail) and total Met. A representative blot from three independent experiments (N=3) are shown and quantification provided for n=3 experiments.
(c) Quantification of (b). The Y1234/35 phosphorylation levels were not found to be significant between Met WT and MetΔex14 clones in DLD-1 and HeLa cells. In contrast, pY1349 levels were significantly different. Two-way ANOVA, mean ± SEM, *p < 0.05, **p < 0.01, ***p < 0.001.

## 2.2 The formation of a symmetrical Met kinase dimer for activation is incompatible with Y1349 phosphorylation

Multiple crystals of the Met kinase domain with various TKI have been solved yet a full understanding of activation of the Met kinase and subsequent tyrosine phosphorylation of C-tail tyrosines is still poorly understood. To understand how loss of exon 14 may contribute to enhanced phosphorylation of Y1349, we analysed previously deposited crystal structures of the Met kinase domain and those with the C-tail. One structure (PDB: 2RFN) revealed a symmetrical kinase dimer formed by an α-helical dimer in the C terminus of the juxtamembrane region. This dimer on closer examination is facilitated by a salt bridge between residues E1061 and H1068 within the α-helix (Figure 2.2 a-d). A comparison between crystal structures of the active and inactive states of Met kinase domain monomers unveiled an initial engagement between the α-C helix and the

juxtamembrane α-helix through hydrophobic interactions (Figure 2.2 g-i). Our extended analysis of the dimer structure proposes that the α-helical dimer within the C-terminus of the juxtamembrane domain serves to dimerize the α-C helix of the kinase domain.

Autoinhibition of protein kinase activity by the JM region has been reported for several RTKs, such as FLT3 (Griffith et al., 2004), KIT (Mol et al., 2004), MuSK (Till et al., 2002), and Ephrin family RTKs (Wybenga-Groot et al., 2001). In each case, sequences in the JM region make extensive contacts with several parts of the kinase domain, including the α-C helix (Figure 4.1), and stabilize an autoinhibited conformation.

To directly test this hypothesis, we conducted an experiment using T47D cells which have diminished Met expression. We utilized the sleeping beauty transposase to stably express Met-WT, MetΔex14, and the Met-H1068D mutants. Our findings demonstrated that in this particular cell line, Y1234/35 phosphorylation was observed even without HGF stimulation. However, we observed that Y1349 phosphorylation remained dependent on HGF stimulation. Furthermore, we observed that the H1068D mutant exhibited reduced capacity to induce Y1349 phosphorylation when exposed to high concentrations of HGF. This crucially indicates that H1068 is indeed a critical site for Met activation (Figure 2.2 j).

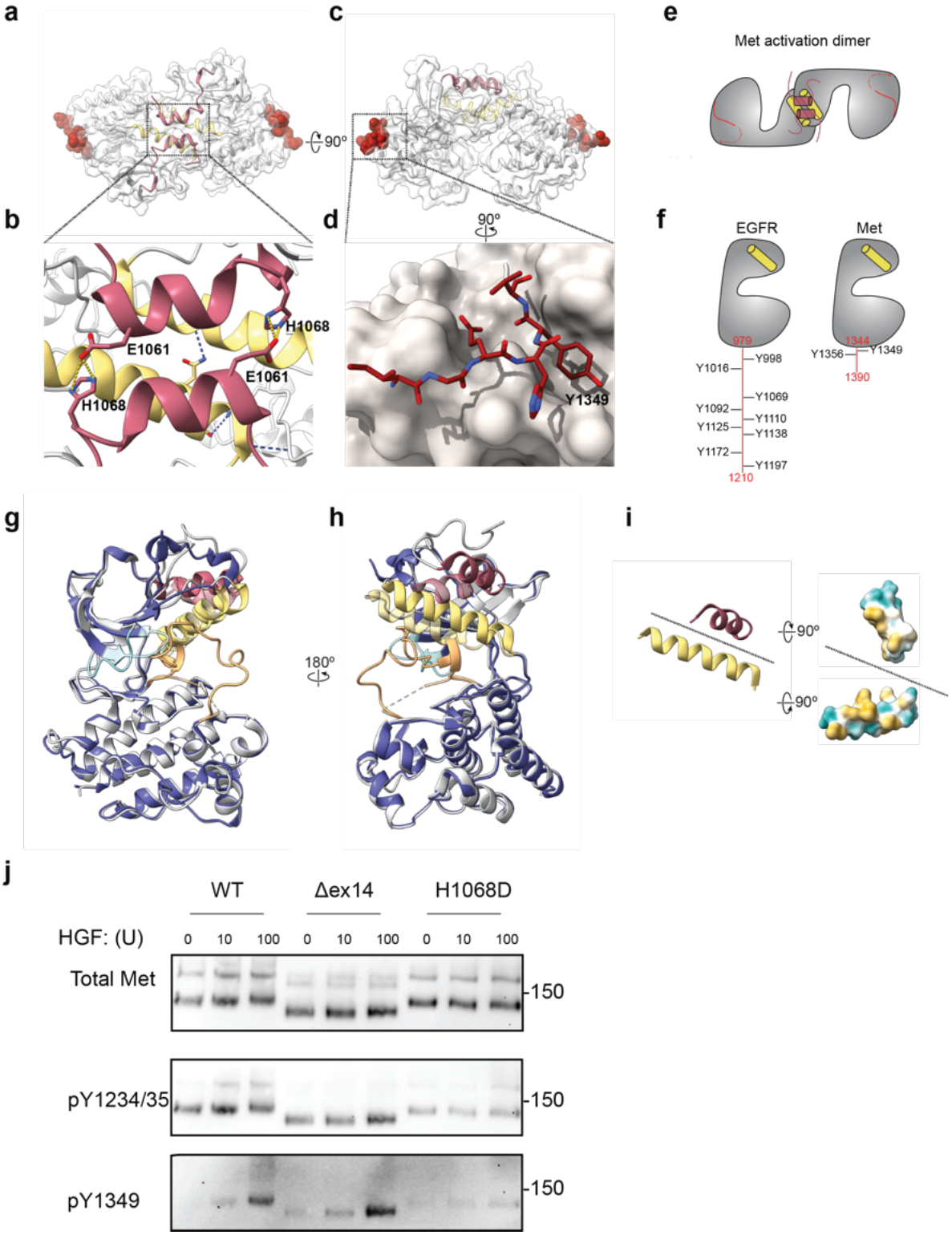


***Figure 2.2 Symmetric Met kinase activation dimer is incompatible with Y1349 phosphorylation.***

(a-d) PDB: 2RFN (Bellon et al., 2008) crystal structure of dimeric Met receptor with compound AM7. Juxtamembrane-C terminal α-helix (colored in red) and the α-C helix in the kinase domain (colored in yellow). Note that the juxtamembrane-C terminal α-helix dimerizes through (b) E1061 and H1068 salt bridges. (d) Met C-tail docked back to the kinase C-lobe. (e) Schematic view of the Met receptor kinase dimer. (f) Schematic view of the comparison between EGFR and Met receptors, featuring a short Met C-tail. (g-h) Structure comparison of the Met receptor tyrosine kinase domain between PDB: 3Q6U (active, shown in purple) (Rickert et al., 2011) and PDB: 2G15 (inactive, shown in gray) (Wang et al., 2006). In 3Q6U, the activation loop is extended and unstructured, while the P-loop is ordered (light blue opaque). In contrast, 2G15 adopts a closed activation loop (brown) with a disordered P-loop (light blue). The juxtamembrane-C terminal a-helix is colored in red, and the α-C helix in the kinase domain is colored in yellow. (i) Hydrophobic interactions between the juxtamembrane-C terminal helix and α-C helix in the kinase domain are shown in the 2G15 structure. (j) T47D stable cell lines expressing Met, MetΔEx14, and the H1068D mutant using the sleeping beauty transposase. Cells were stimulated with the indicated concentration of HGF for 5 minutes. Subsequently, Met tyrosine phosphorylation levels were assessed using immunoblotting of cell lysates, using antibodies that recognise pY1234/35 (located in the kinase activation loop), pY1349 (located in the C-tail) and total Met.

Additionally, the dimeric crystal complex demonstrated that the Met C-tail at Y1349 is docked back into the kinase domain where Y1349 is located within a hydrophobic pocket made by F1168, F1184 and F1216. Notably, when compared to the ERBB family of proteins, which typically possess C-tails averaging 250-300 amino acids in length, the C-tail of Met is short, in comparison consisting of only 46 amino acids (Figure 2.2 f). This proposed structure (Figure 2.2 e) suggests that the dimeric structure of the Met kinase may be unable to readily phosphorylate Y1349 at the junction of the kinase domain within the short Met C-tail.

## 2.3 Met exon 14 region stabilizes through a β-sandwich tetramer

From this proposed structure of the symmetrical Met dimer kinase, it became evident that the presence of Y1349 phosphorylation at the junction of the kinase domain is incompatible with this dimeric state.

we employed a crosslinking approach to investigate the formation of Met and MetΔex14 dimers or tetramers in response to HGF stimulation within a cellular context. While we predominantly observed monomeric bands, it is important to note that crosslinking provides a snapshot of the Met multimeric state and may underestimate the extent of multimeric formation over time. Nevertheless, our results suggest that under high concentrations of HGF, MetΔex14 exhibits a higher propensity to form tetramers compared to the wildtype Met (Figure 2.3).

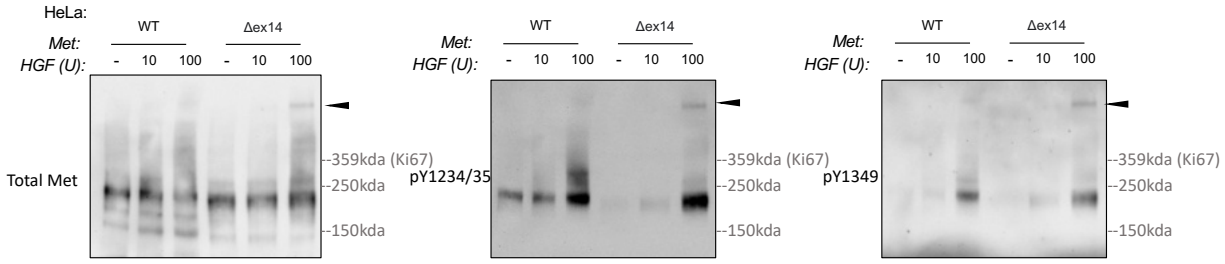


***Figure 2.3 HGF induced Met multimer detection by DSP crosslinking***

HeLa cells harboring WT Met, Δex14 clone were stimulated with the indicated concentration of HGF for 5 minutes. Subsequently, 0.2 mM DSP crosslinker was added and incubated at 37 degrees for 30 minutes. The crosslinking reaction was then stopped by adding 1 M Tris (pH=7.4), Met tyrosine phosphorylation levels were assessed using immunoblotting of cell lysates without reducing reagent, using antibodies that recognise pY1234/35 (located in the kinase activation loop), pY1349 (located in the C-tail) and total Met. A representative blot from three independent experiments (N=3) are shown. The arrow on the blot indicates the band corresponding to tetrameric Met (~680 kDa).

## 2.4 Met exon 14 region is mostly unstructured

To understand this better and because Y1349 displays elevated phosphorylation in MetΔex14 (Figure 2.1 b, c) we proceeded to investigate the role of the exon 14 region in the activation of the Met receptor.

Since the extracellular domain remains unchanged in MetΔex14 when compared to Met-WT expressing cell lines, we reasoned that both RTKs should engage with ligand, HGF, in a similar fashion. Furthermore, we found that loss of exon 14 alone does not result in the activation of the kinase domain of MetΔex14 in the absence of HGF. This is consistent with the current model for activation of Met whereby HGF engagement with the Met extracellular domain promotes the formation of a Met dimer followed by activation and trans-phosphorylation of the kinase activation loop.

Phosphorylation at Y1349 is elevated in MetΔex14 cells when compared to WT Met even in response to sub-physiological levels of HGF (Figure 2.1 b, c). Hence, we hypothesized that Met exon 14 may act to modulate Met kinase domain trans-phosphorylation. To understand this, we synthesized a 47-amino acid peptide corresponding to Met exon 14: (AA:964-1010). We utilized AlphaFold (Jumper et al., 2021), a computational modeling tool now used to predict many structures, to generate structural models of the Met exon 14 to fit data generated by with Small-angle X-ray scattering (SAXS). The Met exon 14 region is highly distinctive, characterized by a considerably lower population in the Multiple Sequence Alignment (MSA) dataset, typically fewer than 35 per position (Figure 2.4 f). AlphaFold has made a relatively lower confidence level for a dimeric structure (pLDDT=50.1, pTM=0.329), (Figure 2.4 b, c) as well as random coil monomer. Interestingly, the SAXS profile does not align well with a large $\chi^2$ when considering the

single model monomer or dimer state. However, employing a multi-state SAXS approach involving 89.1% random coil and 10.9% dimer content significantly improves the fit, yielding a reduced $\chi^2$ value of 5.93. This suggest that an isolated exon 14 peptide when examined in vitro, is largely unstructured.

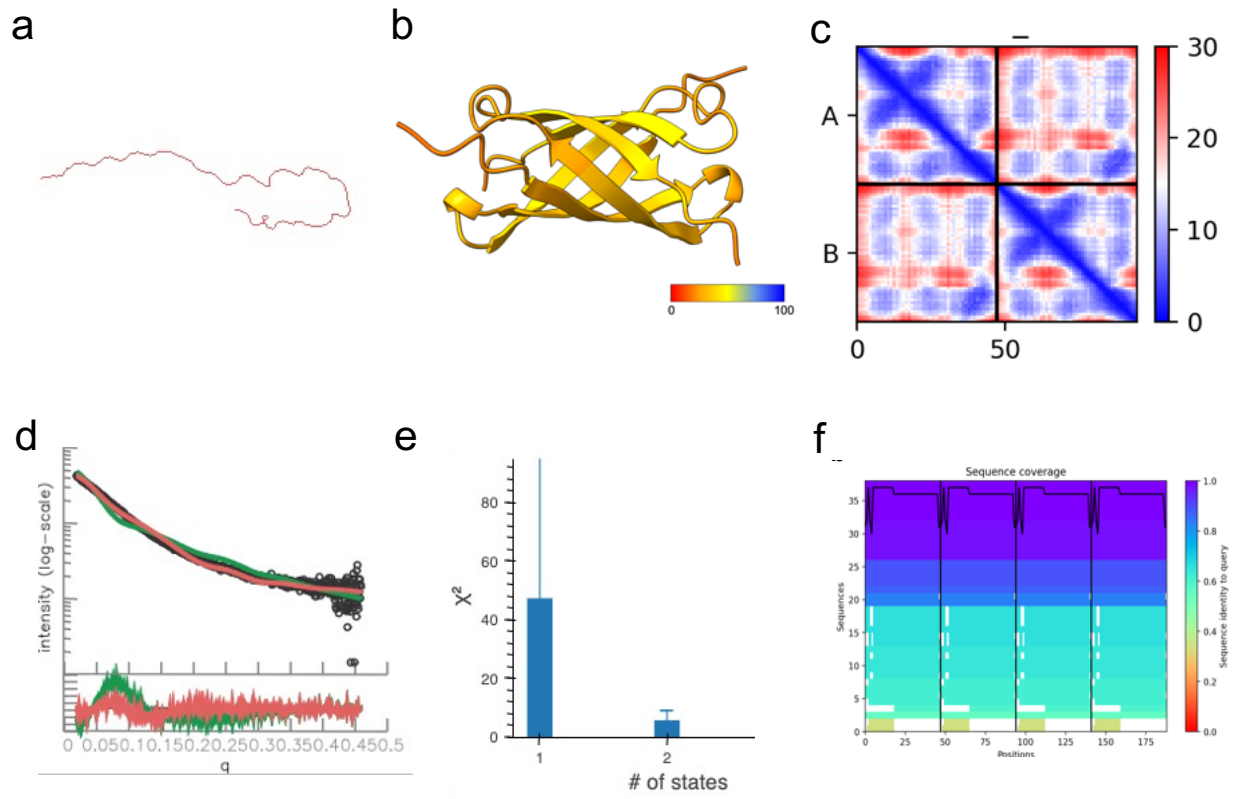


***Figure 2.4 Characterization and prediction of Met exon 14 structure***

(a) Predicted monomeric AlphaFold Met exon 14 structure colored by predicted per-residue scores on the lDDT-Cα metric (pLDDT) score.
(b) Predicted dimeric AlphaFold Met exon 14 structure colored by predicted per-residue scores on the lDDT-Cα metric (pLDDT) score, highlighting regions of low confidence.
(c) Heat map depicting the predicted alignment error for the predicted dimeric Met exon 14 structure.
(d) SAXS profile of experimental data is colored in black while predicted monomeric random coil in red and dimeric structure in blue.
(e) $\chi^2$ value SAXS profile fitting using single model versus multi-model approach.
(f) Multiple Sequence Alignment (MSA) coverage of the Met exon14 sequence using AlphaFold V2.3.1. Featuring a low level of similarity.

## 2.5 Computational prediction of Met exon 14 region tetramerization

We next explored the possibility of the Met exon 14 peptide adopting a tetrameric structure. This inquiry was also prompted by AlphaFold's prediction, which indicated a predominant composition of β sheets and exhibited a high-confidence assessment (pLDDT=79.9, pTM=0.792).

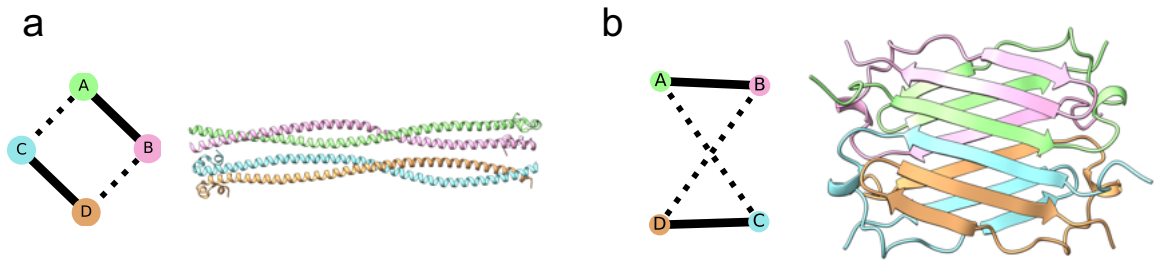


***Figure 2.5 Structural comparison of TPR and Met exon 14 tetramer***

(a) Crystal structure (PDB ID: 5TO6) diagram of the TPR tetramer depicting the four chains and their respective interfaces. Node colors correspond to the predominant colors of the chains. Smaller interfaces, with buried solvent-accessible surface area less than half of the largest interface, are indicated with dotted lines.
(b) Predicted tetrameric structure of Met exon 14 using AlphaFold V2.3.1. Node colors match the predominant colors of the chains. Smaller interfaces, with buried solvent-accessible surface area less than half of the largest interface, are indicated with dotted lines.

Notably, the exon 14 tetramer bears a striking similarity to a structural model proposed for the activation mechanism of the Met kinase domain by TPR (Figure 2.5 a) (Pal et al., 2017), the *MET* fusion partner in the oncogenic TPR-Met complex. Notably, TPR comprises a continuous 124-residue α-helix that constructs an anti-parallel tetramer using two leucine zipper-containing parallel coiled coils. Both TPR and exon 14 exhibit comparable dihedral symmetry (Figure 2.5).

## 2.6 Proposed model of Met activation

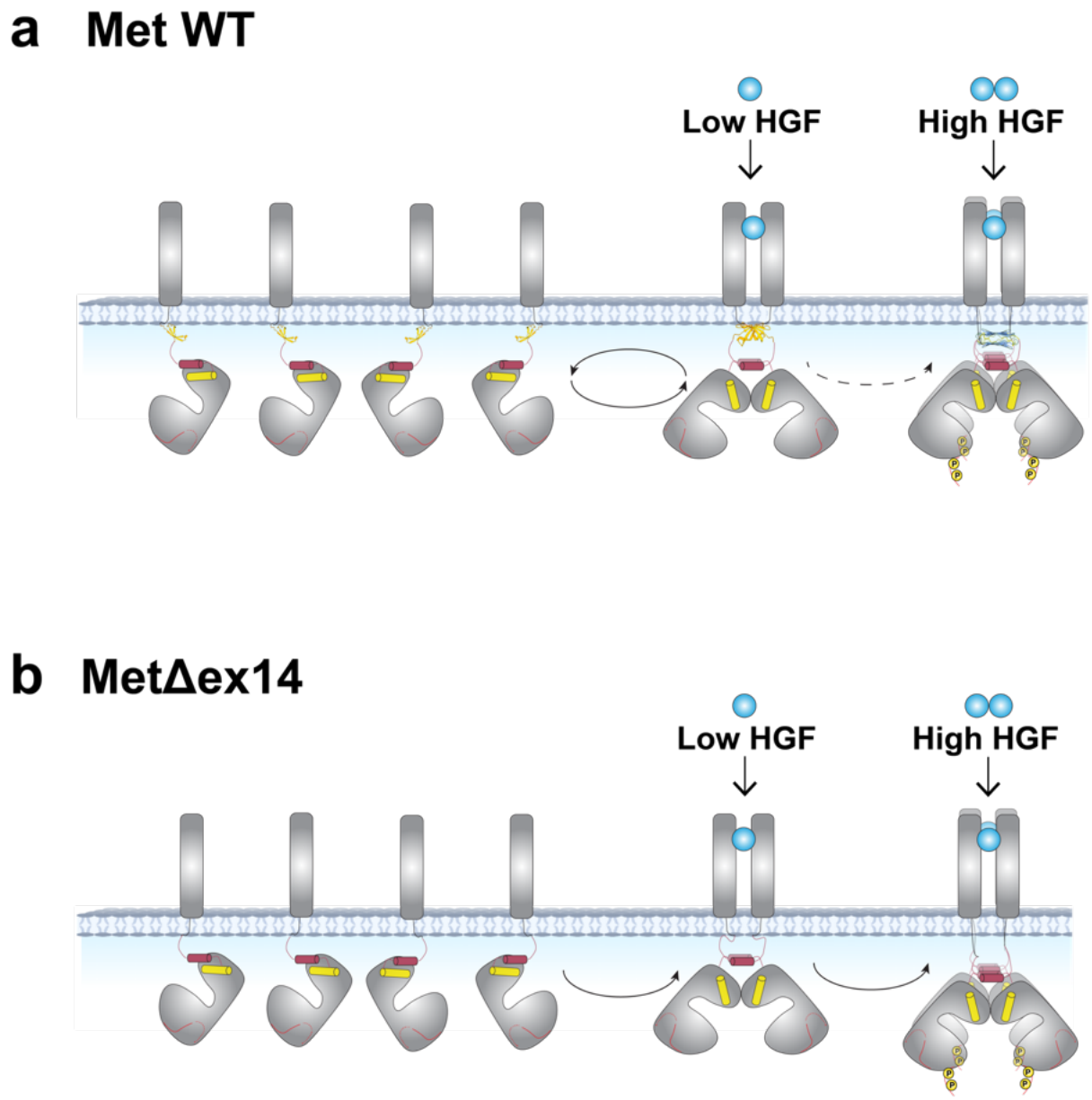


***Figure 2.6 Proposed model for Met WT and MetΔex14 activation***

(a) In Met-WT cells. At low concentrations of HGF, Met activity is weak due to inefficient exon 14 dimerization, Only under high HGF concentration, stable tetrameric Met can form. (b) MetΔex14, lacking the exon 14 region, escapes negative regulation. At low HGF concentration, it may slowly transition into a tetrameric state, and at high HGF concentration, stable tetrameric Met is formed.

Although intriguing, exon 14 doesn't seem to exhibit self-assembled characteristics (Figure 2.4). Instead, we posit that the formation of the exon 14 tetramer might necessitate additional efforts to overcome the inhibitory influence of the exon 14 random coil. In wild-type cells, the elevated concentration of HGF-induced extracellular domain tetramerization holds the potential to transcend this barrier and facilitate the assembly of the exon 14 tetramers and enable phosphorylation and subsequent activation of the Met C-tail, the formation of an exon 14 tetramer becomes necessary. Hence, we predict that deletion of exon 14 allows for the bypassing of this regulatory process (Figure 2.6).

Based on our data and observations, we conclude that the formation of a tetramer through HGF and the exon 14 region serves as an HGF sensing factor in the activation of the Met receptor. This novel insight provides valuable knowledge regarding the regulatory mechanisms that underlie Met signaling and opens up new avenues for investigating the functional implications of Met tetramerization in diverse cellular processes. By elucidating the significance of the exon 14 region, our findings contribute to a better understanding of the overall activation mechanism of the Met receptor and its profound impact on downstream signaling cascades.

# CHAPTER 3 – A POOLED KINOME/DRUGGABLE CRISPR SCREEN IDENTIFIES CELL CYCLE CONTROL OF THE MET RTK

## 3.1 A pooled kinome/druggable CRISPR screen of surface Met in DLD-1 cells

Expanding on the findings and insights obtained from our structural investigations, we aimed to explore additional mechanisms that contribute to the heightened levels of Met protein activation in cancer.

In our quest to identify key regulators of Met protein stability and hence Met protein levels, we developed a Fluorescence-Activated Cell Sorting (FACS)-based pooled CRISPR screen using DLD-1 colorectal cancer cells. Elevated Met protein levels in colorectal cancers, even without direct mutations in the Met RTK transgene, contribute to enhanced tumorigenicity and make DLD-1 cells an appropriate model for screening potential Met regulators (Seiden-Long et al., 2008). This cell line was also chosen due to its intermediate Met protein levels compared to HeLa and T47D cells, which serve as positive and negative controls, respectively, for Met protein levels. This enabled the identification of both positive and negative regulators by selecting cells with enhanced or decreased levels of Met protein on the cell surface. We confirmed similar trends in these levels through both western blot analysis and FACS, demonstrating that FACS is capable of differentiating surface protein levels of Met (Figure 3.1 a).

We assessed the effectiveness of sgRNAs in editing DLD-1 cells and evaluated the associated time frame. By employing sgRNA targeting Met, we observed a decrease in Met levels through Flow cytometry analysis using a PE conjugated Met antibody (Clone # 95106, R&D) that recognises surface Met levels. Furthermore, over time, the cell population depleted of Met increased, indicating that Flow cytometry is capable of sorting

cells based on their surface Met levels. Notably, the depletion of Met did not adversely affect the viability of DLD-1 cells in culture (Figure 3.1 b).

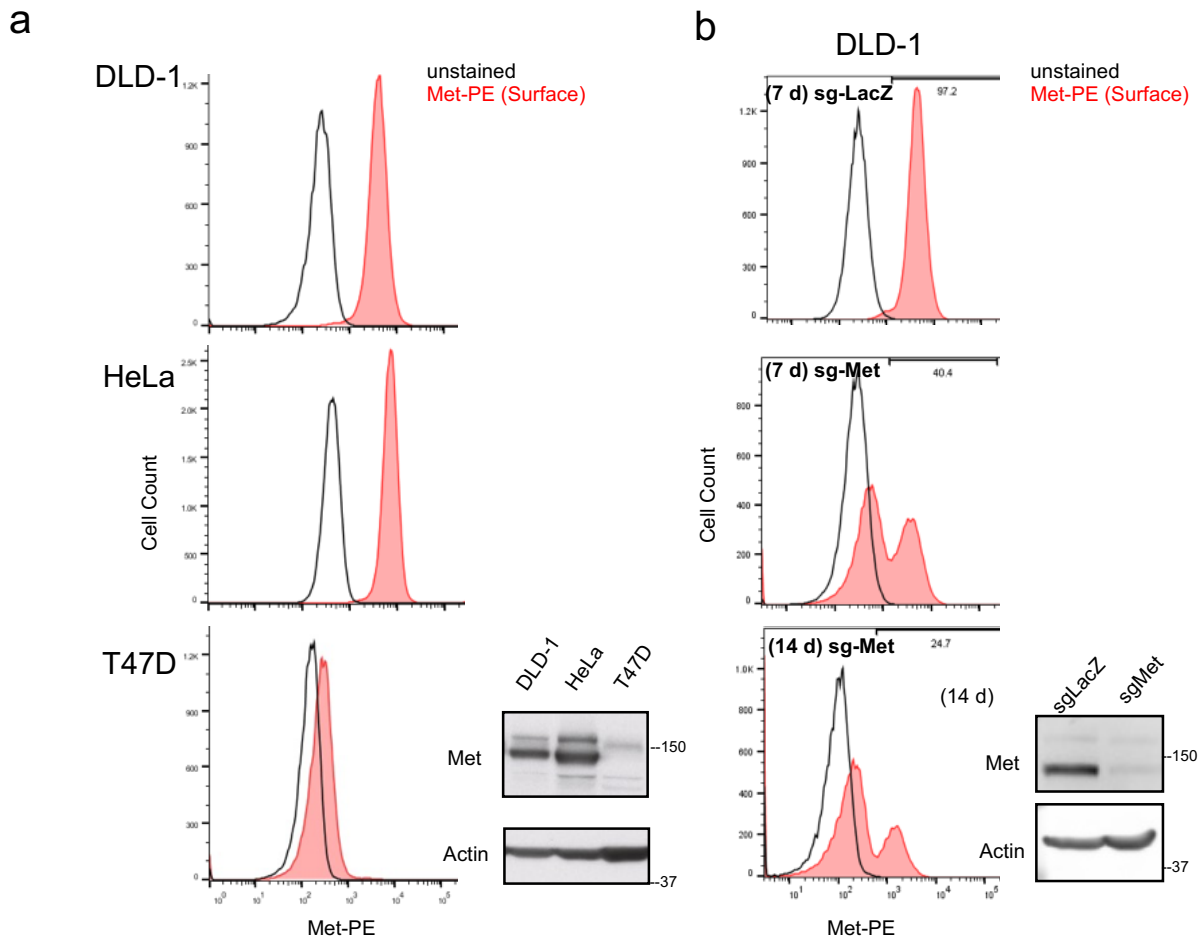


***Figure 3.1 Pre-CRISPR screen optimization***

(a) Surface Met levels detected by flow cytometry positively correlate with total Met levels in various cell lines.
(b) The CRISPR/Cas9 system demonstrates exceptional efficiency in DLD-1 cells. (Middle panel) Seven days after infection, a $Met^{null}$ population is identified using flow cytometry. (Bottom panel) 14 days after infection, the $Met^{null}$ population expands.

For screening, we utilized a custom-made sgRNA library targeting FDA-approved drug targets and the kinome, encompassing 11,991 sgRNAs targeting 1,977 genes, at an average of 6 sgRNAs per gene. After infecting DLD-1 cells with the library at a low

multiplicity of infection (MOI), we maintained cells in culture for 7 days. The cells were then sorted into two populations based on high or low Met protein levels (~1 million cells per bin). Genomic DNA was extracted from each population, and the sgRNAs were PCR amplified and sequenced. To ensure the fidelity of sgRNA representation throughout the experiment, we compared the abundance of sgRNAs from the plasmid library to those amplified from genomic DNAs at 3 days post-infection (T0) and 7 days post-infection (T1), observing a high correlation (R^2=0.722, R^2=0.702, respectively).

The sgRNA-encoding regions were then PCR amplified, sequenced, and subjected to Next Generation Sequencing (NGS). We followed this by mapping the results back to the original sgRNA library design to assess the representation of sgRNA in each population. Using Model-based Analysis of Genome-Wide CRISPR-Cas9 Knockout (MAGeCK) (Li et al., 2014), we ranked the hits based on the relative abundance of the Met-Low and Met-High populations for each CRISPR target, considering significance values calculated by comparing six CRISPR targets against the same gene (Figure 3.2).

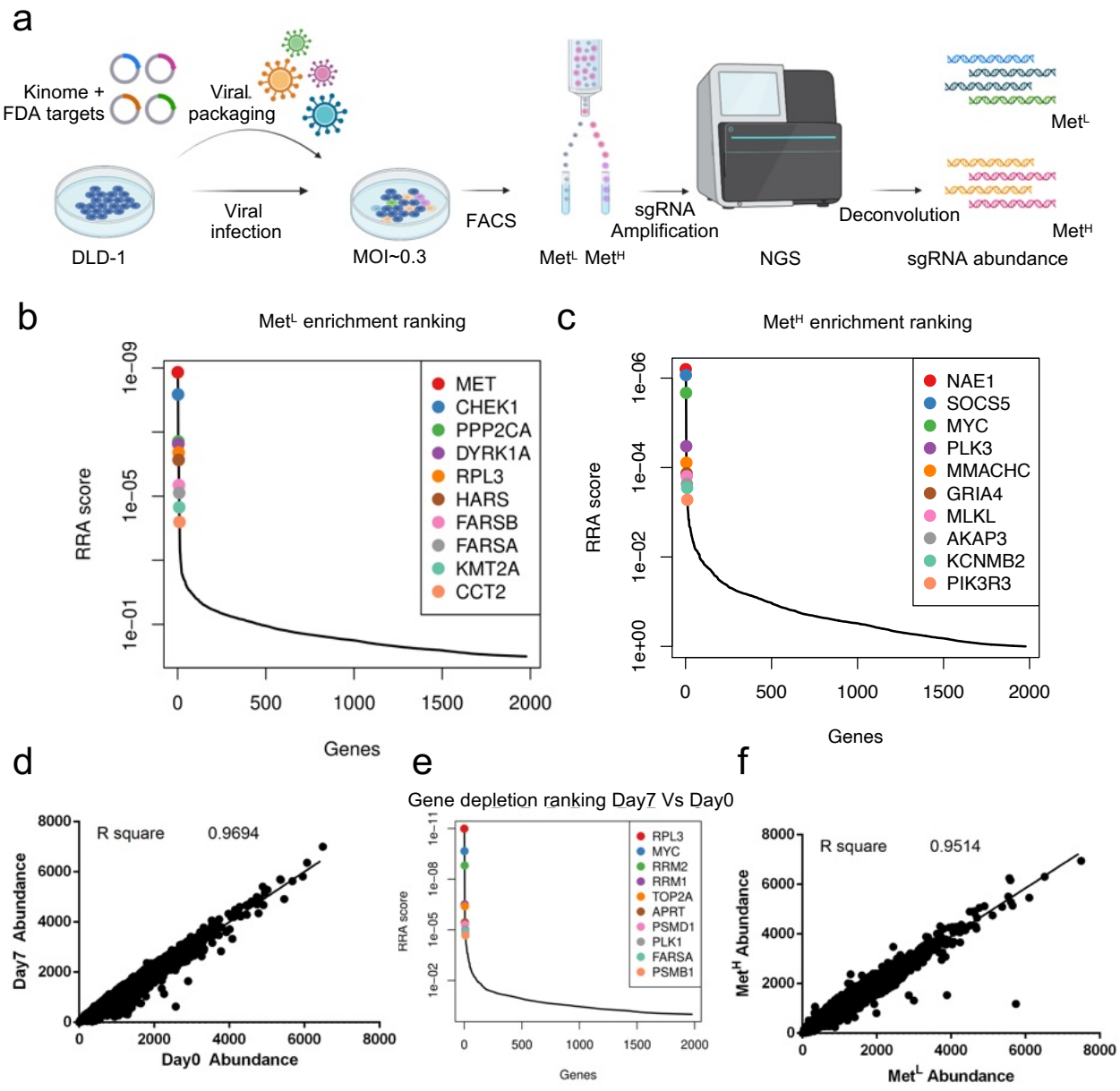


***Figure 3.2 A pooled kinome/druggable CRISPR screen of surface Met regulators***

(a) Schematic representation of CRISPR screen: A custom-synthesized CRISPR library was transduced into DLD-1 cells via viral vectors at a low multiplicity of infection (MOI). After 7 days, cells expressing the Met surface protein were identified and sorted using FACS. The genomic DNA was then extracted from these two populations ($Met^{high}$ and $Met^{low}$), and the incorporated sgRNAs were amplified and subjected to next-generation sequencing.

(b) MAgeCK analysis of $Met^{Low}$ population: The sgRNAs enriched in the $Met^{Low}$ population were identified and ranked based on their significance values using MAgeCK analysis. The x-axis represents the ranking, while the y-axis represents the significance value.

(c) MAGeCK analysis of $Met^{High}$ population: Similarly, the sgRNAs enriched in the $Met^{High}$ population were identified and ranked using MAGeCK analysis. The x-axis signifies the ranking, while the y-axis represents the significance value.
(d) Correlation of sgRNA Abundance in unsorted populations: The sgRNAs identified in the unsorted population, both at the beginning (Day 0) and after 7 days (Day 7), were plotted according to their abundance, demonstrating a high correlation between the two time points.
(e) Ranking of depleted genes: Using MAGeCK analysis, the genes that were depleted between Day 0 and Day 7 in the unsorted population were identified and ranked based on the abundance of their corresponding sgRNAs.
(f) By comparing the abundance of sgRNAs from unsorted populations of Day 0 and Day 7, hits that show a deviation from the high level of correlation were identified. These exceptions indicate sgRNAs that potentially regulate Met.

From this unbiased screen, we identified more than a dozen of potential positive regulators of Met protein levels, including Met itself. Moreover, individual sgRNAs targeting Met were found to be enriched in the $Met^{Low}$ population and depleted in the $Met^{High}$ population. The top-ranked genes induced the most pronounced shift of cells towards either the $Met^{Low}$ (Table 2) or $Met^{High}$ (Table 3) population.

***Table 2 Positive regulators identified from CRISPR screen***

| Gene ID | sgRNA | Score | p-value | FDR | Rank | Good sgRNA | LogFC |
|---|---|---|---|---|---|---|---|
| MET | 6 | 1.35E-09 | 2.50E-06 | 0.001238 | 1 | 4 | -0.85143 |
| CHEK1 | 6 | 6.69E-09 | 2.50E-06 | 0.001238 | 2 | 5 | -0.65786 |
| PPP2CA | 6 | 1.99E-07 | 2.50E-06 | 0.001238 | 3 | 3 | -0.55198 |
| DYRK1A | 6 | 2.36E-07 | 2.50E-06 | 0.001238 | 4 | 6 | -0.90201 |
| RPL3 | 6 | 4.37E-07 | 7.51E-06 | 0.00297 | 5 | 5 | -0.7863 |
| HARS | 6 | 7.37E-07 | 1.25E-05 | 0.004125 | 6 | 6 | -0.60581 |
| FARSB | 6 | 4.51E-06 | 2.75E-05 | 0.007779 | 7 | 5 | -0.32785 |
| FARSA | 6 | 7.90E-06 | 3.76E-05 | 0.009282 | 8 | 6 | -0.5546 |
| KMT2A | 6 | 2.24E-05 | 0.000118 | 0.025853 | 9 | 4 | -0.37792 |
| CCT2 | 6 | 6.39E-05 | 0.000323 | 0.058056 | 10 | 5 | -0.39286 |
| ATR | 6 | 6.41E-05 | 0.000323 | 0.058056 | 11 | 4 | -0.24605 |
| CARD10 | 6 | 0.000184 | 0.001049 | 0.172855 | 12 | 6 | -0.25725 |
| HAL | 6 | 0.000477 | 0.002752 | 0.418507 | 13 | 4 | -0.46054 |
| VARS | 6 | 0.000603 | 0.003363 | 0.474894 | 14 | 3 | -0.12139 |

| | | | | | | | |
|---|---|---|---|---|---|---|---|
| DGKK | 6 | 0.000649 | 0.003613 | 0.476238 | 15 | 5 | -0.31571 |

***Table 3 Negative regulators identified from CRISPR screen***

| Gene ID | sg RNA | Score | p-value | FDR | Rank | Good sgRNA | LogFC |
|---|---|---|---|---|---|---|---|
| NAE1 | 6 | 6.31E-07 | 1.25E-05 | 0.017327 | 1 | 6 | 0.38408 |
| SOCS5 | 6 | 8.55E-07 | 1.75E-05 | 0.017327 | 2 | 4 | 0.4753 |
| MYC | 6 | 2.14E-06 | 2.75E-05 | 0.018152 | 3 | 5 | 0.51667 |
| PLK3 | 6 | 3.33E-05 | 0.00017779 | 0.087871 | 4 | 6 | 0.34049 |
| MMACHC | 6 | 7.79E-05 | 0.00042819 | 0.169307 | 5 | 4 | 0.35608 |
| GRIA4 | 6 | 0.00013412 | 0.00076874 | 0.246818 | 6 | 4 | 0.49218 |
| MLKL | 6 | 0.00015692 | 0.00087391 | 0.246818 | 7 | 5 | 0.30001 |
| AKAP3 | 6 | 0.00023149 | 0.0013347 | 0.329827 | 8 | 4 | 0.42007 |
| KCNMB2 | 6 | 0.00028605 | 0.0016452 | 0.361386 | 9 | 4 | 0.37749 |

Among these, FARSA and FARSB are linked to aminoacyl-tRNA synthetases, while RPL3 is categorized as a ribosomal protein. CCT2 functions as a molecular chaperone, and CARD10 is implicated in apoptosis regulation. HAL contributes to histidine catabolism, while VARS is classified as an aminoacyl-tRNA synthetase. DGKK operates as a kinase, converting diacylglycerol (DAG) into phosphatidic acid (PA) and regulating the balance of these bioactive lipids. MLKL, a pseudokinase, holds a pivotal role in TNF-induced necroptosis. NAE1 and SOCS5 are both part of the E3 ubiquitin ligase pathway.

Initially, we excluded hits directly tied to synthetic pathways or cell death, which encompassed FARSA, FARSB, CCT2, RPL3, CARD10, VARS, as well as MLKL.

MYC, PLK3, ATR, as well as Chk1, DYRK1A, and PP2A are intricately involved in the regulation of the cell cycle. To validate the findings from our initial screen, we employed a complementary shRNA approach to individually validate the identified hits in both DLD-1 and MDA-MB-231 cells. For this we used a similar approach to measure Met protein

levels on the cell surface by Flow. We successfully validated several positive and negative regulators (Figure 3.3).

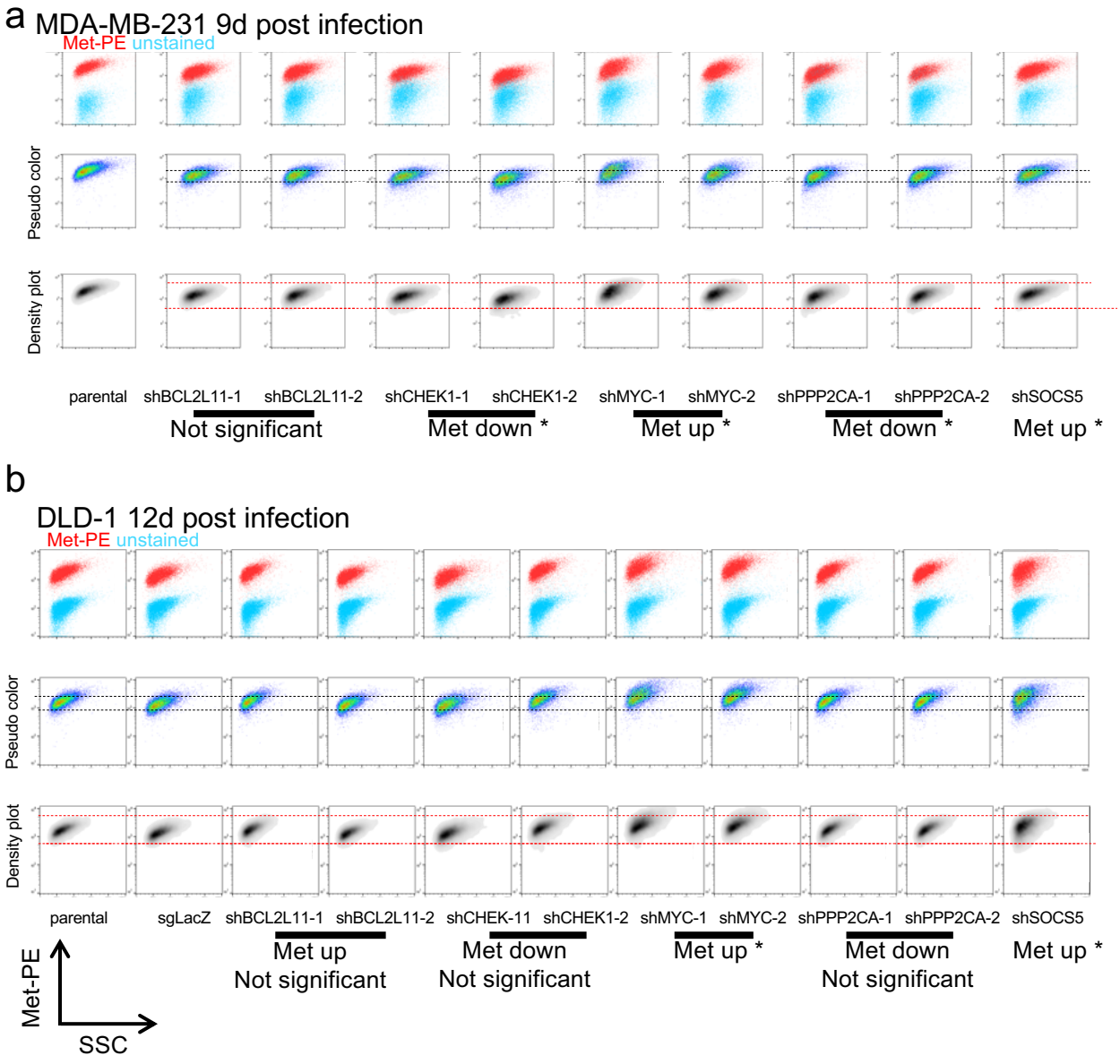


***Figure 3.3 FACS and shRNA-based hits validation in 2 different cell lines.***

MDA-MB-231 (a) and DLD-1(b) cells were infected with individual shRNAs and evaluated for surface Met expression by flow cytometry.

Noteworthy positive regulators, including PPP2CA, CHEK1 and ATR, were identified as crucial mediators of the cell cycle. Among these hits, PP2A (PPP2CA), a gene encoding the core catalytic subunit of the PP2A (protein phosphatase 2) protein complex, identified as a positive regulator was initially prioritized for further validation based on follow-up experiments.

## 3.2 PP2A loss-of-function decreases Met levels and HGF dependent cell migration

CRISPR knockout of the catalytic subunit (PPP2CA) decreased Met protein abundance (Figure 3.4 a). This phenotype was recapitulated by shRNA (Figure 3.4 b) and a small molecule inhibitor (okadaic acid) that selectively inhibits protein phosphatase 2A (PP2A) under the dosage used (25-100 nM). The decrease in Met protein abundance was partially rescued by either proteasomal inhibitor (MG132) or lysosomal inhibitor (bafilomycin) (Figure 3.4 c-e), suggesting that the decreased Met protein abundance caused by okadaic acid inhibition of PP2A can be attributed, at least in part, to proteasomal and lysosomal degradation pathways.

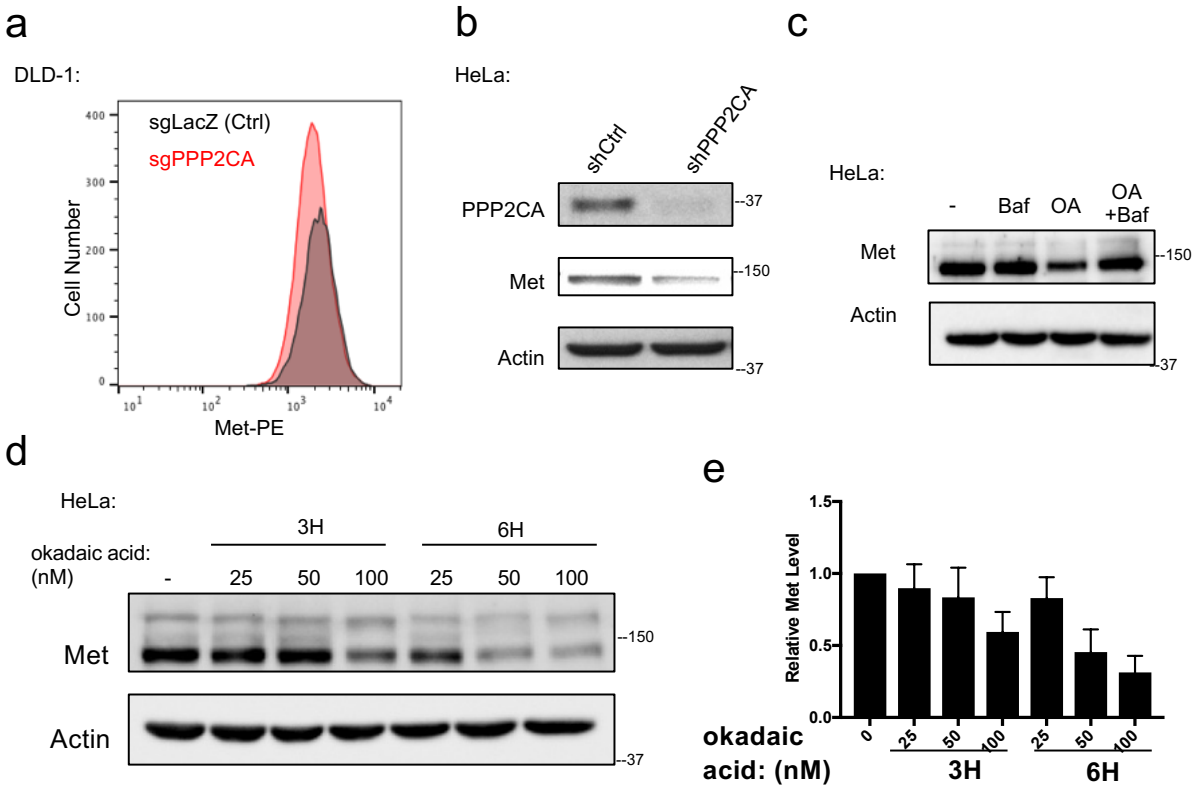


***Figure 3.4 PP2A modulation decreases Met protein levels***

(a) Flow cytometry determination of surface Met in DLD-1 cells. DLD-1 cells were infected with sgPPP2CA or sgLacZ control, after 7 d, cells were assessed for surface Met levels by flow cytometry.
(b) HeLa cells stably infected with shCtrl and PPP2CA with PPP2CA cDNA were analyzed by western blot to detect Met.
(c) Western blot of HeLa cells treated with 50 nM of okadaic acid in presence or absence of 20 nM bafilomycin for 6 h
(d) Western blot of HeLa cells treated with 0, 25, 50, 100 nM Okadaic Acid with indicated time points in absence of serum and in presence of cycloheximide to block protein biosynthesis.
(e) Quantification of (d), mean ± SEM.

## 3.3 MaMTH assay identifies PPP2R2A (regulatory subunit of PP2A complex) can engage with Met

To investigate a potential association between endogenous Met and PP2A we employed two complementary techniques, immunoprecipitation (IP) and MaMTH assay. MaMTH assay is based on the principle of the classical yeast two-hybrid system but modified for use in mammalian cells. The interactions between membrane proteins are investigated by employing split-protein complementation. The assay involves the use of two separate fusion proteins, each consisting of a membrane protein of interest fused to a fragment of a reporter protein, typically split ubiquitin or split enzyme. If the two membrane proteins being studied interact with each other, the split fragments of the reporter protein can come into close proximity, allowing for reconstitution of the functional reporter protein. This reconstitution can be detected and measured, providing evidence of the interaction between the two membrane proteins (Petschnigg et al., 2014).

Both experiments provide evidence for the association between Met and with subunits of PP2A, highlighting potential interaction and regulatory mechanism further supporting involvement of PP2A in Met signaling (Figure 3.5).

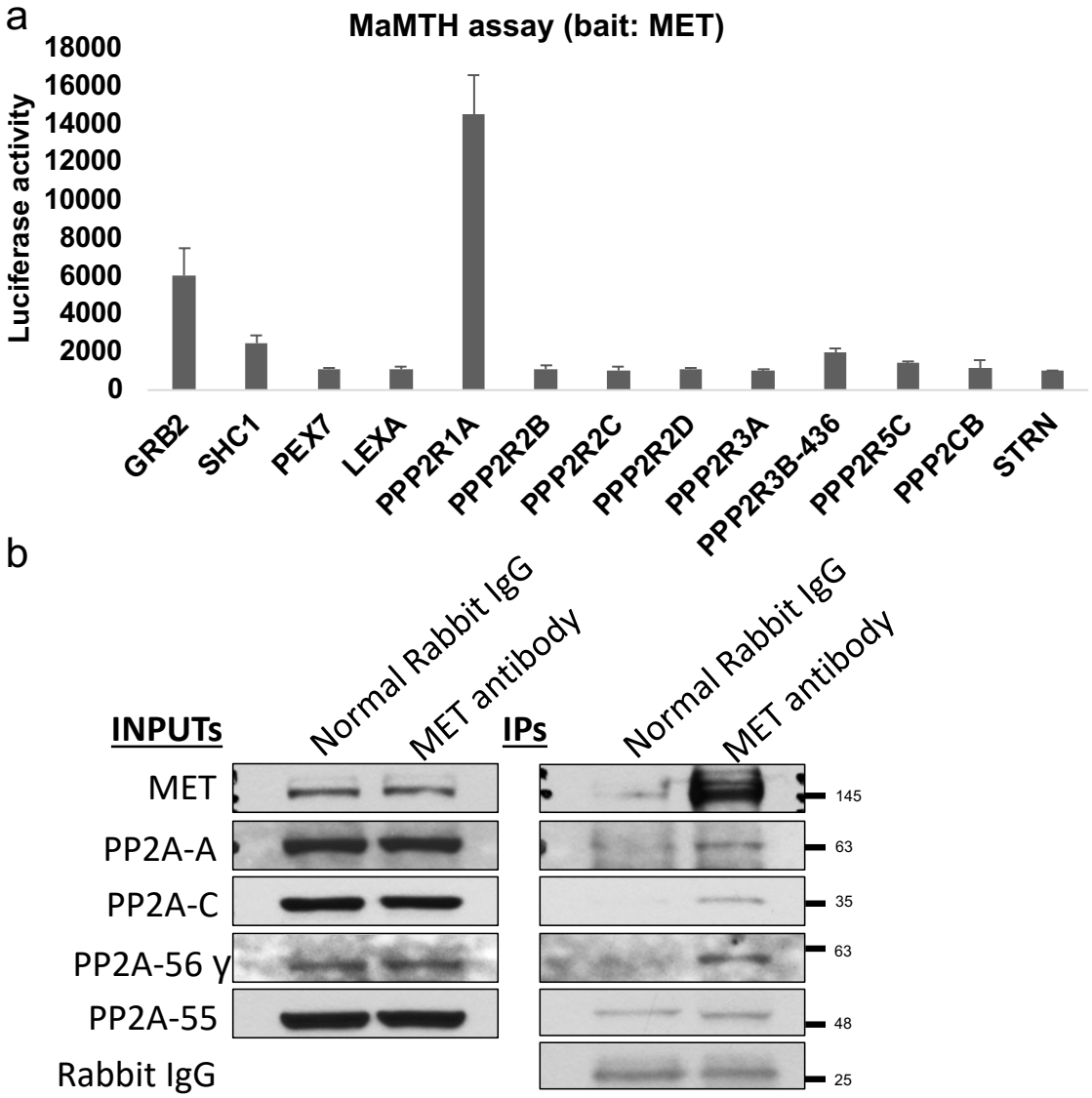


***Figure 3.5 Endogenous Met associates with PP2A.***

(a) Luciferase activity was assessed in HEK293T cells that were stably expressing the 5×GAL4UAS-luciferase reporter and transiently expressing MaMTH-Met-WT-V5 along with prey constructs. Measurement of luciferase activity was conducted 24 hours after transfection.

(b) immunoprecipitation was performed on HeLa S3 cell lysates, followed by probing with antibodies to detect endogenous PP2A subunits.

## 3.4 Impact of okadaic acid in Met related biology

To test if, as supported by decreased Met protein levels (Figure 3.4), okadaic acid treatment impacted HGF-induced cell migration and invasion, we conducted a 2D Transwell migration assay (Figure 3.6) and a 3D invasion assay (Figure 3.7). We observed that okadaic acid treatment resulted in decreased cell migration and invasion mediated by Met in response to HGF, which is consistent with the decreased protein levels observed. These findings support the role of okadaic acid targets in regulating Met-dependent cellular migration and invasion processes.

Collectively, these results demonstrate that okadaic acid inhibition of protein phosphatases such as PP2A, and the ability of PP2A members to associate with Met using MaMTH leads to reduced Met protein levels on the cell surface and, importantly, reduces Met-mediated cell migration and invasion. These findings highlight the significance of protein phosphatases such as PP2A in modulating Met signaling and its potential implications in cellular behaviors associated with metastasis and invasion.

Notably, the influence of PP2A on Met biology potentially extends to the modulation of Gab1 activity downstream of Met signaling. The activation of PKC-alpha and PKC-beta1, arising from PP2A inhibition, contributes to Gab1 hypo-phosphorylation on tyrosine residues. As a consequence, the proficiency of Gab1 in recruiting SH2-containing signal transducers, including PI3 kinase, is subsequently curtailed (Gual et al., 2001).

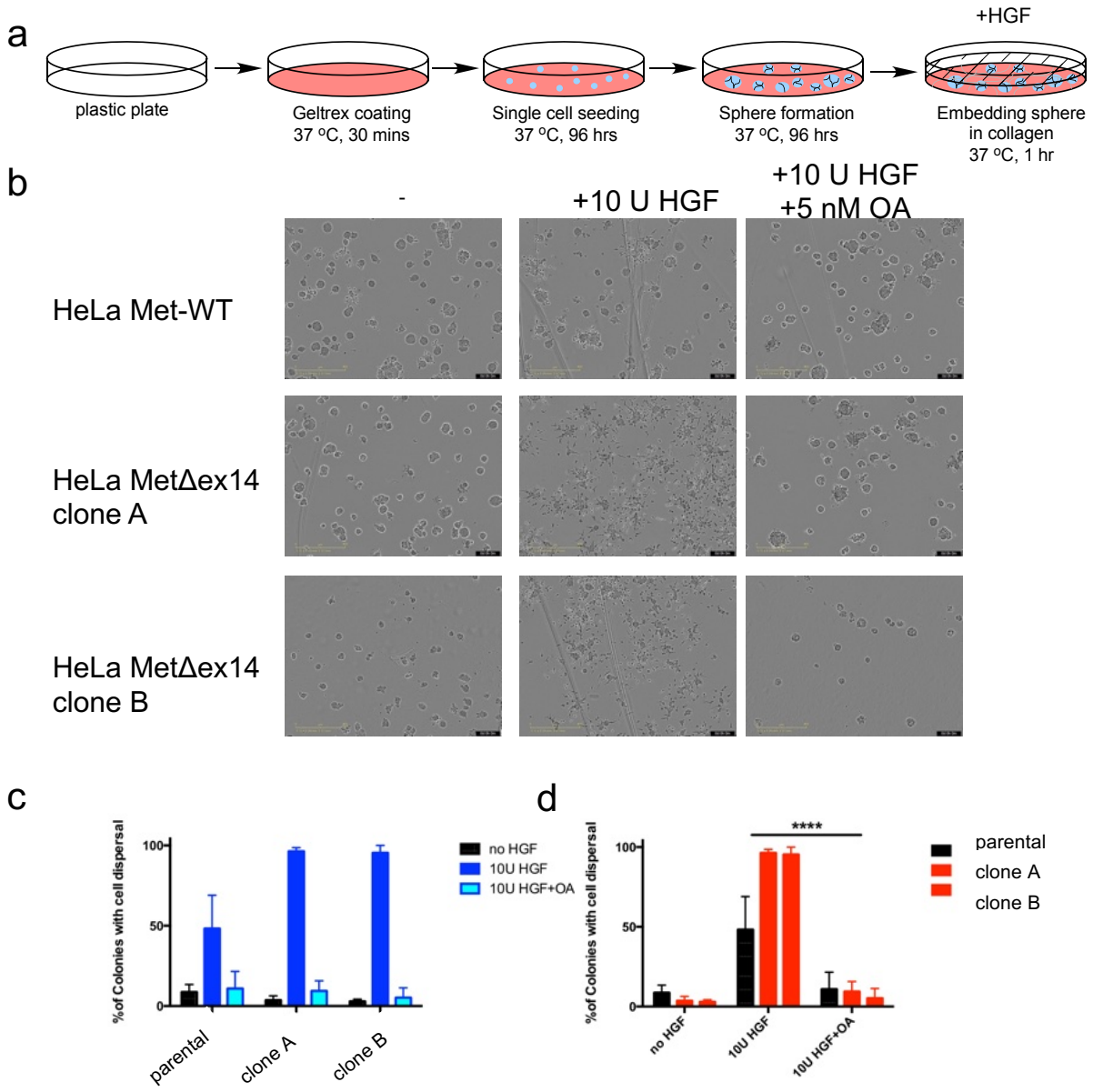


***Figure 3.6 Okadaic acid inhibits HGF dependent 3D invasion***

(a) A schematic model represents the design of a 3D invasion/migration assay. using HeLa Met-WT cells and MetΔex14 clone A and B cell lines stimulated with 10 U HGF.
(b) Phase contrast images of HeLa cells were captured using the IncuCyte S3 system. The images compare the cellular morphology of unstimulated HeLa cells with those stimulated by HGF and okadaic acid for 48 hours.
(c) The percentage of colonies with single cell invasion was quantified and grouped by cell line clones. n = 3, mean ± SEM.
(d) The percentage of colonies with single cell invasion was quantified and grouped by treatment conditions. n = 3, mean ± SEM, ****p < 0.0001, paired t-test.

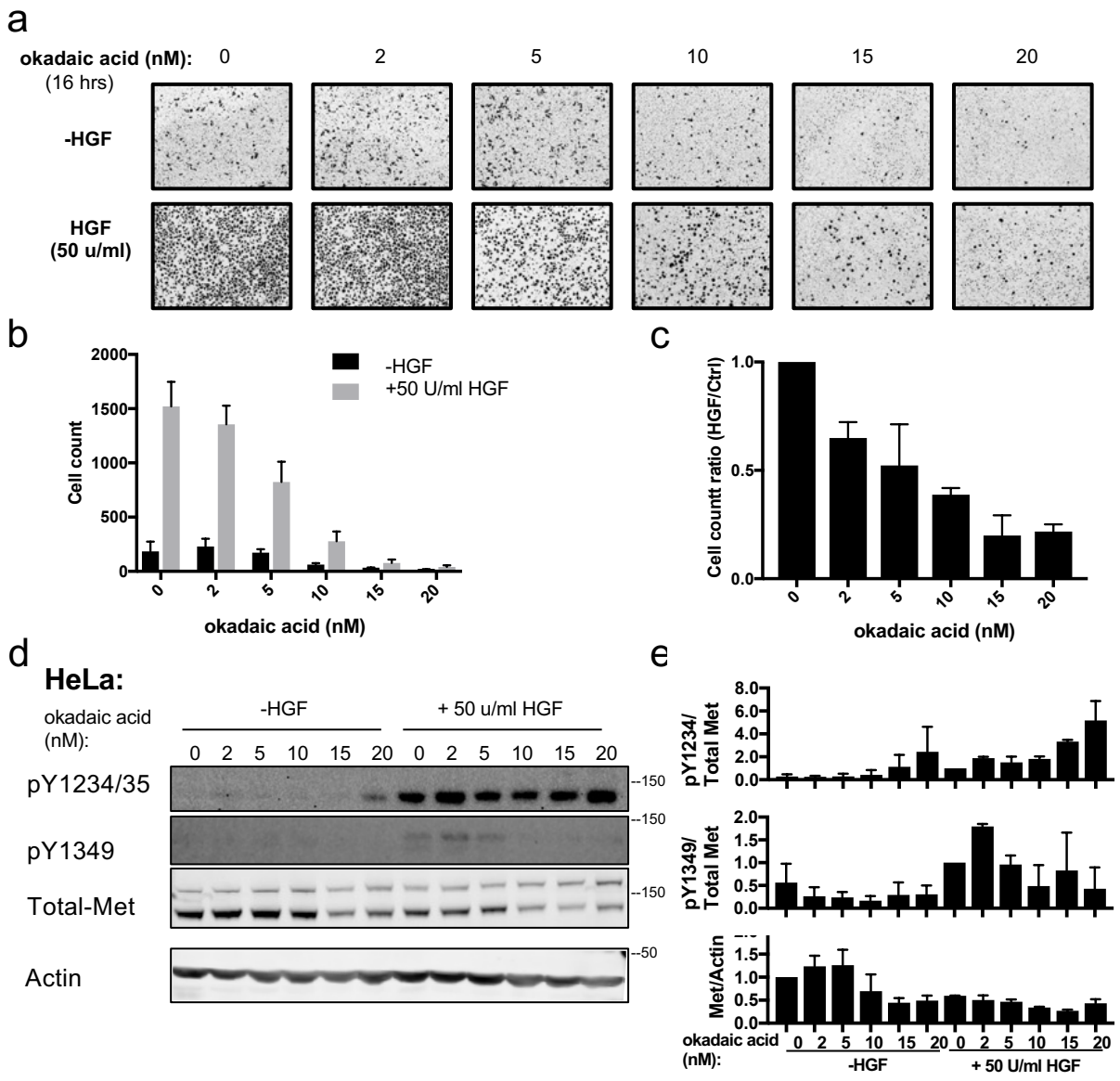


***Figure 3.7 Okadaic acid inhibits HGF dependent cell migration***

(a) Representative phase contrast image of migrated cells after 16 hours. HeLa cells were trypsinized into single cells and seeded into Transwell chambers. The bottom chamber was filled with HGF or okadaic acid at the indicated concentrations. After fixation and crystal violet staining, migrated cells were visualized and photographed under a phase contrast microscope.
(b) Quantification of migrated cells by cell number. Data presented as mean ± SEM (n = 3).
(c) Quantification of migrated cells normalized to the no HGF treatment condition. Data presented as mean ± SEM (n = 3).
(d) Western blot analysis of cell lysates under the same conditions as (a). The blots were probed for total Met and phosphorylated forms of Met (pY1234/35 and pY1349).

(e) Quantification of Met phosphorylation levels (pY1234/35 and pY1349) in (d). Data presented as mean ± SEM (n = 3).

Moreover, a case study showcased a confluence of *MET* amplification and a hyperactivating BRAF mutation (G469A). Intriguingly, efforts to inhibit the BRAF pathway yielded a surprising parallel: a lack of effectiveness. However, from this situation emerged a revelation—an unexpected resurgence of the Met oncoprotein's activity when BRAF was inhibited, bringing to light an unforeseen addiction to Met. Within the context of the BRAF-activating mutation, Met inactivation followed a distinctive mechanistic pathway. This was orchestrated through a negative feedback loop, intricately involving the deactivation of the PP2A phosphatase. The culmination of this cascade led to the inhibitory phosphorylation of Met at Ser985. Importantly, the disruption of this feedback loop proved pivotal. It ushered in the reactivation of PP2A, thereby alleviating the inhibitory phosphorylation and reawakening the kinase activity of Met (Virzì et al., 2018). These observation underscores that PP2A possesses the capacity to negatively impact Met activity, either through direct association or by influencing downstream effector proteins.

## 3.5 Met is internalized at M-phase

During our analysis of Met localization, we observed that Met displayed enhanced localization to the cytosol during cell division. In order to investigate the localization of Met during the M phase of the cell cycle, we conducted an experiment to avoid biases introduced by drug inhibitors. Through the use of immunofluorescence, we utilized DAPI staining to define the M phase and visualize the localization of Met. We were able to

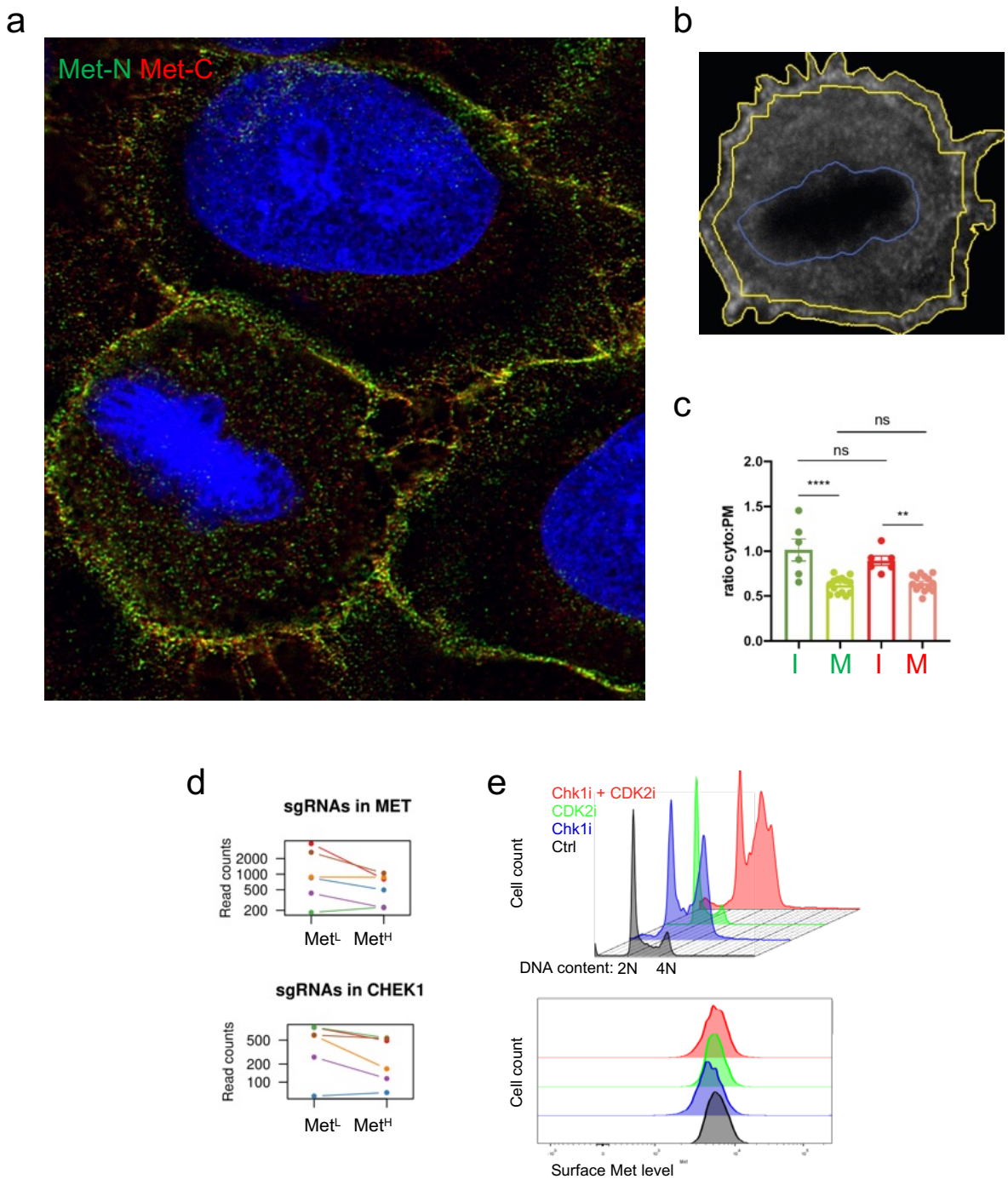


***Figure 3.8 Met is internalized at M-phase.***

(a) Immunofluorescence staining of untreated HeLa cells with antibodies raised against the N and C terminus of Met. DAPI staining was used to identify dividing cells. Images were acquired using super resolution microscopy mode by Zeiss LSM Airyscan 880 microscope.

(b) Example of cell surface and cytoplasmic region definition for quantification using MetaMorph.
(c) Quantification of Met intensity ratio between the cell surface and cytoplasmic region in interphase and mitotic phases. I: interphase, M: mitotic phase. Red: signal from antibody against Met N-terminus, blue: signal from antibody against Met C-terminus. Data presented as mean ± SEM (n = 3). Statistical significance indicated by **p < 0.01, ****p < 0.0001 and as determined by paired t-test.
(d) Relative sgRNA abundance obtained in the original CRISPR screen. Each distinct sgRNA identified in CRISPR screen was represented in different colors.
(e) DNA content profiling of DLD-1 cells treated with LY2603618 (Chk1i) or K03861 (CDK2i) for 24 hours. Methanol-fixed cells were stained with propidium iodide and analyzed by flow cytometry.

observe that Met undergoes internalization specifically during the M phase in the absence of HGF. To ensure the validity of our findings, we employed antibodies targeting both the N- and C- terminus of Met, which converged on the same conclusion. Additionally, this study provides the first evidence of Met dynamic behavior during cell division (Figure 3.8 a-c).

## 3.6 Positive Met regulators converge on cell cycle kinases

The finding that Met is internalized during M phase prompted us to explore the relationship between hits identified in a CRISPR screen and the cell cycle. PP2A, a multifunctional protein, is involved in various biological processes. Notably, during the cell cycle, PP2A plays a critical role in counteracting CDK1 through several mechanisms: 1) Dephosphorylation of CDK1 substrates, 2) Activation of upstream negative regulators of CDK1, such as Wee1 and Cdc25, via PP2A-mediated dephosphorylation, and 3) Direct phosphorylation and inactivation of PPP2CA by CDK1 (Jeong & Yang, 2013; Nasa et al., 2020).

The ATR-CHEK1 signaling pathway is fundamental for responding to DNA replication stress during the S phase of the cell cycle (Karnitz & Zou, 2015). It inhibits origin firing, facilitates fork repair and restart, supports fork stabilization, and ultimately triggers S-phase arrest in a CDK2-dependent manner. Additionally, ATR-CHEK1 is implicated in processes such as S-G2 and G2-M transition, chromosome segregation, double-strand DNA break repair, and mechanical stress response, acting upstream of CDK1 and/or CDK2 (Kabeche et al., 2018; Krämer et al., 2004; Kumar et al., 2014; Saldivar et al., 2018). Based on our results, we hypothesize that inhibition of ATR-CHEK1 and PP2A could potentially influence Met protein levels by activating CDKs. This suggests a potential regulatory connection between the cell cycle machinery and Met protein dynamics.

## 3.7 Met exon 14 region is phosphorylated under basal conditions

Our findings on chapter 2 support that exon 14 plays a role as a rheostat for Met C-tail tyrosine phosphorylation in the presence of low levels of HGF. Indeed, previous research has identified that the Y1003 residue within exon 14 region is phosphorylated and serves as a recognition site for the E3 ubiquitin ligase Cbl, where Y1003F mutation prolonged Met stability, signalling and conferred tumorigenic properties in the presence of HGF (Abella et al., 2005; Peschard et al., 2001). However, exon 14 skipping mutations are more frequent than Y1003F mutations in human tumors suggesting potential other functions (Figure 2.1 a). Hence, we sought to determine whether other sites in this region are phosphorylated. Due to the lack of phospho-specific antibodies for this region, we employed the use of Phos-tag gel electrophoresis to identify distinct phosphorylated Met species (Kinoshita et al., 2009) and detected a prominent HGF independent

phosphorylation species of Met in M-WT cells, but not in MetΔex14 cells (Figure 3.9 a). Further analysis using IP-MS of cell lysates prepared from HeLa cells with WT Met identified pT977 and pS990 located within exon 14 under basal conditions (Figure 3.9 c). This is in agreement with published high-throughput datasets where these sites are identified as phospho sites during G2/M phase cell cycle arrest (Daub et al., 2008; Olsen et al., 2010).

To establish the dependence of this phosphorylation species on kinases elevated at this stage in the cell cycle such as CDK activity, we treated HeLa cells with CDK inhibitors and observed that the Type II Cyclin A/E competitive CDK2 inhibitor K03861 as well as others tested (RO-3306, homoharringtonine, roscovitine) abolished the gel shift detected using Phos-tag gel electrophoresis while nocodazole which induces G2/M cell cycle arrest exacerbated the shifted phosphorylation species (Figure 3.9 b).

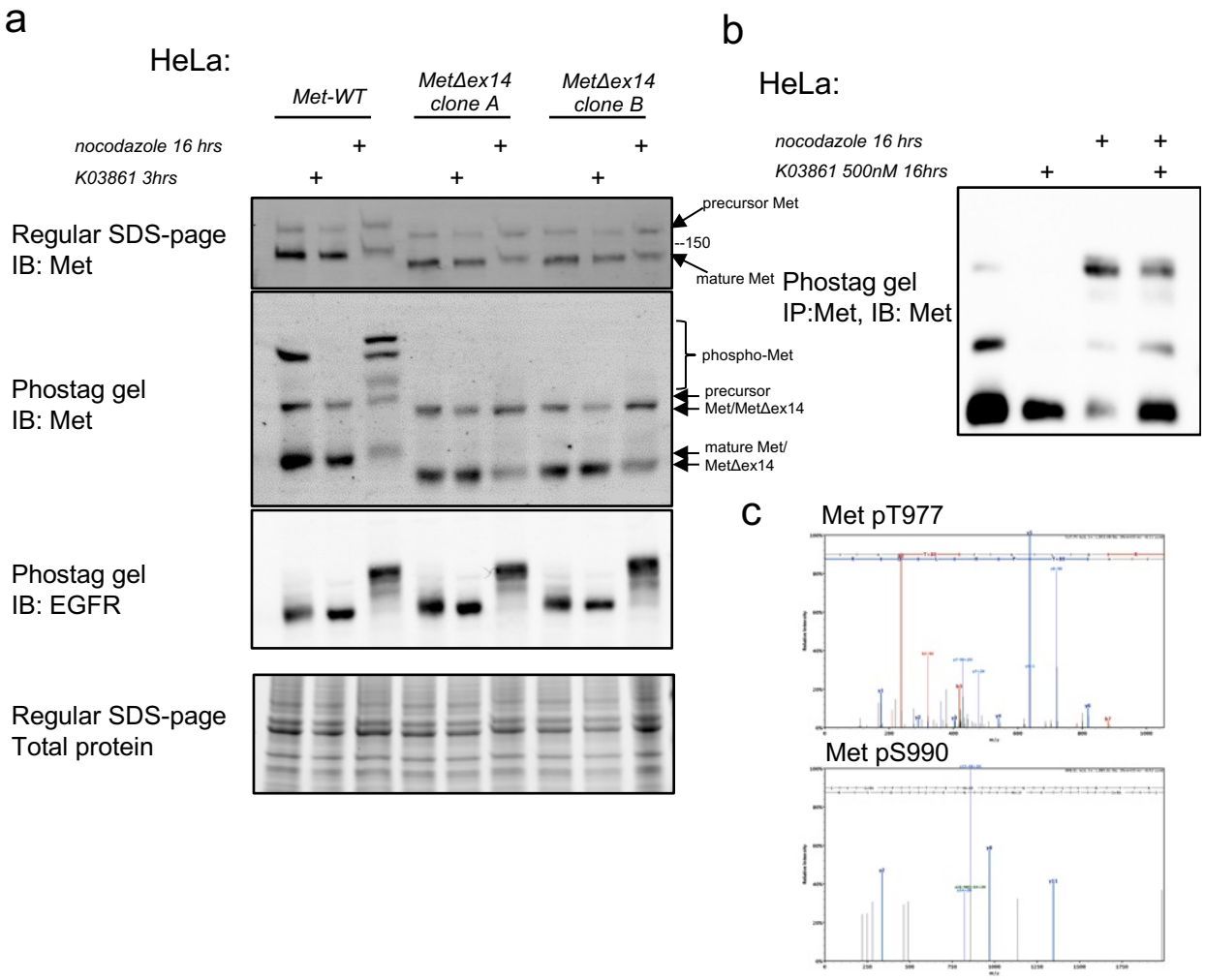


***Figure 3.9 Nocodazole induces exacerbated exon 14 dependent phosphorylation***

(a) The total Met protein in CRISPR-Cas9 engineered HeLa and DLD-1 cells, which endogenously express wild-type (WT) Met, Δex14 clones, and natural Δex14 H596 cells, was evaluated. Immunoblotting of cell lysates was performed, and the resolved proteins were visualized using a 6% polyacrylamide gel containing 20 μM phos-tag. Representative blots from three independent experiments (N=3) are shown.
(b) HeLa cells expressing wild-type (WT) Met or CRISPR-Cas9 engineered Δex14 clones were treated with nocodazole (100 ng/ml) for 16 hours or the CDK2 inhibitor K03861 (5 μM) for 3 hours. Total Met and EGFR protein levels were determined by immunoblotting of cell lysates. Proteins were separated using regular SDS-page or a 6% polyacrylamide gel containing 20 μM Phos-tag. Representative immunoblotting results from three independent experiments (N=3) are shown.
(c) HeLa cells expressing WT Met were treated with nocodazole (100 ng/ml) and/or the CDK2 inhibitor K03861 (5 μM) for 16 hours. Cell lysates were immunoprecipitated with a

Total Met antibody, and total protein levels were assessed by immunoblotting using a 6% polyacrylamide gel containing 20 μM Phos-tag.
(d) To further analyze the phosphorylation status, samples from (c) were subjected to tandem mass spectrometry, and the presence of phosphorylated residues pT977 and pT990 was detected in both non-treated and nocodazole-treated conditions.

To establish a time-dependent activation profile of Met in response to HGF stimulation, we treated HeLa cells harboring 2 Δex14 clones with HGF and employed Phos-tag to resolve different phosphorylation states of Met. Notably, we observed distinct patterns in phosphorylation for two key tyrosine sites. Specifically, pY1234/35 exhibited multiple species distributed from the bottom to the middle of the gel, while pY1349 displayed a singular distinct band in the Δex14 clones. This finding suggests that pY1234/35 represents an early phosphorylation event, whereas pY1349 undergoes phosphorylation in a cascading manner, potentially as a downstream event triggered by the initial phosphorylation. Furthermore, we observed an intriguing phenomenon where the super-shifted species (phospho-exon 14) was present in the wild-type Met samples but absent in the Δex14 clones under unstimulated conditions. Interestingly, upon the addition of HGF over time, the phospho-exon 14 species in the wild-type Met also became phosphorylated. This suggests that the phosphorylation of phospho-exon 14 may be facilitated through neighboring active Met complexes, indicating a potential interplay between different Met signaling complexes in mediating this phosphorylation event (Figure 3.10).

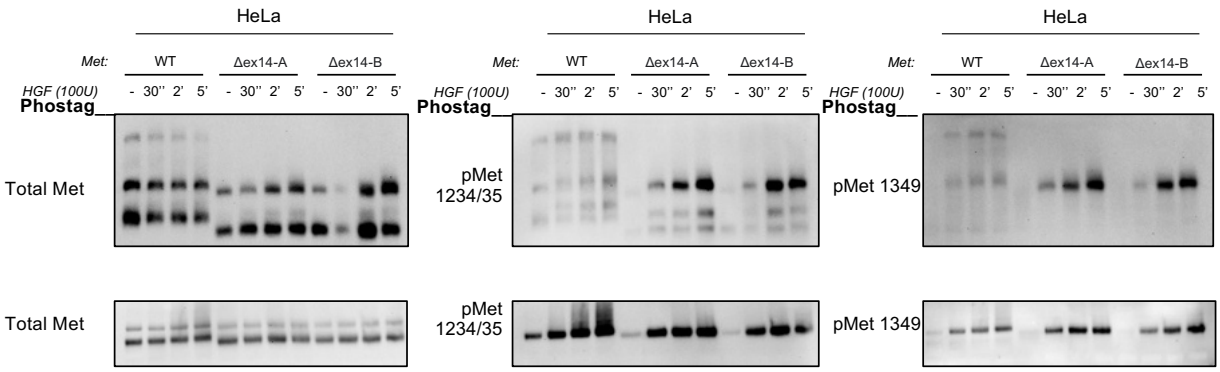


***Figure 3.10 Phos-tag resolved time course activation profile of Met***

HeLa cells expressing WT Met and Δex14 clone were subjected to stimulation with 100 U of HGF for different durations. Following stimulation, Met tyrosine phosphorylation levels were evaluated using either 20 μM Phos-tag or regular SDS-PAGE. Immunoblotting of cell lysates was performed using antibodies specific to pY1234/35 (located in the kinase activation loop), pY1349 (located in the C-tail), and total Met. Representative blots from three independent experiments (N=3) shown.

Notably, the contrast in exon 14 phosphorylation shift brought about by nocodazole is markedly more pronounced (Figure 3.9 b) when compared to that induced by HGF (Figure 3.10). This observation strongly implies the existence of a limited subset of Met receptors on the cellular surface that are susceptible to HGF-induced phosphorylation and its subsequent cascading effects. On the contrary, when exposed to nocodazole, a substantial reservoir of Met receptors becomes a substrate for cell cycle kinases, accentuating the distinction.

## 3.8 Impact of exon 14 phosphorylation

To enhance our understanding of the impact of phosphorylation of T977 and S990 on Met, we investigated the phosphorylation status of Met-amplified cancer cell lines,

specifically MKN45 (gastric adenocarcinoma) and EBC1 (lung squamous cell carcinoma) These cell lines are known to exhibit constitutive Met activation in the absence of HGF (Lai et al., 2014). Notably they display the Met super-shifted species observed in nonamplified Met, HeLa and DLD-1 cell lines. This species is detected with Met C-terminal antibodies as well as antibodies to pY1234/35 and antibodies to pY1349. The lowest Met species in the Phos-tag gel is detected only by Met or pY1234/35 antibodies and not those to pY1349, identifying this species as a kinase active but signalling inactive species. Interestingly a small molecule Met kinase inhibitor, crizotinib, failed to promote a downshift in the WT Met super-shifted species as detected with Met antibodies. although it abrogated all Met Y1234/35 or Y1349 phosphorylation. This supports that the super-shifted Met species observed in WT Met is alternatively modulated in addition to tyrosine phosphorylation. Since T977 and S990 residues are phosphorylated in multiple datasets (Daub et al., 2008; Olsen et al., 2010), we treated WT Met amplified cells with the inhibitor for CDK2 (K03861). Notably, K03861 pre-treatment downshifted the super-shifted species recognised by anti-total-Met, pY1234/35 or pY1349 antibodies supporting this species as harboring CDK2 dependent phosphorylation.

Notably, in the immunoblot results, phosphorylation species A is observed to be less abundant compared to species B, while species C is more abundant than species D. This finding suggests that phosphorylation of the Met exon 14 region leads to a reduction in pY1349 phosphorylation, indicating a potential role of exon 14 phosphorylation in modulating pY1349 phosphorylation levels (Figure 3.11).

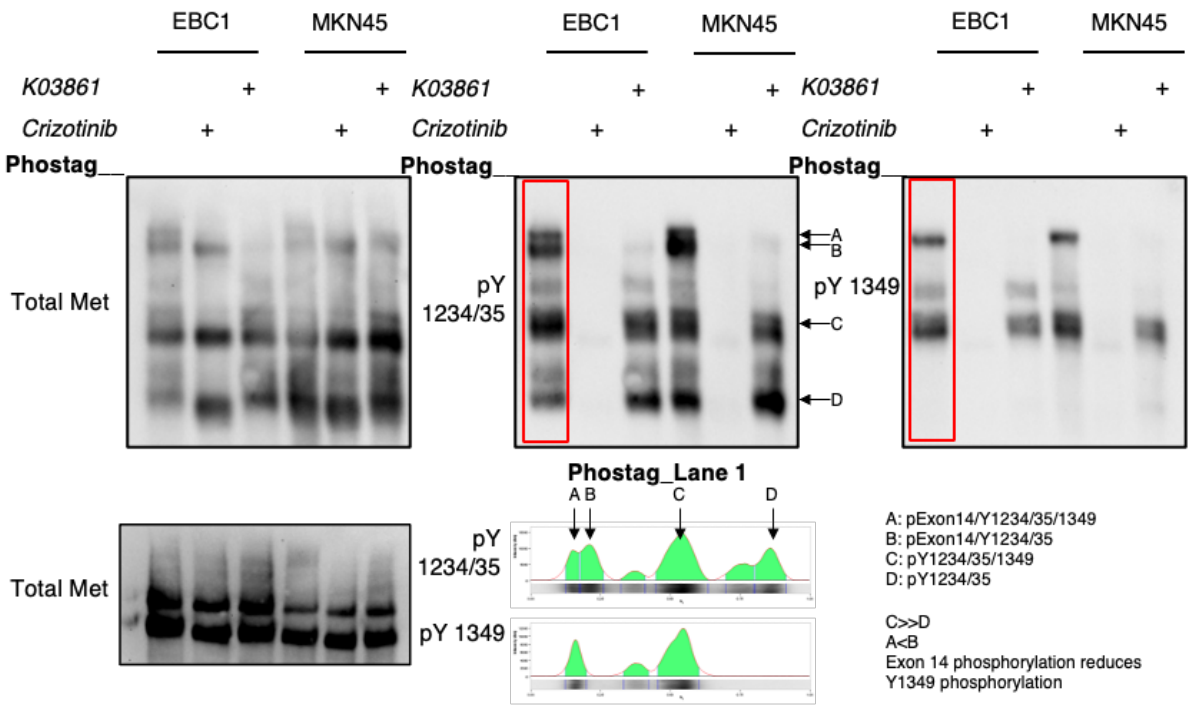


***Figure 3.11 Phos-tag western blot to detect baseline level exon 14 phosphorylation***

Met-amplified EBC1 and MKN45 cells were treated with the Met inhibitor crizotinib (500 nM) or the CDK2 inhibitor K03861 (5 μM) for 1 hour. The phosphorylation status of Met was assessed by immunoblotting of cell lysates, specifically targeting pMet1234/35 (located in the kinase activation loop), pMet1349 (located in the C-tail), and total Met (unphosphorylated C-tail). Regular SDS-page or a 6% polyacrylamide gel containing 20 μM Phos-tag was used for the separation of proteins. Representative blots from three independent experiments (N=3) are shown.

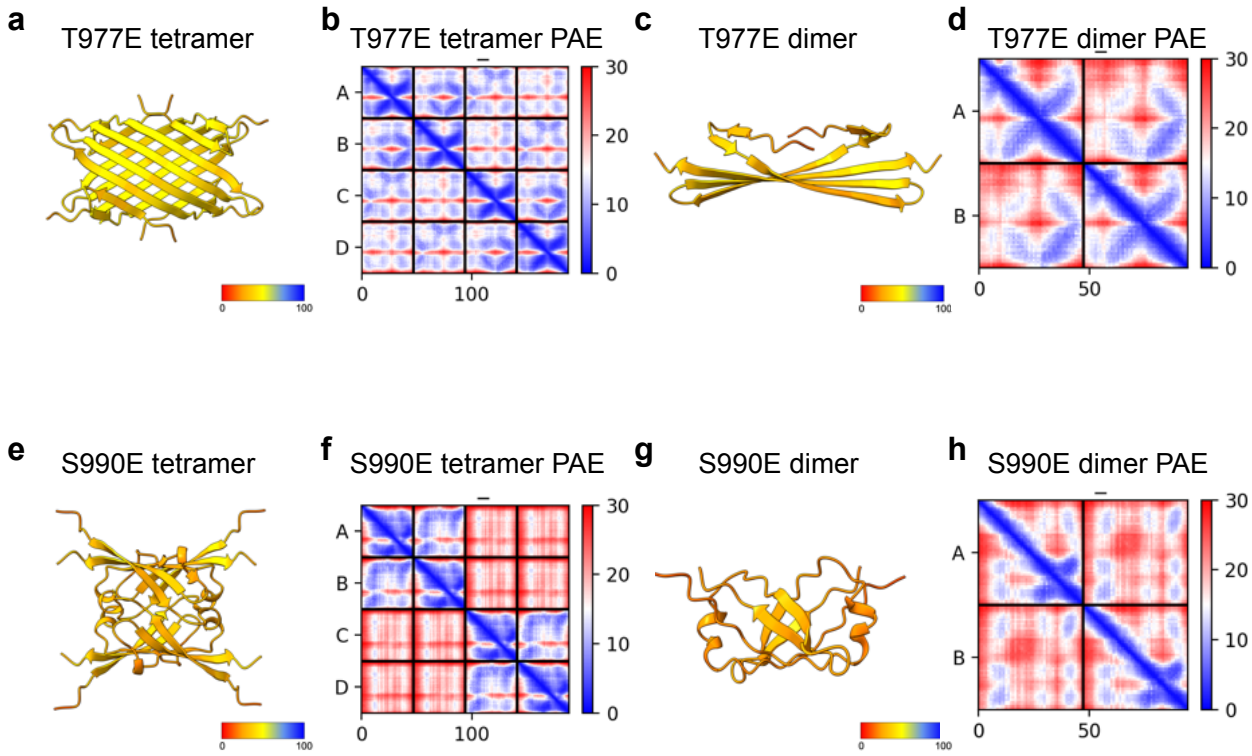


***Figure 3.12 Structural prediction of Met exon 14 T977E and S990E mutant variants***

(a) Predicted tetrameric structure of Met exon 14 T977E colored by predicted per-residue scores on the lDDT-Cα metric (pLDDT) score, indicating the confidence level in the predicted structure.
(b) Heat map displaying the predicted alignment error for the tetrameric Met exon 14 T977E structure.
(c) Predicted dimeric structure of Met exon 14 T977E using AlphaFold, colored by predicted per-residue scores on the lDDT-Cα metric (pLDDT) score.
(d) Heat map depicting the predicted alignment error for the predicted dimeric Met exon 14 T977E structure.
(e) Predicted tetrameric structure of Met exon 14 S990E colored by predicted per-residue scores on the lDDT-Cα metric (pLDDT) score, indicating the confidence level in the predicted structure.
(f) Heat map displaying the predicted alignment error for the tetrameric Met exon 14 S990E structure.
(g) Predicted dimeric structure of Met exon 14 S990E using AlphaFold, colored by predicted per-residue scores on the lDDT-Cα metric (pLDDT) score.
(h) Heat map depicting the predicted alignment error for the predicted dimeric Met exon 14 S990E structure.

To investigate the potential influence of phosphorylation at T977 and S990 on the formation of exon 14 tetramers, computational modeling using AlphaFold revealed a

modification in the ability of phospho-mimetic peptides containing T977E and S990E substitutions to form tetramers. This modeling provides support for the hypothesis that phosphorylation and the introduction of a negative charge at S990 and/or T977 may impact the capacity of exon 14 to form tetramers (Figure 3.12 a-h). In order to further characterize the Met-CDK interaction, we employed a split-Intein approach. This approach involves the use of split-Inteins, which are self-splicing protein domains that can catalyze the ligation of two separate polypeptide fragments. In Split Intein-Mediated Protein Ligation (SIMPL), the protein of interest is split into two fragments, each fused to a complementary split Intein fragment. When the two Intein-fusion proteins interact with each other due to a protein-protein interaction, the split Intein fragments come into close proximity and can reassemble, leading to the splicing of the Intein fragments and the formation of a functional, full-length Intein (Yao et al., 2020). From this we observed that Met transfers the flag tag to both CDK2 and CDK1, albeit to a lesser extent with CDK1, supporting engagement of Met with CDKs at a cellular level (Figure 3.13).

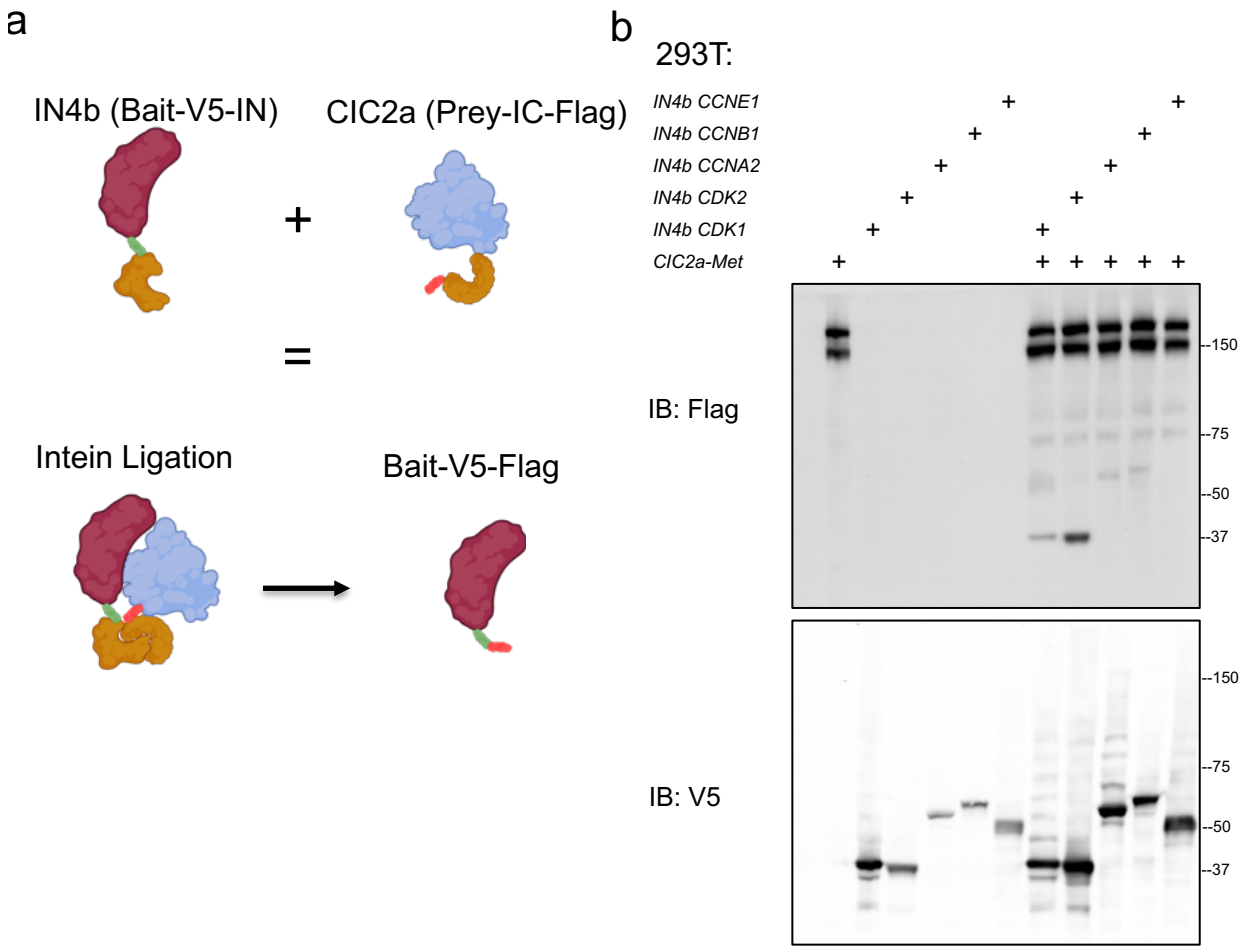


***Figure 3.13 SPLIT-Intein system captures Met-CDK2 engagement via tag transfer***

(a) Schematic Representation of SPLIT-Intein System: The SPLIT-Intein system was utilized in this study. Intein halves were genetically fused to bait or prey proteins, each tagged with distinct Flag and V5 tags. Protein engagement between the bait and prey proteins was assessed by monitoring the transfer of the Flag tag from the Prey to the Bait protein, and subsequently, Intein excision from the Bait protein.
(b) Protein Detection and Co-transfection: 100K 293T cells were transiently transfected with 250 ng of various Bait proteins and Met prey using Lipofectamine 2000. After 24 hours, protein lysates were prepared and subjected to immunoblotting analysis using antibodies specific to the V5 and Flag tags. Note: The transfer of the Flag tag indicates successful engagement between the Bait and Prey proteins, and the observed protein transfer was most evident in the presence of CDK2 co-expression. Representative blots from three independent experiments (N=3) are shown.

## 3.9 Impact of pharmacological drugs on Met levels

Upon treating cells with nocodazole or taxol,G2/M phase-arresting agents (De Brabander et al., 1986), a significant reduction in surface levels of Met was observed. However, when cells were simultaneously treated with a CDK1/2 inhibitor (roscovitine) or endo-lysosomal inhibitor (bafilomycin), the reduction in surface Met levels was rescued. The reduction is Met specific but not EGFR (Figure 3.14). These findings suggest that CDK1/2 activity is involved in maintaining the surface expression of Met during G2/M arrest, and that this process is endo-lysosomal dependent.

Interestingly, Chk1 inhibition also induces G2/M cell cycle arrest (Figure 3.8 e), which is also described in literature (Tang et al., 2006). and it was observed that both the cell cycle progression and Met levels were partially rescued when a CDK2 selective inhibitor (K03861) was applied (Figure 3.8 e). These results imply that CDK2 activity might play a role in regulating both the cell cycle progression and the levels of Met during G2/M arrest, possibly through the Chk1 signaling pathway.

Importantly, the decrease in Met levels on the cell surface, followed by subsequent degradation, is influenced by chemical agents and might not manifest during the typical course of the normal cell cycle. Given the brief duration of the M phase cell cycle (~45 minutes), this limited time frame might not offer ample opportunity for Met to undergo degradation. Instead, Met could potentially be recycled to the cell surface once cells transition out of the cell cycle, marked by diminished CDK2 activity. This narrow temporal window, however, permits the phosphorylation labeling of Met exon 14 by CDK2, discouraging proliferation in the context of Met biology.

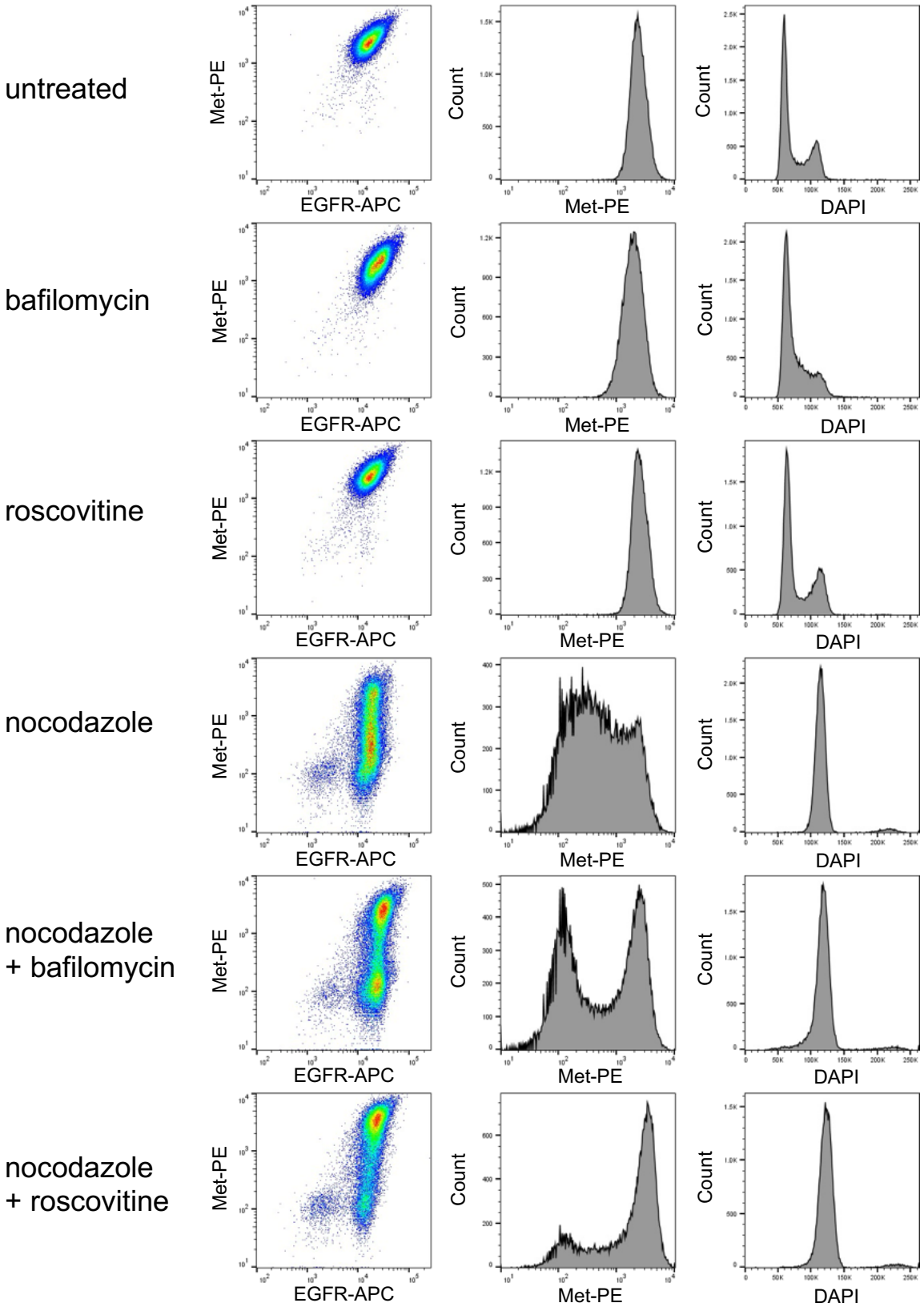
untreated
bafilomycin
roscovitine
nocodazole
nocodazole
+ bafilomycin
nocodazole
+ roscovitine
Met-PE
EGFR-APC
Count
Met-PE
Count
DAPI

***Figure 3.14 Nocodazole induced G2/M arrest decreases surface Met levels and is rescued by CDK1/2 inhibitor.***

HeLa cells were treated with nocodazole (100 ng/ml, G2/M arrest inducer), bafilomycin (20 nM, lysosomal inhibitor), or roscovitine (10 μM/ml, CDK1/2 inhibitor) for 16 hours. Cells were then stained with Met-PE, fixed with 2% PFA, permeabilized with Triton X-100, and subsequently stained with DAPI for DNA content profiling. Flow cytometry was used for data acquisition and analysis.

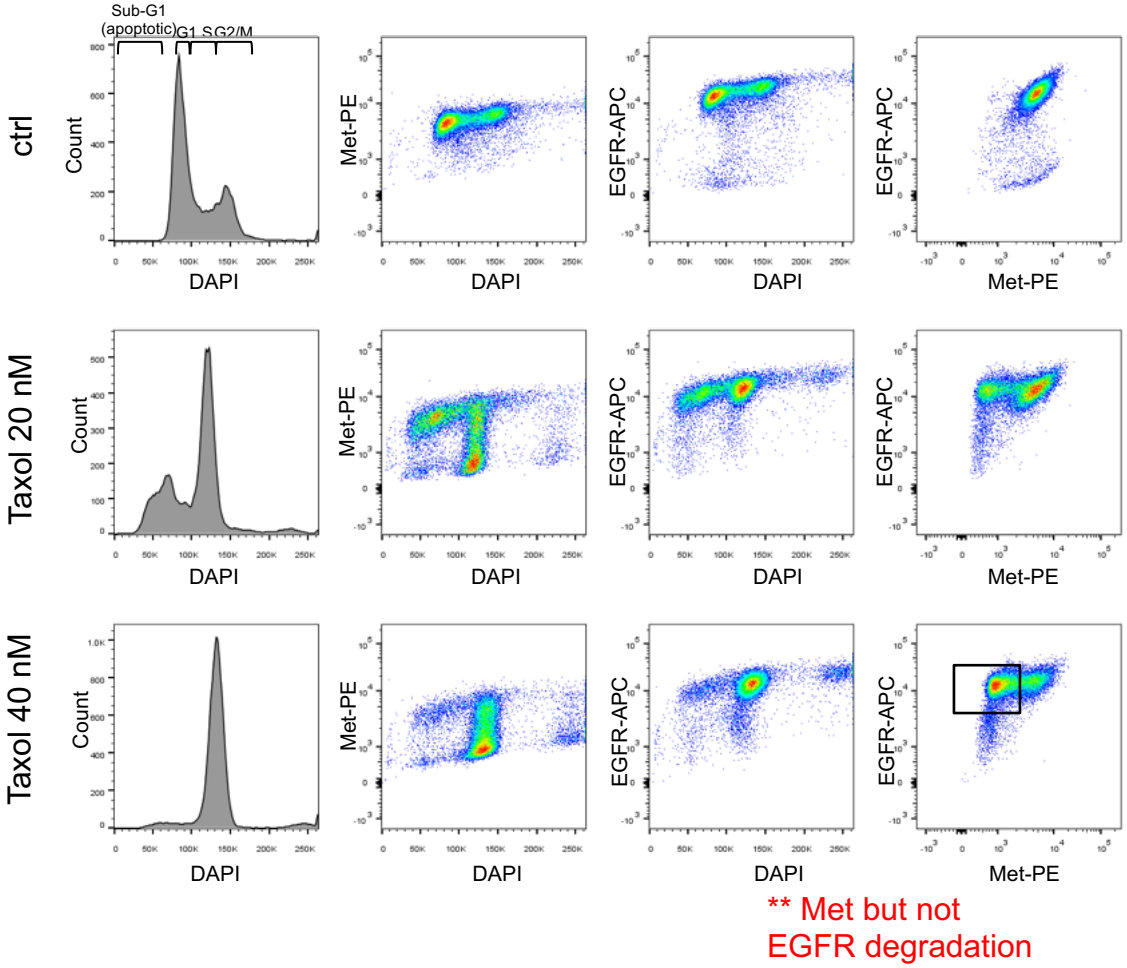


***Figure 3.15 24 hours of paclitaxel treatment on HeLa cells causes Met but not EGFR degradation***

HeLa cells were treated with Taxol with indicated concentration (0 nM, 20 nM, 40 nM,) for 24 hours. Cells were then stained with Met-PE and EGFR-APC, fixed with 2% PFA, permeabilized with Triton X-100, and subsequently stained with DAPI for DNA content profiling. Flow cytometry was used for data acquisition and analysis.

Taxol (Paclitaxel), a chemotherapeutic agent sharing a mode of action akin to nocodazole, has garnered extensive use in cancer treatment. Taxol precipitates cell cycle arrest specifically at the M phase, concurrent with a reduction in surface levels of the Met receptor (Figure 3.15). This intriguing association prompts consideration for potential therapeutic benefits in patients undergoing Taxol-based chemotherapy.

For individuals undergoing Taxol chemotherapy, the concurrent decrease in surface Met levels could hold therapeutic significance. Such an effect might augment the overall efficacy of the treatment strategy. Conversely, patients who exhibit overexpression of the Met receptor might find Taxol-based chemotherapy to be a suitable treatment option. The intersection of Taxol's impact on cell cycle progression and its modulation of Met receptor levels opens intriguing avenues for tailoring chemotherapy regimens to individual patient profiles.

## 3.10 Cyclin B1 and Met protein levels are negatively correlated in tumors

We decided to evaluate the protein levels of TCPA (The Cancer Protein Atlas) dataset. This dataset incorporates 5470 tumors of various origins, generated by the Reverse Phase Protein Array (RPPA) (Li et al., 2017; Li et al., 2013). The tumors were assessed based on a previously described gene expression signature of CDK2 activity (McCurdy et al., 2017). Interestingly, the gene expression signature indicative of CDK2 activity strongly correlated with Cyclin B1 protein levels in tumors (r=0.84, Spearman correlation), and protein levels of Cyclin B1 and Met – but not other RTKs – exhibited a negative correlation (r=-0.45, Spearman correlation) (Figure 3.16 a, b). This was also analyzed by segmenting the tumors into different subtypes (Figure 3.17).

a

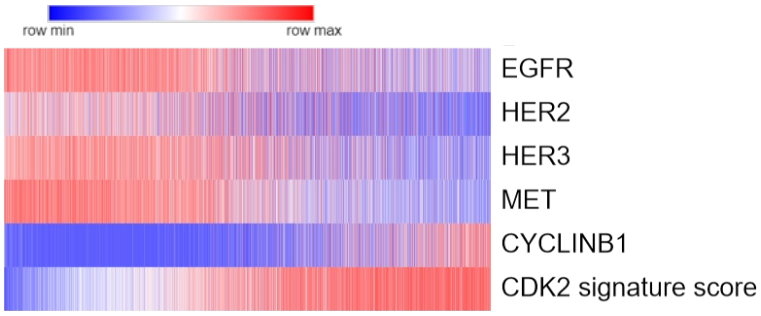


b

Spearman rank correlation

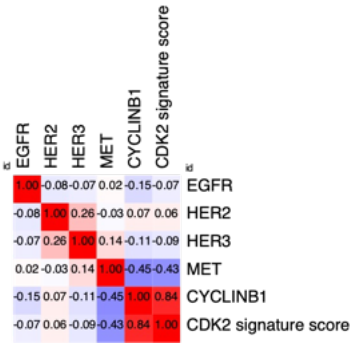


c Breast Cancer PDX 7087:

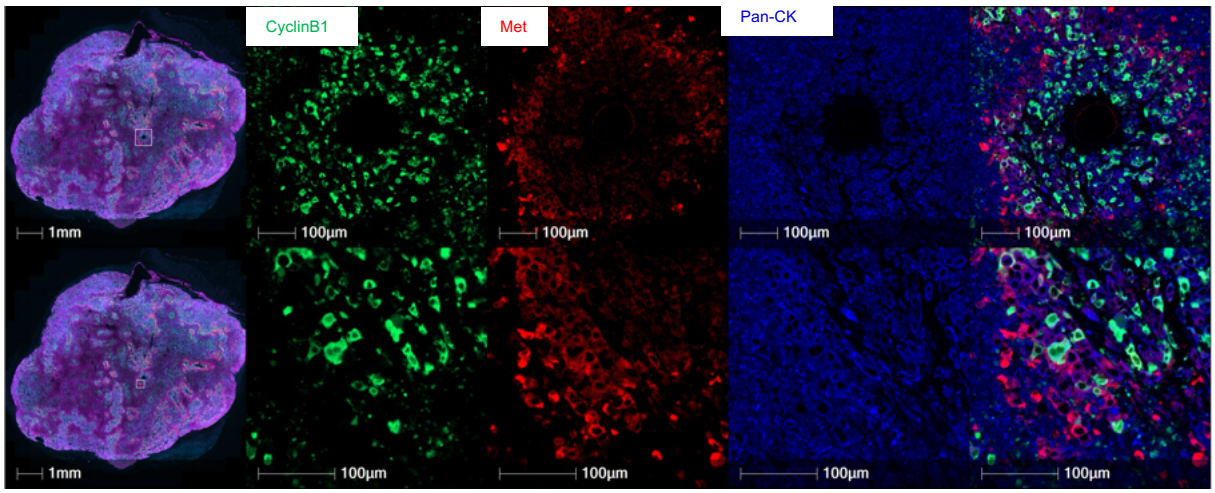


d

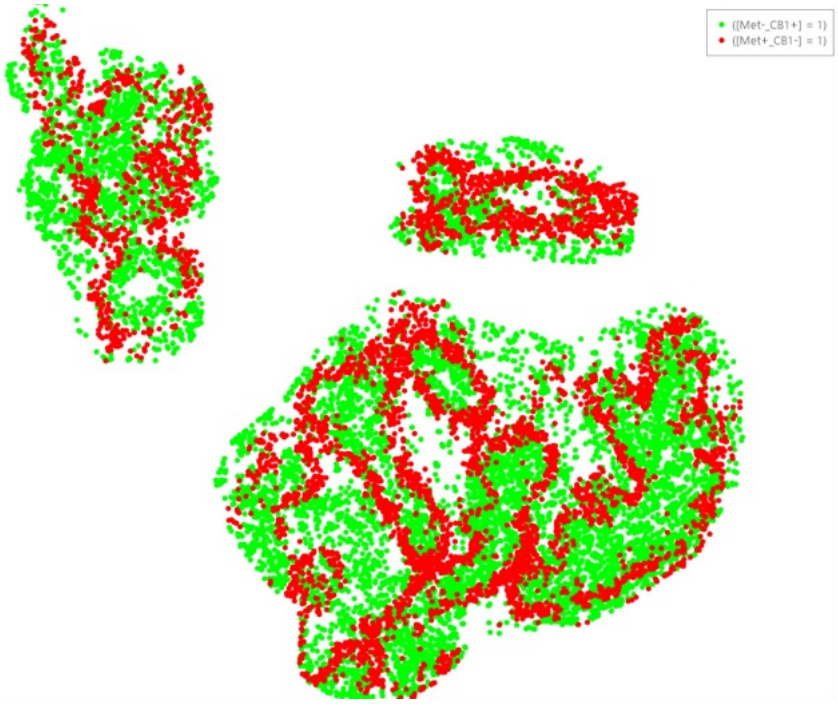

***Figure 3.16 CDK2 activity and Met protein levels but not other RTKs are negatively correlated in TCGA tumors***

(a) Evaluation of TCPA dataset reveals correlations between CDK2 activity and protein levels in tumors. The dataset includes 5470 tumors of various origins assessed by Reverse Phase Protein Array (RPPA).
(b) The gene expression signature indicative of CDK2 activity strongly correlates with Cyclin B1 protein levels (r=0.84, Spearman correlation). Additionally, a negative correlation is observed between protein levels of Cyclin B1 and Met (r=-0.45, Spearman correlation), while no significant correlations are found with other RTKs.
(c) Immunofluorescence staining of breast cancer patient-derived xenograft (PDX) model 7087.
(d) HALO analysis visualization of immunofluorescence staining in breast cancer PDX 7087. The image displays the expression patterns of Cyclin B1 and Met proteins within the tumor tissue. Cyclin B1-positive + Met-negative cells are represented in green, while Cyclin B1-negative + Met-positive cells are shown in red. The distinct color-coding highlights the differential expression patterns of Cyclin B1 and Met proteins within the tumor tissue.

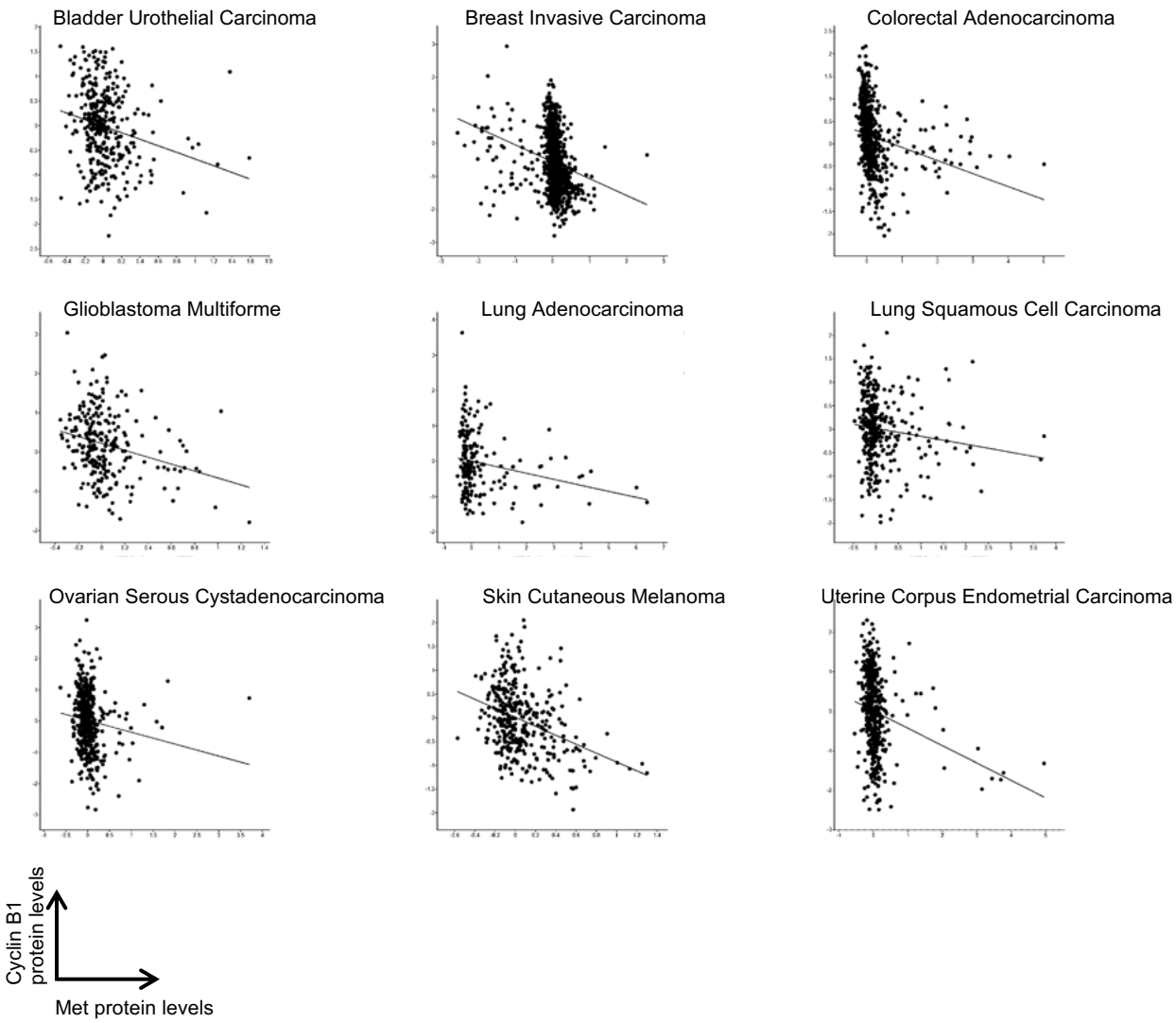


***Figure 3.17 Met and Cyclin B1 protein levels are inversely correlated in different cancer origins of the TCGA datasets***

Inverse correlation of Met and Cyclin B1 protein levels across various cancer origins in the TCGA datasets. Scatter plots represent the protein levels of Met and Cyclin B1 in different cancer types derived from the TCGA datasets. A negative correlation is observed, indicating an inverse relationship between the protein levels of Met and Cyclin B1 across the different cancer origins. The analysis suggests that higher Met protein levels are associated with lower Cyclin B1 protein levels in the examined TCGA datasets, irrespective of the cancer types.

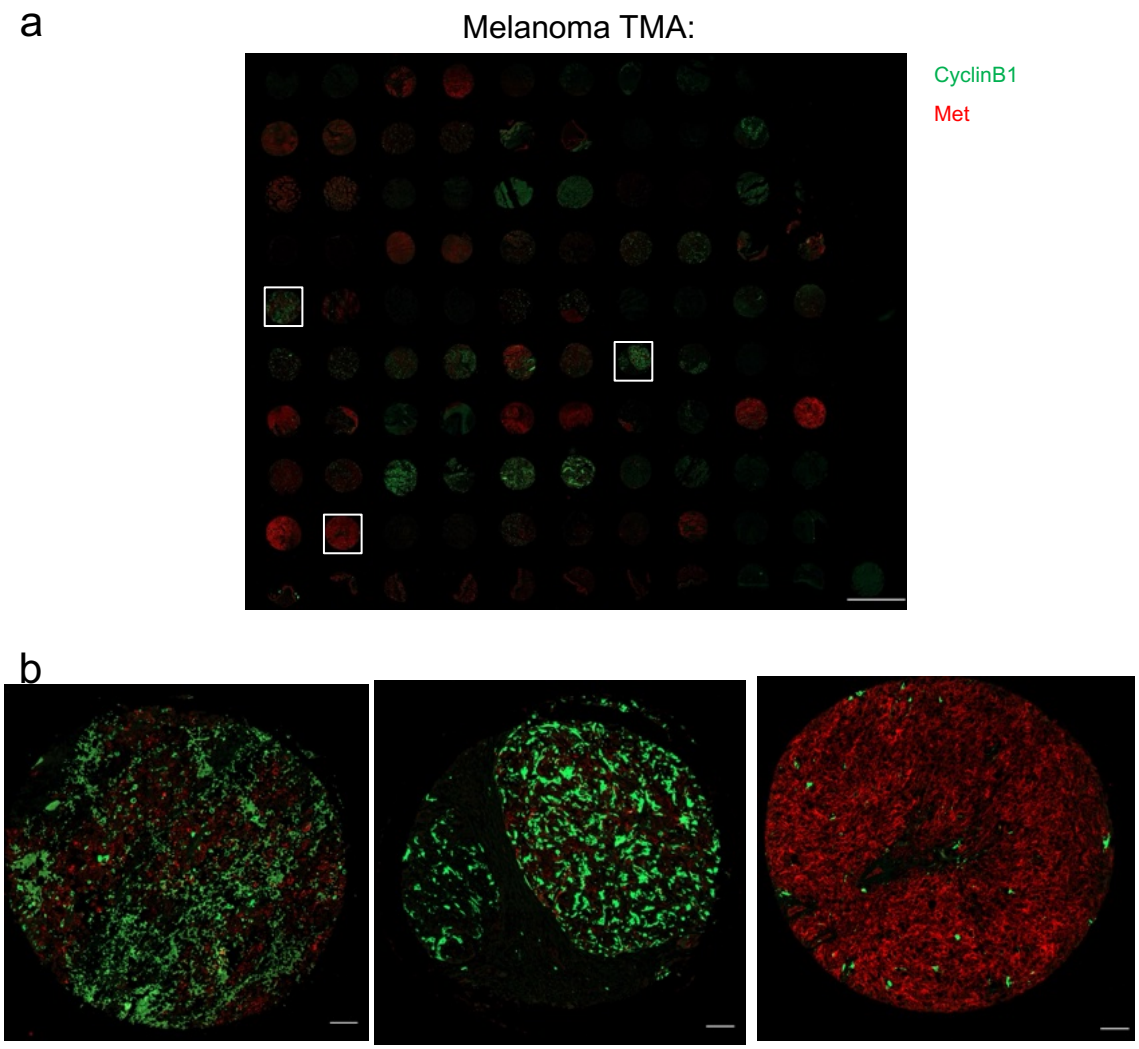


***Figure 3.18 Met and CyclinB1 protein levels negatively correlated in a cohort of patient Melanoma tumor microarrays***

(a) Immunofluorescence staining of a patient Melanoma tumor microarray cohort. The image depicts the expression patterns of Met (red) and Cyclin B1 (green) within the tumor samples.
(b) Representative tumor cores with three distinct patterns are shown.

To confirm the RPPA results, we employed melanoma tumor microarrays encompassing primary patient tumors (N=50, 100 cores, ME1002b, US Biomax Inc). Immunofluorescent imaging of Met and Cyclin B1 co-staining substantiated the pattern of mutual exclusivity noted in the RPPA data (Figure 3.18).

Collectively, these findings present compelling evidence that the cell cycle axis functions as a potent negative regulator of Met. They further suggest that Cyclin B1 protein level could serve as a reliable diagnostic tool to anticipate CDK2 activity and Met protein levels in addition to its previously described predictive utility for patients survival (Aaltonen et al., 2009; Cooper et al., 2009; Soria et al., 2000).

# CHAPTER 4 – GENERAL DISCUSSION

In the tapestry of cell communication, RTKs, G-protein Coupled Receptors (GPCRs), and ion channels are all integral components of cell communication. They act as "gatekeepers" to control the flow of information into and out of cells, and they play key roles in many cellular processes, including cell proliferation and migration.

While we now have a deep understanding of GPCRs and ion channels, including many high-resolution structures determined by cryo-EM, the same cannot be said for RTKs. This may be due in part to the technical challenges associated with determining the full-length receptor structures due to a dynamic single pass transmembrane helix.

In this chapter, I will provide an overview of the current comprehension of the structural regulation between Met and other RTKs, focusing on their structural characteristics and distinct signaling outputs that set Met apart from the rest.

## 4.1 Modulation of RTK activation by juxtamembrane region

While the ligand-binding extracellular domain and the intracellular kinase domain of RTKs have been extensively studied, the juxtamembrane region has often been overlooked. This flexible and dynamic region, typically consisting of over 40 amino acid residues, connects the C-terminus of the transmembrane helix to the intracellular protein kinase domain. In recent years, researchers have shifted their focus to understanding the entire receptor structure, including the JM region, using a combination of experimental and computational approaches such as X-ray crystallography, NMR, and cryo-EM.

Contrary to its initial characterization as a simple linker, the JM region plays a critical role in the regulation of RTK function. The region is essential for dimerization and activation of protein kinase activity, and often contains trafficking signal motifs and binding sites for

calmodulin. Autoinhibition of protein kinase activity by the JM region has been reported for several RTKs, such as FLT3 (Griffith et al., 2004), KIT (Mol et al., 2004), MuSK (Till et al., 2002), and Ephrin family RTKs (Wybenga-Groot et al., 2001). In each case, sequences in the JM region make extensive contacts with several parts of the kinase domain, including the α-C helix (Figure 4.1), and stabilize an autoinhibited conformation. Receptor dimerization promotes trans-phosphorylation of key tyrosines in the JM region, which disrupts the cis-autoinhibitory interactions and promotes receptor activation. For EGFR, the JM region functions as an activation domain and is essential for receptor activation (Jura et al., 2009).

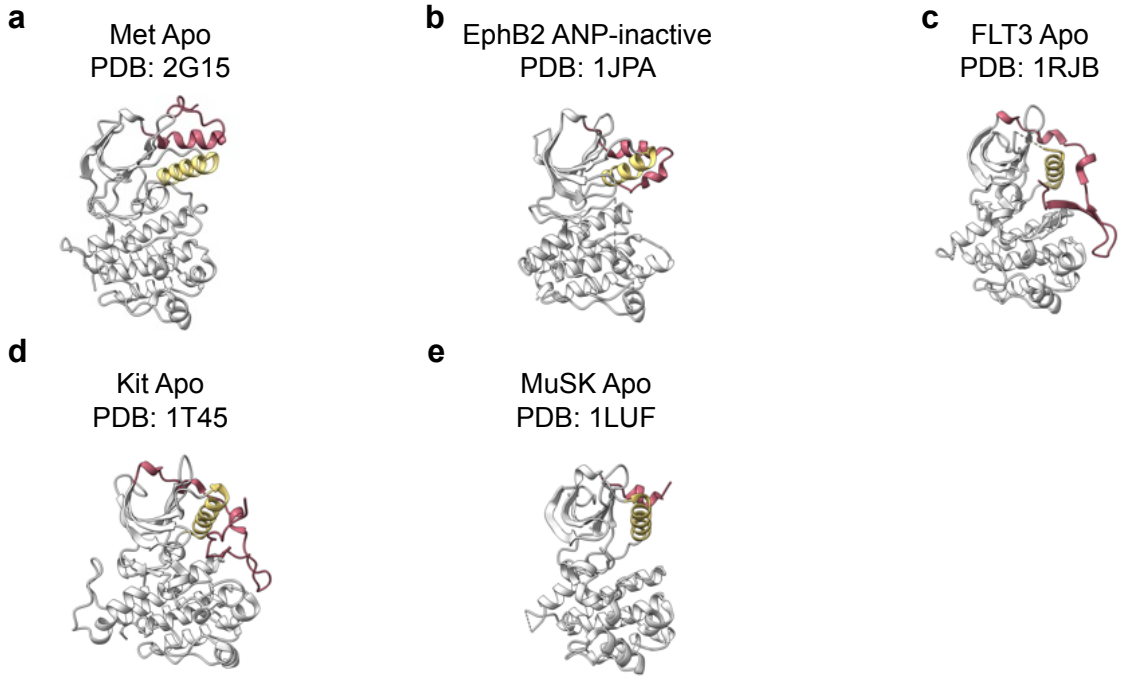


***Figure 4.1 JM autoinhibition across several RTKs***

Crystal structures of autoinhibited receptor tyrosine kinases highlighting the kinase αC helix in yellow and the juxtamembrane region in red. (a) Structure of Met (PDB: 2G15), (b) Structure of EphA2 (PDB: 1JPA), (c) Structure of FLT3 (PDB: 1RJB), (d) Structure of Kit (PDB: 1T45), and (e) Structure of MuSK (PDB: 1LUF). The crystal structures depict

the autoinhibited conformations of these RTKs, with the α-C helix and JM region playing critical roles in maintaining their inactive states. The coloring scheme highlights these regions, providing insights into the structural basis of autoinhibition in the respective RTKs.

RTKs are tightly regulated to maintain basal activity, and autoinhibition manifests through various mechanisms. Similar to TGFβ receptors, phosphorylation of the JM domain in RTKs can remove inhibition upon ligand-induced oligomerization (Schlessinger, 2000). The structural mechanisms underlying these phosphorylation events remain largely unknown, and other kinases may be involved in releasing the autoinhibitory locks established by the JM domains on the receptor kinase domains.

The interactions between JM regions and anionic lipids, particularly phosphatidylinositol 4,5-bisphosphate (PIP2), have been investigated mainly in ErbB1. In vitro Fluorescence Resonance Energy Transfer (FRET) labeling studies and surface plasmon resonance studies have demonstrated that the EGFR JM region is capable of inducing PIP2 clustering and exhibits strong binding to PIP2 These interactions are believed to be mediated through electrostatic interactions between a cluster of basic residues in the JM region and the multiple phosphoryl groups of the PIP2 headgroup (Abd Halim et al., 2015). Molecular dynamics simulations also revealed a conserved interaction pattern shared across all human RTKs. In particular, predominantly the N-terminal residues of the JM region are involved in the interactions with PIP2 (Hedger et al., 2015).

## 4.2 Modulation of RTK activation by carboxy-terminal tail

The ERBB family of proteins are well characterized in cell signaling pathways. These proteins interact through their tail regions, which function as a hub for protein-protein interactions regulated by phosphorylation. Such interactions often involve adapter

proteins that trigger various downstream signaling pathways, including RAS/MAPK, PI3K/Akt, Src kinases, and STAT3 transcription factor-dependent pathways (Schulze et al., 2005).

A striking characteristic of the ERBB family, specifically EGFR and ErbB2, is the long C-terminal tail of about 300 amino acids (AAs). The Met protein has a significantly shorter C-tail, with just 46 AAs. Despite their diverse sequences, the ERBB proteins show a high degree of conservation within the helix and tail regions, highlighting their importance in protein function.

Current research illuminates the pivotal role of the elongated C-terminal tail of ERBB proteins in modulating kinase activity. These tails, hypothesized to possess an intrinsically disordered structure, previously were deemed as simplistic connectors between phosphorylation sites and the rest of the receptor. However, the lack of a definitive, rigid structure is now understood to potentially facilitate their involvement in post-translational modifications, particularly phosphorylation.

Investigations into the EGFR structure have revealed the considerable influence of the C-terminal portion of EGFR's juxtamembrane region on its kinase activity. During EGFR's inactive periods, a structure known as the AP-2 helix arises from the C-terminal tail, interacting with the kinase region. This interaction has implications for the kinase's activity and the way ATP binds to the kinase domain. Subsequent to the AP-2 helix, a segment identified as the "electrostatic hook" interacts with a different part of the kinase (Kovacs et al., 2015). Notably, there seems to be a competition between this hook and the JMB segment for interaction with the kinase. The complexity of this interaction becomes apparent during the kinase's active state when the electrostatic hook binds with another

region of the kinase, allowing the JMB segment to engage with the kinase (Zhang et al., 2006). Emerging studies have proposed that the early portion of the EGFR tail region might inhibit the formation of the active asymmetric dimer, a crucial factor in kinase activity (Pines et al., 2010).

Contrary to the trans-autophosphorylation of the activation loop observed in a multitude of RTKs, ErbB kinases undergo allosteric activation via asymmetric dimerization (Zhang et al., 2006). In contrast, my research reveals that Met activation is facilitated through a symmetric dimerization mechanism, subsequently leading to trans-autophosphorylation of its activation loop. Additionally, a conspicuous difference between Met and ErbB family of receptors is the relatively diminutive C-tail of Met. An intriguing observation, however, is that in the context of this dimeric activation complex, the Met C-tail is docked back onto its respective kinase domain. This poses a conundrum as this docking process renders the C-tail unreachable for trans-phosphorylation. Consequently, the structure of this dimerization does not sufficiently elucidate the mechanism of Met C-tail phosphorylation.

## 4.3 'Go or Grow' - RTK modulated cell fate decision between proliferation and migration

Cellular proliferation and migration are fundamental in numerous biological contexts, such as embryonic development, tissue repair, immune response, and cancer metastasis. These two processes are often regulated by RTKs, with any disruption in this regulatory mechanism potentially leading to pathological conditions like cancer, marked by uncontrolled cell proliferation and migration.

RTKs are known to control cell proliferation by initiating a sequence of intracellular signals once binding with growth factors occurs. Significantly, RTKs activate the Ras/Raf/MEK/ERK pathway, governing the expression of genes vital for cell cycle progression and cell division, thereby regulating cell proliferation. Dysregulation of this pathway can potentially result in pathological conditions, such as cancer.

RTKs also serve a critical role in cell migration, an essential process for development, wound healing, and cancer metastasis. Moreover, RTK signaling can stimulate the release of proteases to degrade the extracellular matrix, thus facilitating cellular movement.

These processes of cell proliferation and migration have an integral role in embryonic development, wound healing, and cancer metastasis. During embryonic development, cellular proliferation and migration cooperate to form the diverse structures of a living organism. Cells proliferate and differentiate into various types, subsequently migrating to their assigned locations to establish different tissues and organs. Regarding wound healing, the body responds by augmenting cell proliferation at the site of the wound to replace damaged cells and regenerate the tissue. Concurrently, specific cells, such as immune cells and fibroblasts, migrate to the wound site to assist the healing process. In cancer, cells often undergo uncontrolled proliferation, leading to tumor formation. Some of these cancer cells may then migrate away from the primary tumor and form secondary tumors in other parts of the body, a process known as metastasis, highlighting a complex interplay between cell proliferation and migration (De Donatis & Cirri, 2008; Schlessinger, 2000).

Often, cell proliferation and migration occur in a mutually exclusive and sequential manner, yet many of the signaling pathways and molecular mechanisms involved are shared. Signals from RTKs can stimulate both processes. Moreover, there is often a balance or trade-off between proliferation and migration, especially in cancer cells that may oscillate between a proliferative and migratory state, a phenomenon known as the "go or grow" phenomenon (Garay et al., 2013). The processes of cell division and migration present striking contrasts. The irreversible nature of cell division is in stark contrast with the reversibility of cell migration. This dichotomy allows for swift alterations or cessation of the signaling mechanisms supporting migration, thereby enabling a change in the cell's phenotypic response. It is also important to highlight that unlike cell proliferation, cell migration is mediated by non-symmetric cell polarization (De Donatis et al., 2010).

The biological response variability to cytokines can be primarily attributed to two key factors: the direct regulation of RTKs and the selective activation of downstream signaling pathways.

### 4.3.1 Control of cell fate by direct RTK regulation

RTKs frequently exhibit biased activation, resulting from varied ligand modulation or differing activation intensities on the same RTK. This bias becomes particularly evident when identical ligands at disparate concentrations produce unique responses. For instance, low-concentration PDGF primarily induces clathrin-mediated endocytosis, recycling the receptor to the plasma membrane to serve as a directional movement sensor.

Significant transformations in cellular behavior transpire when the surrounding cytokine concentration surpasses a certain limit. In these circumstances, high levels of RTK ligand engagement instigate receptor internalization through Rafts/Caveolin-mediated endocytosis (Sigismund et al., 2005). The signaling from the endosomally localized PDGFR is proficient in engaging crucial signaling pathways that bolster cell proliferation (Wang et al., 2004). The translocation of the receptor from plasma or sub-plasma membrane sites to intracellular locations modifies the assortment of intracellular signaling proteins that the receptor recruits. This change concurrently diminishes the rate of PDGFR recycling to the cell surface, as the receptor is directed towards late endosome/lysosomal compartments for degradation (Polo & Di Fiore, 2006). This sequence of events aligns with the cellular commitment to irreversible mitosis, indicating the fulfillment of the RTK's role for the remaining duration of the cell cycle.

Under these conditions, a transition in cellular phenotypes occurs, from migratory to proliferative, signifying an adaptive response to environmental shifts. This dynamic process of RTK activation is intricately connected to the cell cycle, which exercises additional regulatory influence. Specific phases in the cell cycle, notably the G2/M phase (Wee et al., 2015), are linked with a decreased migratory capacity, further modulating the operational flexibility of RTKs.

RTK activation can lead to the formation of ERK pulses/waves, which coordinate cell fate decisions during processes like mammary acinar morphogenesis (Ender et al., 2022). ERK pulses could triggered by the cleavage of pro-EGF ligands by Matrix Metalloproteinases (MMPs), leading to the activation of EGFR (Hiratsuka et al., 2015).

This process can translate slight variations in EGFR input into frequency-modulated regimes of ERK pulses that can specify proliferation, survival, and apoptosis.

### 4.3.2 Control of cell fate by modulation of the ERK signaling pathway

The Raf-MEK-ERK protein kinase cascade is posited to transmit signals from RTKs to the ERK with precise temporal fidelity, a process that is crucial for ERK's accurate interpretation and subsequent initiation of appropriate biological responses. The distinct biological consequences that emerge as a result of ERK activation by various RTKs hinge on the duration and pattern of such activation. This intricate mechanism has been the subject of rigorous scientific scrutiny over several decades, and the collective efforts and sophisticated computational models has significantly augmented our understanding of this phenomenon.

ERK response to different RTKs triggers divergent biological outcomes, a variability that is tied to the duration and modality of ERK activation. This pivotal insight was gleaned from studies conducted on rat pheochromocytoma (PC12) cells in the 1990s, which suggested that the specificity of signaling could be partially attributed to the dynamic features of downstream network responses. The research revealed that the divergent responses of PC12 cells to EGF and nerve growth factor (NGF) were linked to fluctuations in ERK activation. Specifically, transient activation of ERK was associated with cell proliferation, while sustained ERK activation corresponded to cell differentiation (Marshall, 1995). This complex mechanism involves a fine-tuned balance of feedback systems, receptor-level mechanisms, and RTK activation kinetics, all of which are faithfully transmitted via the Raf-MEK-ERK protein kinase cascade.

Although the specific modalities behind these distinct modes of ERK activation remain somewhat elusive, several theories have been proposed. It is postulated that multiple feedback mechanisms, each operating at different downstream levels in the ERK pathway, contribute to defining the dynamics of ERK activation by individual RTKs (Toettcher et al., 2013). Additionally, other studies propose that receptor-level mechanisms and the kinetics of RTK activation also play significant roles in influencing the dynamics of ERK activation (Kiyatkin et al., 2020). The ongoing advancements in computational modelling are poised to further illuminate our understanding of these intricate processes.

## 4.4 Limitations and future directions

While our present study is not devoid of limitations, it highlights that exon 14 tetramerization provides a structural framework that facilitates Met C-tail phosphorylation. Intriguingly, in the absence of exon 14, Met C-tail is also phosphorylated in an HGF dependent manner. This suggests that other regions of Met may have a predisposition to undergo tetramerization upon HGF binding. This interaction could be facilitated by higher-order HGF binding, given that the flexible N-K1-K2-K3 segment of HGF-B presents a compelling potential to interact with a third Met receptor via its K1-SEMA binding site (E. Uchikawa et al., 2021). As a result, there is a possibility for a higher-order assembly of Met and HGF complexes to form on the cellular membrane.

Besides the potential higher order assembly induced by HGF, a careful analysis of the crystal lattice of the Met kinase domain uncovers a potentially vital asymmetric dimer formed crystallographically (PDB: 3QTI) (Tiedt et al., 2011). Here, two kinase domains engage in a head-to-tail interaction through a mainly electrostatic interface. This

interaction takes place primarily at residues Y1307 and E1306, which form salt bridges with K1161. This asymmetric dimer configuration brings the C-lobe of one kinase domain (monomer B) into close contact with the hinge region of the other domain (monomer A). These electrostatic interactions might have a significant impact on the stability and functional activity of this dimer structure (Figure 4.2 a).

Additionally, an asymmetric kinase domain tetramer is observed (PDB: 4KNB) (Steinig et al., 2013). This tetramer is assembled in a manner akin to the asymmetric dimer, with monomers A and C bolstered through the same contacts as monomers AB and BC. This structure suggests a plausible dynamic interchange of positions between the two kinase domains in the AB and BC dimers (Figure 4.2 b).

What makes these interactions within the Met kinase domain particularly noteworthy is their unique occurrence as shown by sequence alignment with EGFR family and other Met family RTKs within the kinase region. The crucial residues K1161, Y1307, and E1306 are specific to Met and do not occur in other RTKs, implying a unique mechanism of interaction and regulation exclusive to Met (Figure 4.2 c). Moving forward, these initial findings necessitate more comprehensive and detailed investigations. Future research should aim to confirm the structure function of these sites biochemically and in cells.

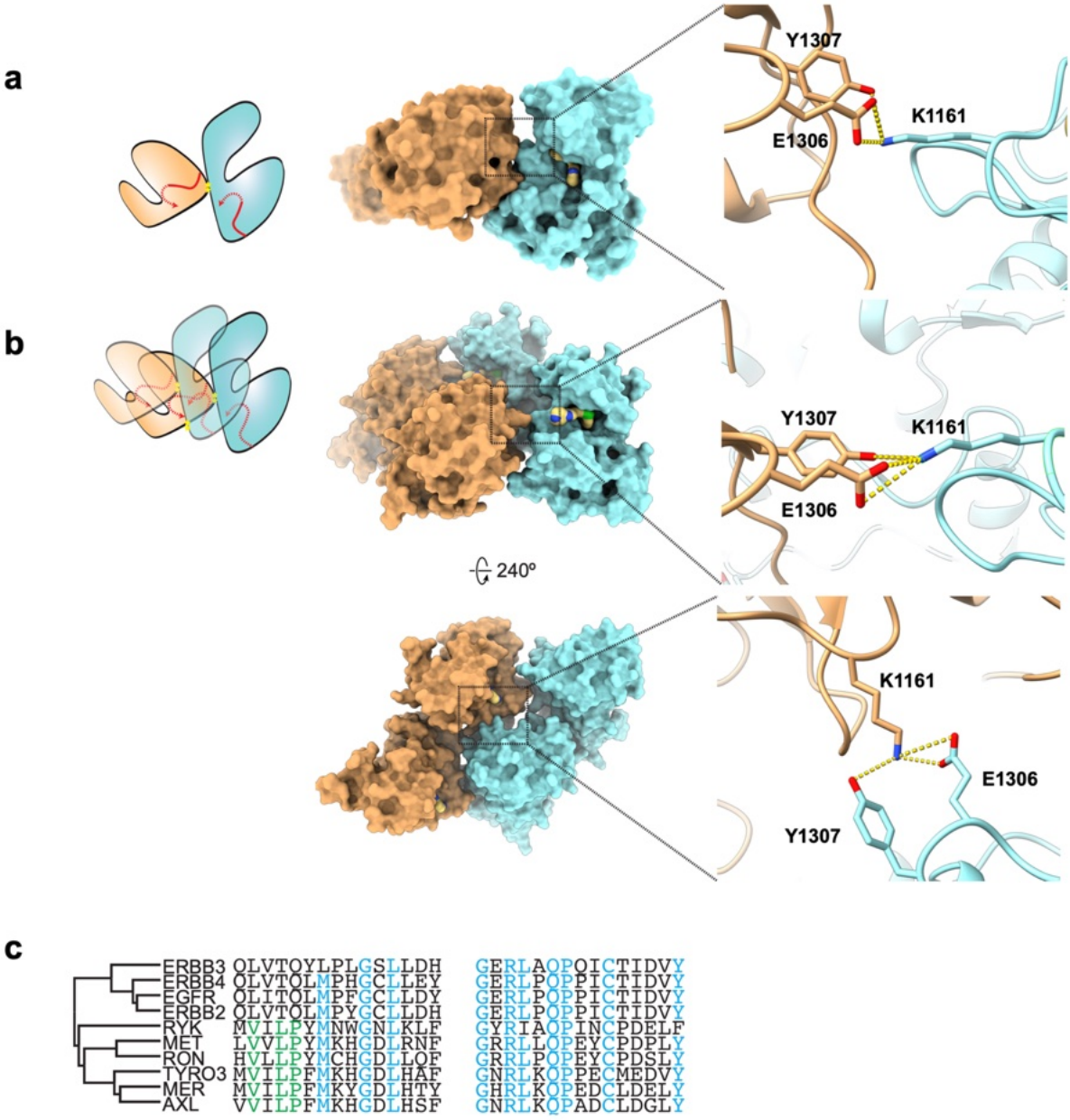


***Figure 4.2 Asymmetrical Met dimer and tetramer***

(a) Crystal structure of Met kinase in complex with NVP-BVU972 (PDB: 3QTI). Monomer A of Met kinase is shown in green, while monomer B is shown in blue. Y1307 and E1306 residues on the kinase c lobe of monomer A are forming salt bridges with K1161 on the hinge region of monomer B.

(b) Crystal structure of Met kinase domain in complex with OSI ligand (PDB: 4KNB). Monomer A and B of Met kinase are shown in green and blue, respectively. Y1307 and E1306 residues on the kinase c lobe of monomer A and B are forming salt bridges with K1161 on the hinge region of monomer C and D, respectively. Additionally, monomer B and C are also connected through the same salt bridge.

(c) Sequence alignment of EGFR and Met family RTKs kinase region. K1161, Y1307, and E1306 residues are unique in Met and not found in other RTKs.

Previous lab work has revealed through gene expression analysis that MetΔex14 elicits a more robust MAPK signaling response in HeLa cells compared to its counterpart, Met-WT (Golenar, 2022).

Intriguingly, my results showed that native HeLa cells did not display enhanced proliferation upon the addition of HGF (Figure 4.3 a). However, when the cells were either subjected to continuous serum starvation or exposed to the CDK2 inhibitor K03861 for 8 hours, the negative regulation of Met by CDK2 was diminished (Figure 4.3 b, c). This suggests the possibility that removing the regulatory influence of CDK2 may potentially boost cellular proliferation, further emphasizing its role in controlling Met.

This inference was validated when we introduced HGF to two MetΔex14 HeLa cell clones. Despite the presence of serum and active CDK2, the cells demonstrated a small but consistent growth advantage at physiological levels of HGF (10U) (Figure 4.3 d, e). This indicates that even in the presence of CDK2, HGF can enhance Met signaling and drive proliferation, especially in cells with Met exon14 skipping.

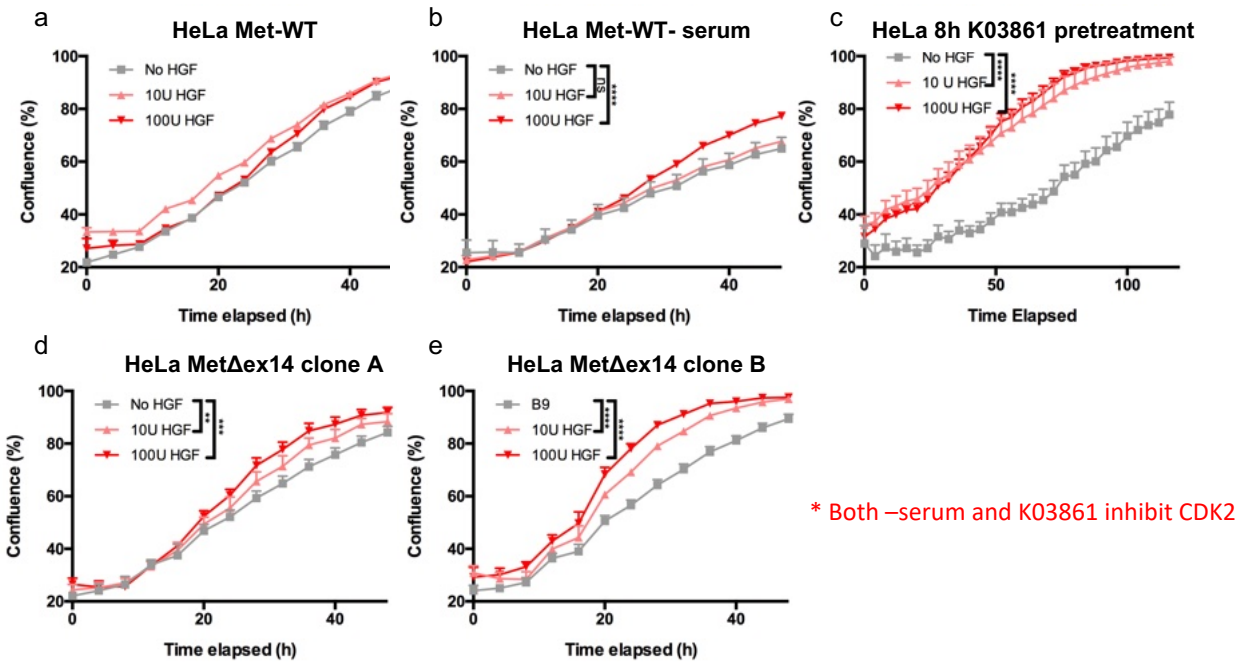


***Figure 4.3 HGF/ MetΔex14 displays growth advantages***

Time course proliferation of wild-type (WT) Met-expressing HeLa cells (a-c) and CRISPR-Cas9 engineered Δex14 clones (d and e). Cells were seeded at a density of 2000 cells per well in 96-well plates (N=3, 5 biological replicates per condition). They were stimulated with HGF at concentrations of 10 U and 100 U. For samples (a, c-e), 10% serum was present, while sample (b) was serum-free. (c) was pre-treated with 10 μM of the CDK2 inhibitor, K03861, for 8 hours before replacing it with a complete medium. Cell growth was monitored by evaluating cell confluency using the Incucyte S3 live-cell analysis system.

Building upon the insights provided by Min et al. (Min et al., 2020), who uncovered the intricate interplay between cumulative MAPK signaling output throughout the cell cycle and the delicate balance between cell proliferation and quiescence, they also demonstrated that not only the intensity but also the duration of MAPK signaling actively influence proliferative outcomes. My biochemical findings support this logic, where we discovered that the Met exon 14 region is phosphorylated in a CDK2 dependent manner, potentially acting as a mechanism to negatively regulate Met-dependent proliferation.

Consequently, if Met exon 14 skipping occurs, cells bypass the regulatory influence of both CDK2 and Cbl. This results in enhanced MAPK signaling intensity coupled with an extended half-life of the signal, thereby favoring cellular proliferation.

These findings corroborate the hypothesis that 'transiently quiescent cells' — those that are temporarily out of the cell cycle — are prevalent in most cell lines, including HeLa (Spencer et al., 2013). In such cells, HGF-induced Met signaling could potentially trigger re-entry into the cell cycle, resulting in enhanced proliferation.

Projecting into the future, the role of a CDK2 inhibitor on MetΔex14 cell lines bears profound implications. Rather than showing resistance to CDK2 regulation, these cells might present a different response, especially when HGF and CDK2 are simultaneously inhibited. This combination could drastically reduce MetΔex14 growth, possibly leading to cell death, signifying a potential partial dependency of MetΔex14 cancers on both Met and CDK2 for survival and growth. Therefore, exploring this complex interplay in future research could lead to the identification of novel therapeutic strategies and enhance our understanding of the involved molecular pathways.

## 4.5 Conclusion

The Met receptor tyrosine kinase, initially characterized as an oncogenic transforming factor, is widely acknowledged for its role in enhancing foci formation and overcoming contact inhibition. The comprehensive characterization of Met developmentally oriented pro-migratory and pro-survival role is well-documented. Previous studies from our laboratory have underscored that Met overexpression, in combination with the loss of p53, triggers tumorigenesis in a mouse model of breast cancer, thereby accentuating the pivotal role of Met in fostering stemness and initiating tumor formation (Knight et al., 2013). One of the frequently occurring mutations in NSCLC and sGBM involves the skipping of Met exon 14 (Hu et al., 2018; Jee et al., 2022; Network, 2014), yet our understanding of the influence of this mutation on the initiation and progression of these cancers still remains limited. The work in this thesis observed that MetΔex14 in these cancers is still dependent on HGF for activation as it lacks intrinsic activity. Our insights have shed light on the role of MetΔex14 in enhancing the sensitivity to physiological levels of HGF, which bears considerable clinical implications as many experimental models utilize saturated levels of HGF. This research further justifies the potential of targeting MetΔex14 cancers, even in the absence of *METΔEX14* amplification, given the frequent detection of HGF in plasma of healthy or diseased patients. In agreement with this, recent studies demonstrated promising therapeutic outcomes with tepotinib and capmatinib, both FDA approved drugs targeting MetΔex14 regardless of the amplification status.

My research further enhances the molecular understanding of Met activation in Met-WT cells. We found that HGF mechanically leads to the creation of extracellular domain

tetramers and subsequent transphosphorylation of the kinase domain Y1234/35 and multi-substrate docking sites Y1349/56. This study also revealed that exon 14 is most stable in a tetrameric form when an isolated peptide is examined. Furthermore, we discovered that a portion of exon 14 is baseline phosphorylated and that this is reversed using inhibitors to CDK1/2 with some preference for CDK2 specificity. This may reflect a feedback inhibitory loop as a consequence of cellular signals or stage of the cell cycle and highlights that phospho-exon 14 might act to decrease responsiveness to HGF following hybridization with non-phosphorylated Met, which based on our substitution studies of a charged residue for S or T may act to restrict exon 14 tetramerization and full activation of Met by HGF. (Figure 4.4)

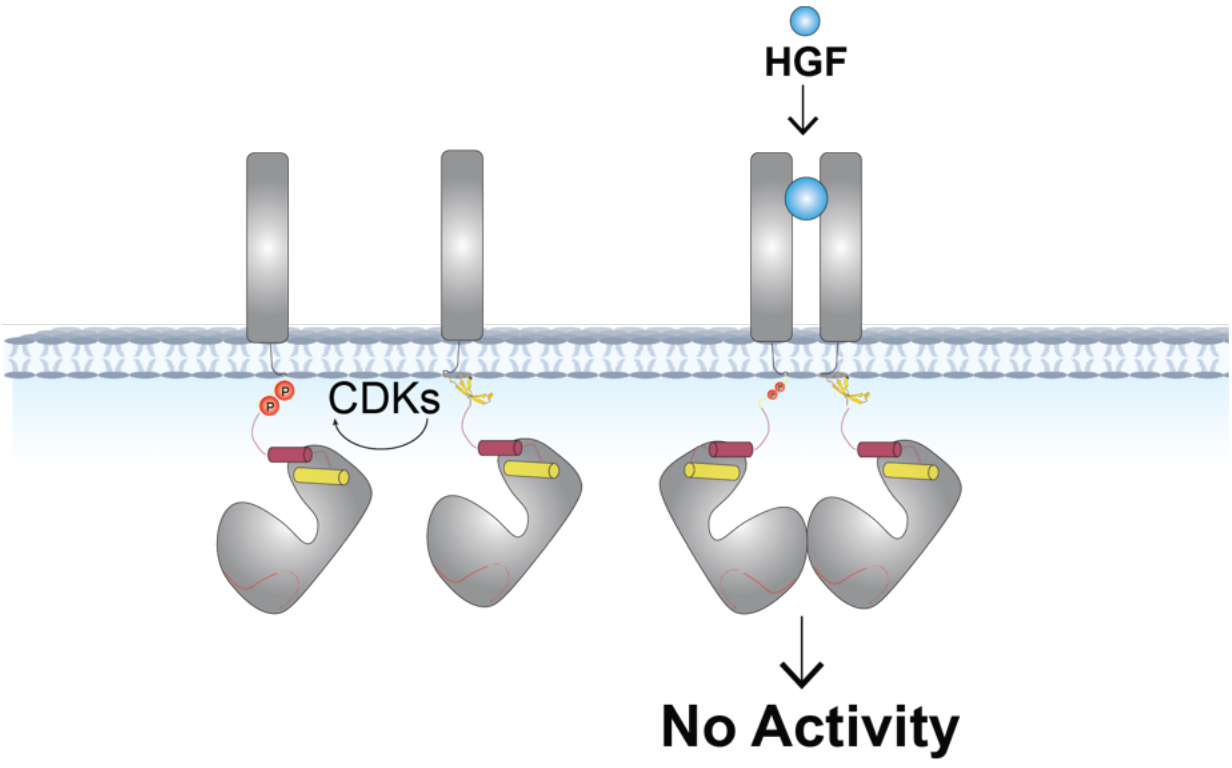


***Figure 4.4 Proposed model for exon 14 phosphorylation on dimerization***

The schematic overview illustrates the negative impact of exon 14 phosphorylation on Met activation. The exon 14 region is susceptible to phosphorylation by other kinases,

including CDKs, under steady-state conditions. This phosphorylation subsequently affects intracellular Met dimerization upon HGF treatment.

As the docking of the Met C-tail to the kinase domain renders it inaccessible for trans-phosphorylation, this structure configuration is incongruous with phosphorylation of the Met C-tail. In such instances, the formation of the Met tetrameric assembly could address this limitation. The Met C-tail phosphorylation is reminiscent of the GS domain of ALK2, a glycine-serine rich area located in the intracellular juxtamembrane portion of the receptor. Upon ligand binding and the formation of the ALK2/BMPR2 tetramer, the GS domain undergoes trans-phosphorylation by the BMPR2 kinase domain. The compatibility of the C-lobe/C-lobe ALK2/BMPR2 dimer with the GS domain further substantiates this binding mechanism (Agnew et al., 2021).

Taken together, my work offers a more improved understanding of the Met activation mechanisms and the driving factors behind exon 14 skipping in cancers.

# CHAPTER 5 – MATERIALS AND METHODS

## CELL CULTURE

The cell lines utilized in this study included HeLa, HEK293T, MKN45, MDA-MB-231, DLD-1, H596, and EBC1. The HeLa, HEK293T, MKN45, MDA-MB-231, and DLD-1 cells were cultured in Dulbecco's Modified Eagle Medium (DMEM), free of antibiotics, but supplemented with 10% fetal bovine serum (FBS). The MKN45, H596, and EBC1 cells were cultured following the ATCC guidelines. All cell lines were maintained at 37°C in a 5% $CO_2$ atmosphere and were confirmed to be mycoplasma-free using the MycoAlert Mycoplasma Detection Kit (Lonza).

## ANTIBODIES AND REAGENTS

The antibodies and reagents used in this study were sourced from various suppliers. Antibodies against phosphorylated Met at Y1234/1235, Y1349, and total Met were obtained from Cell Signaling Technologies. Antibodies against M2-FLAG peptide, actin, and tubulin were from Sigma, while the antibody against the V5 peptide was purchased from Abcam. The HRP-conjugated secondary antibody was sourced from Thermo Fisher, and the IRDye infrared secondary antibodies were acquired from Mandel Scientific. The small molecule inhibitors crizotinib (LC Laboratories), okadaic acid against PP2A, Roscovitine (MedChemExpress), K03861 (Selleck Chemicals), nocodazole, bafilomycin a1 (Sigma) and Taxol (paclitaxel) (Cedarlane) were utilized in the study. HGF was generously provided by Genentech, where one unit (U) was defined as the lowest amount of factor per ml that clearly demonstrates scatter (Zhu, Naujokas, & Park, 1994), Dimethyl sulfoxide (DMSO) was purchased from Sigma and used in comparable volumes as a vehicle control. Dithiobis succinimidyl propionate (DSP) (Thermo Fisher Scientific).

## CLONING

The DNA mutations introduced in this study were generated using in vivo Assembly, a variant of the Gibson assembly method (García-Nafría et al., 2016). The MAMTH and SIMPL vectors were produced using the Gateway system (Invitrogen), and vector recombination was achieved using the Gateway LR Clonase II enzyme kit (Thermo Fisher).

## TRANSIENT TRANSFECTION

Transient transfection was conducted after seeding 50,000 cells in 24-well plates and incubating them in complete medium for 16 hours. A total of 250-500 ng of DNA and 1.5 µl of Lipofectamine 2000 were each diluted separately in 25 µl of Opti-MEM and incubated at room temperature for 5 minutes. The diluted Lipofectamine 2000 was then combined with the diluted DNA and incubated at room temperature for an additional 15 minutes. This mixture was then added dropwise to the HEK293T cells, which were collected for Western blot analysis 24 hours later.

## STABLE CELL LINES

HeLa MetΔex14 clones were used in described (Golenar, 2022). DLD-1 MetΔex14 cell lines were generated using synthetic sgRNAs against the intronic exon 14 region (Integrated DNA Technologies) along with purified Cas9 enzyme (Integrated DNA Technologies). The components were transfected into the cells using RNAi MAX, following the manufacturer's recommendations. To establish clones, a serial dilution was performed by seeding 50 cells into 96-well plates.

T47D stably expressing Met mutants were made by electroporating 1 million T47D cells with 4500ng pSB100X together with 500ng pSB-Bi-GP-Met constructs, 30 hours after transfection, stably integrated cells were selected by 1ug/ml puromycin.

## SMALL-ANGLE X-RAY SCATTERING

A 14 mg peptide correspond to Met exon 14 region (LGSELVRYDARVHTPHLDRLVSARSVSPTTEMVSNESVDYRATFPED) was synthesized by GenScript and verified by mass-spectrometry. Small-angle X-ray scattering data were collected on an in-house SAXSLAB Bio-Nordic beamline at University of Montreal. Scattering data of Met exon 14 region peptide were collected for 10X 120 s at 22°C at concentration of 1 and 4 mg/ml Background scattering from the buffer (25 mM Tris-HCl and 150 mM NaCl at pH 7.5.) was measured for 10X 600 s. Scaling, buffer subtraction, and merging were performed using ScÅtter (https://github.com/rambor/scatterIV ) The merged scattering curve was fitted to AlphaFold predicted random coil and dimeric structures by FoXS using multi-state structural modeling (Schneidman-Duhovny et al., 2016).

## CROSSLINKING

Crosslinking was performed using dithiobis succinimidyl propionate (DSP) at 0.2 mM (Thermo Fisher Scientific) for 30 min at 37 degrees and quenched by 3X wash with 1 M Tris (pH 7.4) after crosslinking, lysates were collected with 1% hot SDS buffer and added 4X Laemmli buffer without reducing reagent, boiled for 5 min, and analysed by SDS–PAGE (4–15%)

## ALPHAFOLD ANALYSIS

For AlphaFold predictions, we used the "alphafold2_multimer_v3" model type, with no templates and 24 recycle iterations. The following parameters were set:

- "num_queries": 1,
- "use_templates": false,
- "num_relax": 0,
- "msa_mode": "mmseqs2_uniref_env",
- "model_type": "alphafold2_multimer_v3",
- "num_models": 5,
- "num_recycles": 24,
- "recycle_early_stop_tolerance": 0.0.

The analysis was conducted using version 1.5.2 of the ColabFold suite. Structure was rendered by ChimeraX1.6

## SHRNA KNOCKDOWN

Knockdown validation in DLD-1 and MDA-MB-231 cells were carried out using shRNAs cloned into pLKO.1 lentiviral vectors. The following clones were used: DYRK1A with TRC Clone IDs TRCN0000000526, TRCN0000199188, TRCN0000197202, TRCN0000199464, and TRCN0000273347; PPP2CA with TRC Clone IDs TRCN0000002482, TRCN0000002484, TRCN0000002485, TRCN0000002483, TRCN0000002486, and TRCN0000380015; MLL with TRC Clone IDs TRCN0000005955, TRCN0000005957, TRCN0000010978, TRCN0000005954, and TRCN0000005956; BCL2L11 with TRC Clone IDs TRCN0000001053 and TRCN0000001054; NAE1 with TRC Clone IDs TRCN0000007240 and TRCN0000007242; ATR with TRC Clone IDs TRCN0000039615 and TRCN0000039616; MYC with TRC Clone IDs TRCN0000039642

and TRCN0000174055; CHEK1 with TRC Clone IDs TRCN0000009942 and TRCN0000009947; and finally, SOCS5 with TRC Clone IDs TRCN0000226420, TRCN0000218055, and TRCN0000218597

## IMMUNOBLOTTING AND IMMUNOPRECIPITATION

Cell lysis for protein extraction was achieved by washing the cells with 1x PBS, followed by lysis using 1% SDS hot lysis buffer (10 mM Tris-HCl, pH 8.0). The lysis mixture was homogenized at 2000 rpm for 5 minutes on a shaker. Total protein concentration was determined using A280 readings on a Nanodrop device. For immunoblotting, the resultant lysate supernatant was mixed in a 3:1 ratio with 4x Laemmli sample buffer (40% glycerol, 240 mM Tris-Cl (pH 6.8), 0.04% bromophenol blue, 8% SDS and 10% beta-mercaptomethanol). The samples were heated at 95°C for 5 minutes, centrifuged, and then electrophoresed on an SDS-PAGE gel. Protein transfer onto a PVDF membrane was followed by blocking with 5% non-fat dry milk powder in TBST. Specific primary antibodies were applied overnight at 4°C in a 5% BSA in TBST solution. Subsequent washes in TBST preceded the application of HRP-conjugated secondary antibodies. Protein bands were visualized using SuperSignal™ West Femto chemiluminescent substrate on a Bio-Rad ChemiDoc MP system.

Immunoprecipitation entailed overnight incubation of 1-2 mg total protein with Met antibody, followed by a 1-hour incubation with pre-washed protein A/G beads at 4°C. After centrifugation and supernatant removal, the beads were washed thrice with cell lysis buffer. The bound protein was eluted using 2x Laemmli buffer.

## PHOS-TAG IMMUNOBLOTTING

For Phos-tag gel immunoblotting, cellular lysates were prepared using 1% SDS lysis buffer. Subsequently, the lysates were separated via 6% SDS-PAGE containing 20 μM Phos-tag (Wako, AAL-107) and 40 uM $MnCl_2$. The resolved proteins were then transferred to PVDF membranes utilizing a wet transfer system, involving Towbin buffer enriched with 25 mM Tris, 192 mM glycine, 20% (v/v) methanol, and 0.1% SDS (pH 8.3). Following the transfer, the PVDF membranes were subjected to blocking using 5% non-fat dry milk for 1 hour at room temperature with gentle agitation. Subsequent steps involved washing the blots with PBST and subsequently incubating them with the specified antibodies. To visualize the protein bands, the SuperSignal™ West Femto chemiluminescent substrate was employed, and the imaging was conducted using a Bio-Rad ChemiDoc MP system.

## FACS-BASED CRISPR SCREEN

sgRNA libraries were transduced at a multiplicity of infection (MOI) of 0.3, targeting a coverage of approximately 1000 cells per sgRNA reagent. The MOI was determined through a 12-point dose-response evaluation, ranging from 0 to 400 μL of viral supernatants in the presence of 5 μg/mL polybrene, with the infection rate gauged via FACS as the percentage of RFP-positive cells. Selection optimization was achieved by calculating the puromycin dose required to effect >95% cell mortality within 72 hours across a six-point dose response ranging from 0 to 5 μg of puromycin.

For the CRISPR screen, 10 million cells were seeded at 30% confluency. After 24 hours, the culture medium was substituted with fresh media supplemented with 5 μg/mL polybrene and lentivirus at an MOI of 0.3. At 30 hours post-infection, cells were trypsinized and transferred into new plates containing 1 ug/ml puromycin. Following 7 days of

infection, cells were harvested, resuspended at a density of 30 million cells/mL, and incubated with Met-PE antibody in the dark for 30 minutes at 4°C. After straining through a 40 μm mesh filter, cells were sorted (BD Fortessa II) either from the lower 10% quartile (Met-Low) or from the upper 10% quartile (Met-high). From each quartile and the unsorted population, 1 million and 2 million cells were collected respectively for DNA extraction.

## ILLUMINA LIBRARY CONSTRUCTION AND SEQUENCING

Genomic DNA from viable cells was isolated using the QIAamp DNA Blood Maxi kit (Qiagen, Germany) and quantified using Nanodrop 2000 (Thermo Fisher) as per the manufacturer's guidelines. Illumina sequencing libraries were generated via PCR amplification, using primers specific to the integrated lentiviral vector backbone sequence. Four PCR reactions, each containing 0.25 μg of transduced sample, were performed per sample. Each 100 μl PCR reaction incorporated 0.5 μM of each PCR primer (Integrated DNA Technologies, Coralville, IA), 0.5 mM dNTPs (Clontech), and 1x Titanium Taq and buffer (Clontech). The PCR cycling protocol was as follows: 1 cycle at 98°C for 5 min; 28 cycles at 95°C for 15 s, 65°C for 15 s, 72°C for 30 s; 1 cycle at 72°C for 5 min. The Illumina libraries were pooled and sequenced on a HiSeq 2500 instrument (Illumina, San Diego, CA). The sgRNA libraries were sequenced with 1x30 b (sgRNA) and 1x11 b (sample index) reads, following the manufacturer's recommendations, using custom sequencing. The read count was adjusted to provide coverage for each sgRNA at approximately 1000 reads. Model-based Analysis of Genome-wide CRISPR-Cas9 Knockout (MAGeCK) (Li et al., 2014) was used to identify genes that are significantly enriched or depleted in the screen.

## MASS SPECTROMETRY ANALYSIS

In our analysis, we utilized tandem mass spectrometry to analyze protein digests. Protein samples ranging from 2 to 10 µg were denatured using Laemmli buffer, subsequently purified through Bio-Rad's TGX precast gels, and digested with trypsin at a ratio of 1:100 for 2 hours at 37°C. The digested peptides were then processed using an EVOQ Triple Quadrupole Mass Spectrometer system at the MUHC. The resultant extracted ion chromatograms were analyzed using Bruker's Data Analysis software.

## MAMTH ASSAY

Transfected reporter cells were lysed 48 hours post-transfection, and their wells were washed with PBS. Reporter lysis buffer from Promega, complemented with Complete EDTA protease inhibitor (Roche), was added before freezing the plates at -80°C to ensure thorough cell lysis. Firefly luciferase activity was measured from cell lysates using a Berthold luminometer, with readings taken across at least three independent experiments.

## CELL MIGRATION

For migration assays, $5 \times 10^4$ cells were seeded directly onto 6.5-mm Corning Costar Transwells. Complete media was added to both top and bottom wells, and the setup was incubated overnight at 37°C. For HGF stimulations, 100 U of HGF was added to the lower wells. The subsequent 20-minute formalin phosphate fixation at room temperature was followed by washing with double-distilled water and staining with 0.1% crystal violet in 20% methanol. Cells on the top layer were removed, and the membranes were left to dry overnight. Imaging was performed using a Retiga 1300 digital camera (QIMAGING,

Burnaby, Canada) and a Zeiss AxioVert 135 microscope (Carl Zeiss Canada Ltd., Toronto, Canada).

## THREE-DIMENSIONAL CELL INVASION ASSAY

A three-dimensional (3D) cell invasion assay was conducted as detailed (Bell et al., 2020). Briefly, each well of a 24-well cell culture treated multidish (Thermo Fisher Scientific) was coated with 25 µl of Geltrex-reduced growth factor basement membrane matrix (Life Technologies) following a 10-minute pre-treatment with 100% ethanol. Cells were then seeded onto the coated wells in a medium consisting of 2% Geltrex and 2% FBS, and cultivated for three days to encourage the formation of spherical colonies. The spheres were subsequently enveloped in 120 µl/well of 3 mg/ml Type I Human Collagen Solution (Advanced BioMatrix) in 10X DMEM and 0.01N NaOH and incubated for an hour at 37 °C. This was succeeded by the introduction of a medium devoid of Geltrex and supplemented with variable concentrations (0.364-36.4 ng/ml) of HGF and okadaic acid targeting PP2A. Using the Incucyte® S3 Live-Cell Analysis System, images were acquired every 30 minutes over a period of 48 hours under standard culture conditions (37 °C, 5% $CO_2$). HeLa cells were plated at a density of 5,000 cells/well in DMEM with 2% FBS and 2% Geltrex. The dispersal of cells from the spheres was quantified using the formula: (spheres with dispersed cells / total spheres) x 100.

## IMMUNOFLUORESCENCE

Cells were plated on glass coverslips at a density of 15,000 cells/well within a 24-well plate, then washed and fixed in 2% paraformaldehyde. Subsequent permeabilization with 0.1% Triton X-100 (Sigma) was followed by a blocking step using 2% BSA. The cells were

then incubated for an hour at 4°C with the primary antibody in a solution of 2% BSA, 0.1% Triton X-100, and 0.05% Tween-20 (Sigma). Following several washes in Triton/Tween buffer, coverslips were incubated at room temperature for 45 minutes with secondary antibodies, washed further, and counterstained with DAPI. Image acquisition was performed on an LSM800 microscope or via Airyscan microscopic imaging (Zeiss), with subsequent analysis conducted using Zen software (Zeiss).

## FLOW CYTOMETRY

For flow cytometry, single cells were stained with fluorophore-conjugated antibodies in 100µl of PBS with 2% FBS for 30 minutes on ice in light-protected conditions. Following two washes, cells were resuspended in PBS with 2% FBS and supplemented with the viability dye 7-AAD (eBioscience 00-6993). Multi-color cell sorting was executed on a FACS CantoII (BD Biosciences) system, and data analysis was performed utilizing the FlowJo software (Tree Star Inc.).

## PROLIFERATION ASSAY

For the proliferation assay, H596 and HeLa cells were seeded in 96-well plates at a density of 2,000 cells/well. Cell confluence was measured over a period of 3-5 days using the IncuCyte® S3 Live-Cell Analysis System, which captured phase-contrast images every four hours.

## RPPA ANALYSIS

RPPA data from TCGA were obtained from: (https://bioinformatics.mdanderson.org/public-datasets/) under the ‘TCGA Level 3 data’.

CDK2 activity signature of TCGA tumors were previously described (McCurdy et al., 2017). The visualization of the data was facilitated using Morpheus (https://software.broadinstitute.org/morpheus/).

## STATISTICAL ANALYSIS

Statistical evaluations of the experimental data were executed using the GraphPad Prism software. Depending on the specific requirements of the data set, either a two-tailed Student's t-test or an analysis of variance (ANOVA) was employed.

# CHAPTER 6 – BIBLIOGRAPHY

Aaltonen, K., Amini, R.-M., Heikkilä, P., Aittomäki, K., Tamminen, A., Nevanlinna, H., & Blomqvist, C. (2009). High cyclin B1 expression is associated with poor survival in breast cancer. *British journal of cancer*, *100*(7), 1055-1060.

Abd Halim, K. B., Koldsø, H., & Sansom, M. S. (2015). Interactions of the EGFR juxtamembrane domain with PIP2-containing lipid bilayers: Insights from multiscale molecular dynamics simulations. *Biochimica et Biophysica Acta (BBA)-General Subjects*, *1850*(5), 1017-1025.

Abella, J. V., Peschard, P., Naujokas, M. A., Lin, T., Saucier, C., Urbé, S., & Park, M. (2005). Met/Hepatocyte growth factor receptor ubiquitination suppresses transformation and is required for Hrs phosphorylation. *Molecular and cellular biology*, *25*(21), 9632-9645.

Abou-Alfa, G. K., Meyer, T., Cheng, A.-L., El-Khoueiry, A. B., Rimassa, L., Ryoo, B.-Y., Cicin, I., Merle, P., Chen, Y., & Park, J.-W. (2018). Cabozantinib in patients with advanced and progressing hepatocellular carcinoma. *New England Journal of Medicine*, *379*(1), 54-63.

Agnew, C., Ayaz, P., Kashima, R., Loving, H. S., Ghatpande, P., Kung, J. E., Underbakke, E. S., Shan, Y., Shaw, D. E., & Hata, A. (2021). Structural basis for ALK2/BMPR2 receptor complex signaling through kinase domain oligomerization. *Nature Communications*, *12*(1), 4950.

Ahn, R., Sabourin, V., Ha, J. R., Cory, S., Maric, G., Im, Y. K., Hardy, W. R., Zhao, H., Park, M., Hallett, M., Siegel, P. M., Pawson, T., & Ursini-Siegel, J. (2013). The

ShcA PTB domain functions as a biological sensor of phosphotyrosine signaling during breast cancer progression. *Cancer Res*, *73*(14), 4521-4532.

Ancot, F., Leroy, C., Muharram, G., Lefebvre, J., Vicogne, J., Lemiere, A., Kherrouche, Z., Foveau, B., Pourtier, A., & Melnyk, O. (2012). Shedding-generated Met receptor fragments can be routed to either the proteasomal or the lysosomal degradation pathway. *Traffic*, *13*(9), 1261-1272.

Bai, X., Sun, P., Wang, X., Long, C., Liao, S., Dang, S., Zhuang, S., Du, Y., Zhang, X., & Li, N. (2023). Structure and dynamics of the EGFR/HER2 heterodimer. *Cell Discovery*, *9*(1), 18.

Bao, Z.-S., Chen, H.-M., Yang, M.-Y., Zhang, C.-B., Yu, K., Ye, W.-L., Hu, B.-Q., Yan, W., Zhang, W., & Akers, J. (2014). RNA-seq of 272 gliomas revealed a novel, recurrent PTPRZ1-MET fusion transcript in secondary glioblastomas. *Genome research*, *24*(11), 1765-1773.

Bardelli, A., Basile, M. L., Audero, E., Giordano, S., WennstroÈm, S., Ménard, S., Comoglio, P. M., & Ponzetto, C. (1999). Concomitant activation of pathways downstream of Grb2 and PI 3-kinase is required for MET-mediated metastasis. *Oncogene*, *18*(5), 1139-1146.

Bardelli, A., Corso, S., Bertotti, A., Hobor, S., Valtorta, E., Siravegna, G., Sartore-Bianchi, A., Scala, E., Cassingena, A., & Zecchin, D. (2013). Amplification of the MET receptor drives resistance to anti-EGFR therapies in colorectal cancer. *Cancer discovery*, *3*(6), 658-673.

Bardelli, A., Longati, P., Gramaglia, D., Basilico, C., Tamagnone, L., Giordano, S., Ballinari, D., Michieli, P., & Comoglio, P. M. (1998). Uncoupling signal transducers

from oncogenic MET mutants abrogates cell transformation and inhibits invasive growth. *Proceedings of the National Academy of Sciences*, *95*(24), 14379-14383.

Barrow-McGee, R., Kishi, N., Joffre, C., Ménard, L., Hervieu, A., Bakhouche, B. A., Noval, A. J., Mai, A., Guzmán, C., & Robbez-Masson, L. (2016). Beta 1-integrin–c-Met cooperation reveals an inside-in survival signalling on autophagy-related endomembranes. *Nature Communications*, *7*(1), 11942.

Bastola, P., Stratton, Y., Kellner, E., Mikhaylova, O., Yi, Y., Sartor, M. A., Medvedovic, M., Biesiada, J., Meller, J., & Czyzyk-Krzeska, M. F. (2013). Folliculin contributes to VHL tumor suppressing activity in renal cancer through regulation of autophagy. *PLoS One*, *8*(7), e70030.

Bell, E. S., Coelho, P. P., & Park, M. (2020). LC3C mediates selective autophagy of the MET RTK, inhibiting cancer cell invasion. *Autophagy*, *16*(5), 959-961.

Bell, E. S., Coelho, P. P., Ratcliffe, C. D., Rajadurai, C. V., Peschard, P., Vaillancourt, R., Zuo, D., & Park, M. (2019). LC3C-mediated autophagy selectively regulates the Met RTK and HGF-stimulated migration and invasion. *Cell Reports*, *29*(12), 4053-4068. e4056.

Bell, E. S., Coelho, P. P., Ratcliffe, C. D. H., Rajadurai, C. V., Peschard, P., Vaillancourt, R., Zuo, D., & Park, M. (2019). LC3C-Mediated Autophagy Selectively Regulates the Met RTK and HGF-Stimulated Migration and Invasion. *Cell Reports*, *29*(12), 4053-4068.e4056.

Bellon, S. F., Kaplan-Lefko, P., Yang, Y., Zhang, Y., Moriguchi, J., Rex, K., Johnson, C. W., Rose, P. E., Long, A. M., O'Connor, A. B., Gu, Y., Coxon, A., Kim, T. S., Tasker, A., Burgess, T. L., & Dussault, I. (2008). c-Met inhibitors with novel binding mode

show activity against several hereditary papillary renal cell carcinoma-related mutations. *J Biol Chem*, *283*(5), 2675-2683.

Berthou, S., Aebersold, D. M., Schmidt, L. S., Stroka, D., Heigl, C., Streit, B., Stalder, D., Gruber, G., Liang, C., & Howlett, A. R. (2004). The Met kinase inhibitor SU11274 exhibits a selective inhibition pattern toward different receptor mutated variants. *Oncogene*, *23*(31), 5387-5393.

Birchmeier, C., Birchmeier, W., Gherardi, E., & Vande Woude, G. F. (2003). Met, metastasis, motility and more. *Nature reviews Molecular cell biology*, *4*(12), 915-925.

Birchmeier, C., & Gherardi, E. (1998). Developmental roles of HGF/SF and its receptor, the c-Met tyrosine kinase. *Trends in cell biology*, *8*(10), 404-410.

Bladt, F., Friese-Hamim, M., Ihling, C., Wilm, C., & Blaukat, A. (2014). The c-Met inhibitor MSC2156119J effectively inhibits tumor growth in liver cancer models. *Cancers*, *6*(3), 1736-1752.

Bladt, F., Riethmacher, D., Isenmann, S., Aguzzi, A., & Birchmeier, C. (1995). Essential role for the c-met receptor in the migration of myogenic precursor cells into the limb bud. *Nature*, *376*, 768-771.

Bolanos-Garcia, V. M. (2005). MET meet adaptors: functional and structural implications in downstream signalling mediated by the Met receptor. *Mol Cell Biochem*, *276*(1-2), 149-157.

Bottaro, D. P., Rubin, J. S., Faletto, D. L., Chan, A. M., Kmiecik, T. E., Vande Woude, G. F., & Aaronson, S. A. (1991). Identification of the hepatocyte growth factor receptor as the c-met proto-oncogene product. *Science*, *251*(4995), 802-804.

Bubendorf, L., Dafni, U., Schöbel, M., Finn, S. P., Tischler, V., Sejda, A., Marchetti, A., Thunnissen, E., Verbeken, E. K., & Warth, A. (2017). Prevalence and clinical association of MET gene overexpression and amplification in patients with NSCLC: Results from the European Thoracic Oncology Platform (ETOP) Lungscape project. *Lung Cancer*, *111*, 143-149.

Camidge, D. R., Moran, T., Demedts, I., Grosch, H., Di Mercurio, J.-P., Mileham, K. F., Molina, J. R., Juan Vidal, O., Bepler, G., & Goldman, J. W. (2016). A randomized, open-label, phase 2 study of emibetuzumab plus erlotinib (LY+ E) and emibetuzumab monotherapy (LY) in patients with acquired resistance to erlotinib and MET diagnostic positive (MET Dx+) metastatic NSCLC. In: American Society of Clinical Oncology.

Catenacci, D. V., Tebbutt, N. C., Davidenko, I., Murad, A. M., Al-Batran, S.-E., Ilson, D. H., Tjulandin, S., Gotovkin, E., Karaszewska, B., & Bondarenko, I. (2017). Rilotumumab plus epirubicin, cisplatin, and capecitabine as first-line therapy in advanced MET-positive gastric or gastro-oesophageal junction cancer (RILOMET-1): a randomised, double-blind, placebo-controlled, phase 3 trial. *The Lancet Oncology*, *18*(11), 1467-1482.

Caton, A., Hacker, A., Naeem, A., Livet, J., Maina, F., Bladt, F., Klein, R., Birchmeier, C., & Guthrie, S. (2000). The branchial arches and HGF are growth-promoting and chemoattractant for cranial motor axons. *Development*, *127*(8), 1751-1766.

Chen, B., Brinkmann, K., Chen, Z., Pak, C. W., Liao, Y., Shi, S., Henry, L., Grishin, N. V., Bogdan, S., & Rosen, M. K. (2014). The WAVE regulatory complex links diverse receptors to the actin cytoskeleton. *Cell*, *156*(1-2), 195-207.

Chen, H. H., Su, W.-C., Lin, P.-W., Guo, H.-R., & Lee, W.-Y. (2007). Hypoxia-inducible factor-1α correlates with MET and metastasis in node-negative breast cancer. *Breast cancer research and treatment*, *103*, 167-175.

Chirgadze, D. Y., Hepple, J. P., Zhou, H., Byrd, R. A., Blundell, T. L., & Gherardi, E. (1999). Crystal structure of the NK1 fragment of HGF/SF suggests a novel mode for growth factor dimerization and receptor binding. *Nat Struct Biol*, *6*(1), 72-79.

Chou, P. Y., & Fasman, G. D. (1977). β-turns in proteins. *Journal of Molecular Biology*, *115*(2), 135-175.

Clark, D., Smith, S., Sharkey, A., Sowter, H., & Charnock-Jones, D. (1996). Hepatocyte growth factor/scatter factor and its receptor c-met: localisation and expression in the human placenta throughout pregnancy. *Journal of Endocrinology*, *151*(3), 459-467.

Coelho, P. P., Hesketh, G. G., Pedersen, A., Kuzmin, E., Fortier, A.-M. N., Bell, E. S., Ratcliffe, C. D., Gingras, A.-C., & Park, M. (2022). Endosomal LC3C-pathway selectively targets plasma membrane cargo for autophagic degradation. *Nature Communications*, *13*(1), 3812.

Cooper, C. S., Park, M., Blair, D. G., Tainsky, M. A., Huebner, K., Croce, C. M., & Vande Woude, G. F. (1984). Molecular cloning of a new transforming gene from a chemically transformed human cell line. *Nature*, *311*(5981), 29-33.

Cooper, W. A., Kohonen-Corish, M. R., McCaughan, B., Kennedy, C., Sutherland, R. L., & Lee, C. S. (2009). Expression and prognostic significance of cyclin B1 and cyclin A in non-small cell lung cancer. *Histopathology*, *55*(1), 28-36.

Cui, Q., Cai, C.-Y., Gao, H.-L., Ren, L., Ji, N., Gupta, P., Yang, Y., Shukla, S., Ambudkar, S. V., & Yang, D.-H. (2019). Glesatinib, a c-MET/SMO dual inhibitor, antagonizes P-glycoprotein mediated multidrug resistance in cancer cells. *Frontiers in Oncology*, *9*, 313.

D'Arcangelo, M., & Cappuzzo, F. (2013). Focus on the potential role of ficlatuzumab in the treatment of non-small cell lung cancer. *Biologics: Targets and Therapy*, 61-68.

Dance, M., Montagner, A., Salles, J.-P., Yart, A., & Raynal, P. (2008). The molecular functions of Shp2 in the Ras/Mitogen-activated protein kinase (ERK1/2) pathway. *Cellular signalling*, *20*(3), 453-459.

Daub, H., Olsen, J. V., Bairlein, M., Gnad, F., Oppermann, F. S., Körner, R., Greff, Z., Kéri, G., Stemmann, O., & Mann, M. (2008). Kinase-selective enrichment enables quantitative phosphoproteomics of the kinome across the cell cycle. *Molecular cell*, *31*(3), 438-448.

De Brabander, M., Geuens, G., Nuydens, R., Willebrords, R., Aerts, F., De Mey, J., & McIntosh, J. (1986). Microtubule dynamics during the cell cycle: the effects of taxol and nocodazole on the microtubule system of Pt K2 cells at different stages of the mitotic cycle. In *International review of cytology* (Vol. 101, pp. 215-274). Elsevier.

De Donatis, A., & Cirri, P. (2008). Understanding the specificity of receptor tyrosine kinases signaling. *Communicative & Integrative Biology*, *1*(2), 156-157.

De Donatis, A., Ranaldi, F., & Cirri, P. (2010). Reciprocal control of cell proliferation and migration. *Cell Communication and Signaling*, *8*(1), 1-4.

de Jong, R. M., & Dijkstra, B. W. (2003). Structure and mechanism of bacterial dehalogenases: different ways to cleave a carbon-halogen bond. *Curr Opin Struct Biol*, *13*(6), 722-730.

Deheuninck, J., Foveau, B., Goormachtigh, G., Leroy, C., Ji, Z., Tulasne, D., & Fafeur, V. (2008). Caspase cleavage of the MET receptor generates an HGF interfering fragment. *Biochemical and biophysical research communications*, *367*(3), 573-577.

Desai, A., Menon, S. P., & Dy, G. K. (2016). Alterations in genes other than EGFR/ALK/ROS1 in non-small cell lung cancer: trials and treatment options. *Cancer Biol Med*, *13*(1), 77-86.

Di Renzo, M. F., Olivero, M., Giacomini, A., Porte, H., Chastre, E., Mirossay, L., Nordlinger, B., Bretti, S., Bottardi, S., & Giordano, S. (1995). Overexpression and amplification of the met/HGF receptor gene during the progression of colorectal cancer. *Clinical cancer research: an official journal of the American Association for Cancer Research*, *1*(2), 147-154.

Diwanji, D., Trenker, R., Thaker, T. M., Wang, F., Agard, D. A., Verba, K. A., & Jura, N. (2021). Structures of the HER2–HER3–NRG1β complex reveal a dynamic dimer interface. *Nature*, *600*(7888), 339-343.

Drilon, A., Cappuzzo, F., Ou, S.-H. I., & Camidge, D. R. (2017). Targeting MET in lung cancer: will expectations finally be MET? *Journal of Thoracic Oncology*, *12*(1), 15-26.

Duan, Z., Choy, E., Nielsen, G. P., Rosenberg, A., Iafrate, J., Yang, C., Schwab, J., Mankin, H., Xavier, R., & Hornicek, F. J. (2010). Differential expression of

microRNA (miRNA) in chordoma reveals a role for miRNA-1 in Met expression. *Journal of Orthopaedic Research*, *28*(6), 746-752.

Ebens, A., Brose, K., Leonardo, E. D., Hanson Jr, M. G., Bladt, F., Birchmeier, C., Barres, B. A., & Tessier-Lavigne, M. (1996). Hepatocyte growth factor/scatter factor is an axonal chemoattractant and a neurotrophic factor for spinal motor neurons. *Neuron*, *17*(6), 1157-1172.

El Bezawy, R., De Cesare, M., Pennati, M., Deraco, M., Gandellini, P., Zuco, V., & Zaffaroni, N. (2017). Antitumor activity of miR-34a in peritoneal mesothelioma relies on c-MET and AXL inhibition: persistent activation of ERK and AKT signaling as a possible cytoprotective mechanism. *J Hematol Oncol*, *10*(1), 19.

Ender, P., Gagliardi, P. A., Dobrzyński, M., Frismantiene, A., Dessauges, C., Höhener, T., Jacques, M.-A., Cohen, A. R., & Pertz, O. (2022). Spatiotemporal control of ERK pulse frequency coordinates fate decisions during mammary acinar morphogenesis. *Developmental cell*, *57*(18), 2153-2167. e2156.

Engstrom, L. D., Aranda, R., Lee, M., Tovar, E. A., Essenburg, C. J., Madaj, Z., Chiang, H., Briere, D., Hallin, J., & Lopez-Casas, P. P. (2017). Glesatinib Exhibits Antitumor Activity in Lung Cancer Models and Patients Harboring MET Exon 14 Mutations and Overcomes Mutation-mediated Resistance to Type I MET Inhibitors in Nonclinical ModelsGlesatinib Circumvents Resistance to Type I MET Inhibitors. *Clinical Cancer Research*, *23*(21), 6661-6672.

Fixman, E. D., Fournier, T. M., Kamikura, D. M., Naujokas, M. A., & Park, M. (1996). Pathways downstream of Shc and Grb2 are required for cell transformation by the tpr-Met oncoprotein. *Journal of Biological Chemistry*, *271*(22), 13116-13122.

Fixman, E. D., Holgado-Madruga, M., Nguyen, L., Kamikura, D. M., Fournier, T. M., Wong, A. J., & Park, M. (1997). Efficient cellular transformation by the Met oncoprotein requires a functional Grb2 binding site and correlates with phosphorylation of the Grb2-associated proteins, Cbl and Gab1. *Journal of Biological Chemistry*, *272*(32), 20167-20172.

Forman-Kay, J. D., & Pawson, T. (1999). Diversity in protein recognition by PTB domains. *Current opinion in structural biology*, *9*(6), 690-695.

Fournier, T. M., Kamikura, D., Teng, K., & Park, M. (1996). Branching tubulogenesis but not scatter of madin-darby canine kidney cells requires a functional Grb2 binding site in the Met receptor tyrosine kinase. *Journal of Biological Chemistry*, *271*(36), 22211-22217.

Foveau, B., Ancot, F., Leroy, C., Petrelli, A., Reiss, K., Vingtdeux, V., Giordano, S., Fafeur, V., & Tulasne, D. (2009). Down-regulation of the met receptor tyrosine kinase by presenilin-dependent regulated intramembrane proteolysis. *Mol Biol Cell*, *20*(9), 2495-2507.

Foveau, B., Leroy, C., Ancot, F., Deheuninck, J., Ji, Z., Fafeur, V., & Tulasne, D. (2007). Amplification of apoptosis through sequential caspase cleavage of the MET tyrosine kinase receptor. *Cell Death & Differentiation*, *14*(4), 752-764.

Franco, M. L., Nadezhdin, K. D., Goncharuk, S. A., Mineev, K. S., Arseniev, A. S., & Vilar, M. (2020). Structural basis of the transmembrane domain dimerization and rotation in the activation mechanism of the TRKA receptor by nerve growth factor. *Journal of Biological Chemistry*, *295*(1), 275-286.

Furge, K. A., Zhang, Y.-W., & Vande Woude, G. F. (2000). Met receptor tyrosine kinase: enhanced signaling through adapter proteins. *Oncogene*, *19*(49), 5582-5589.

Furge, K. A., Zhang, Y. W., & Vande Woude, G. F. (2000). Met receptor tyrosine kinase: enhanced signaling through adapter proteins. *Oncogene*, *19*(49), 5582-5589.

Garay, T., Juhász, É., Molnár, E., Eisenbauer, M., Czirók, A., Dekan, B., László, V., Hoda, M. A., Döme, B., & Tímár, J. (2013). Cell migration or cytokinesis and proliferation?–revisiting the "go or grow" hypothesis in cancer cells in vitro. *Experimental cell research*, *319*(20), 3094-3103.

Garcia-Guzman, M., Dolfi, F., Zeh, K., & Vuori, K. (1999). Met-induced JNK activation is mediated by the adapter protein Crk and correlates with the Gab1–Crk signaling complex formation. *Oncogene*, *18*(54), 7775-7786.

García-Nafría, J., Watson, J. F., & Greger, I. H. (2016). IVA cloning: A single-tube universal cloning system exploiting bacterial In Vivo Assembly. *Scientific Reports*, *6*(1), 27459.

Garzotto, D., Giacobini, P., Crepaldi, T., Fasolo, A., & De Marchis, S. (2008). Hepatocyte growth factor regulates migration of olfactory interneuron precursors in the rostral migratory stream through Met–Grb2 coupling. *Journal of Neuroscience*, *28*(23), 5901-5909.

Gebreyohannes, Y. K., Schöffski, P., Van Looy, T., Wellens, J., Vreys, L., Cornillie, J., Vanleeuw, U., Aftab, D. T., Debiec-Rychter, M., Sciot, R., & Wozniak, A. (2016). Cabozantinib Is Active against Human Gastrointestinal Stromal Tumor Xenografts Carrying Different KIT Mutations. *Mol Cancer Ther*, *15*(12), 2845-2852.

Gelsomino, F., Facchinetti, F., Haspinger, E., Garassino, M., Trusolino, L., De Braud, F., & Tiseo, M. (2014). Targeting the MET gene for the treatment of non-small-cell lung cancer. *Critical reviews in oncology/hematology*, *89*(2), 284-299.

Gherardi, E., Birchmeier, W., Birchmeier, C., & Vande Woude, G. (2012). Targeting MET in cancer: rationale and progress. *Nat Rev Cancer*, *12*(2), 89-103.

Gherardi, E., Love, C. A., Esnouf, R. M., & Jones, E. Y. (2004). The sema domain. *Curr Opin Struct Biol*, *14*(6), 669-678.

Gherardi, E., Sandin, S., Petoukhov, M. V., Finch, J., Youles, M. E., Ofverstedt, L. G., Miguel, R. N., Blundell, T. L., Vande Woude, G. F., Skoglund, U., & Svergun, D. I. (2006). Structural basis of hepatocyte growth factor/scatter factor and MET signalling. *Proc Natl Acad Sci U S A*, *103*(11), 4046-4051.

Gherardi, E., Youles, M. E., Miguel, R. N., Blundell, T. L., Iamele, L., Gough, J., Bandyopadhyay, A., Hartmann, G., & Butler, P. J. (2003). Functional map and domain structure of MET, the product of the c-met protooncogene and receptor for hepatocyte growth factor/scatter factor. *Proc Natl Acad Sci U S A*, *100*(21), 12039-12044.

Giordano, S. (2009). Rilotumumab, a mAb against human hepatocyte growth factor for the treatment of cancer. *Curr Opin Mol Ther*, *11*(4), 448-455.

Giordano, S., Di Renzo, M. F., Narsimhan, R. P., Cooper, C. S., Rosa, C., & Comoglio, P. M. (1989). Biosynthesis of the protein encoded by the c-met proto-oncogene. *Oncogene*, *4*(11), 1383-1388.

Glodde, N., Bald, T., van den Boorn-Konijnenberg, D., Nakamura, K., O'Donnell, J. S., Szczepanski, S., Brandes, M., Eickhoff, S., Das, I., Shridhar, N., Hinze, D., Rogava,

M., van der Sluis, T. C., Ruotsalainen, J. J., Gaffal, E., Landsberg, J., Ludwig, K. U., Wilhelm, C., Riek-Burchardt, M., . . . Hölzel, M. (2017). Reactive Neutrophil Responses Dependent on the Receptor Tyrosine Kinase c-MET Limit Cancer Immunotherapy. *Immunity*, *47*(4), 789-802.e789.

Glück, A. A., Orlando, E., Leiser, D., Poliaková, M., Nisa, L., Quintin, A., Gavini, J., Stroka, D. M., Berezowska, S., Bubendorf, L., Blaukat, A., Aebersold, D. M., Medová, M., & Zimmer, Y. (2018). Identification of a MET-eIF4G1 translational regulation axis that controls HIF-1α levels under hypoxia. *Oncogene*, *37*(30), 4181-4196.

Golenar, T. (2022). Oncogenic activity of met receptor tyrosine kinase exon 14 deletion variant.

Griffith, J., Black, J., Faerman, C., Swenson, L., Wynn, M., Lu, F., Lippke, J., & Saxena, K. (2004). The structural basis for autoinhibition of FLT3 by the juxtamembrane domain. *Molecular cell*, *13*(2), 169-178.

Gual, P., Giordano, S., Anguissola, S., Parker, P. J., & Comoglio, P. M. (2001). Gab1 phosphorylation: a novel mechanism for negative regulation of HGF receptor signaling. *Oncogene*, *20*(2), 156-166.

Gual, P., Giordano, S., Williams, T. A., Rocchi, S., Van Obberghen, E., & Comoglio, P. M. (2000). Sustained recruitment of phospholipase C-γ to Gab1 is required for HGF-induced branching tubulogenesis. *Oncogene*, *19*(12), 1509-1518.

Gui, Y., Yeganeh, M., Donates, Y. C., Tobelaim, W. S., Chababi, W., Mayhue, M., Yoshimura, A., Ramanathan, S., Saucier, C., & Ilangumaran, S. (2015). Regulation of MET receptor tyrosine kinase signaling by suppressor of cytokine signaling 1 in hepatocellular carcinoma. *Oncogene*, *34*(46), 5718-5728.

Gunasekaran, K., Gomathi, L., Ramakrishnan, C., Chandrasekhar, J., & Balaram, P. (1998). Conformational interconversions in peptide β-turns: analysis of turns in proteins and computational estimates of barriers. *Journal of Molecular Biology*, *284*(5), 1505-1516.

Hammond, D. E., Carter, S., McCullough, J., Urbé, S., Vande Woude, G., & Clague, M. J. (2003). Endosomal dynamics of Met determine signaling output. *Molecular biology of the cell*, *14*(4), 1346-1354.

Hammond, D. E., Urbé, S., Vande Woude, G. F., & Clague, M. J. (2001). Down-regulation of MET, the receptor for hepatocyte growth factor. *Oncogene*, *20*(22), 2761-2770.

Hashigasako, A., Machide, M., Nakamura, T., Matsumoto, K., & Nakamura, T. (2004). Bi-directional regulation of Ser-985 phosphorylation of c-met via protein kinase C and protein phosphatase 2A involves c-Met activation and cellular responsiveness to hepatocyte growth factor. *J Biol Chem*, *279*(25), 26445-26452.

He, A. R., Cohen, R. B., Denlinger, C. S., Sama, A., Birnbaum, A., Hwang, J., Sato, T., Lewis, N., Mynderse, M., & Niland, M. (2019). First-in-human phase I study of merestinib, an oral multikinase inhibitor, in patients with advanced cancer. *The oncologist*, *24*(9), e930-e942.

Hedger, G., Sansom, M. S., & Koldsø, H. (2015). The juxtamembrane regions of human receptor tyrosine kinases exhibit conserved interaction sites with anionic lipids. *Scientific Reports*, *5*(1), 1-10.

Heigener, D. F., & Reck, M. (2014). Crizotinib. *Recent Results Cancer Res*, *201*, 197-205.

Heigener, D. F., & Reck, M. (2018). Crizotinib. *Recent Results Cancer Res*, *211*, 57-65.

Heist, R. S., Shim, H. S., Gingipally, S., Mino-Kenudson, M., Le, L., Gainor, J. F., Zheng, Z., Aryee, M., Xia, J., & Jia, P. (2016). MET exon 14 skipping in non-small cell lung cancer. *The oncologist*, *21*(4), 481-486.

Hemler, M. E. (2001). Retooling of the beta 4 integrin in tumor cells--ligands lost and kinase gained. *Dev Cell*, *1*(6), 728-730.

Hiratsuka, T., Fujita, Y., Naoki, H., Aoki, K., Kamioka, Y., & Matsuda, M. (2015). Intercellular propagation of extracellular signal-regulated kinase activation revealed by in vivo imaging of mouse skin. *Elife*, *4*, e05178.

Hong, D. S., LoRusso, P., Hamid, O., Janku, F., Kittaneh, M., Catenacci, D. V., Chan, E., Bekaii-Saab, T., Gadgeel, S. M., & Loberg, R. D. (2019). Phase I Study of AMG 337, a Highly Selective Small-molecule MET Inhibitor, in Patients with Advanced Solid TumorsAMG 337 in Patients with Advanced Solid Tumors. *Clinical Cancer Research*, *25*(8), 2403-2413.

Hu, H., Mu, Q., Bao, Z., Chen, Y., Liu, Y., Chen, J., Wang, K., Wang, Z., Nam, Y., Jiang, B., Sa, J. K., Cho, H. J., Her, N. G., Zhang, C., Zhao, Z., Zhang, Y., Zeng, F., Wu, F., Kang, X., . . . Jiang, T. (2018). Mutational Landscape of Secondary Glioblastoma Guides MET-Targeted Trial in Brain Tumor. *Cell*, *175*(6), 1665-1678 e1618.

Huang, Y., Ognjenovic, J., Karandur, D., Miller, K., Merk, A., Subramaniam, S., & Kuriyan, J. (2021). A molecular mechanism for the generation of ligand-dependent differential outputs by the epidermal growth factor receptor. *Elife*, *10*.

Huh, C.-G., Factor, V. M., Sánchez, A., Uchida, K., Conner, E. A., & Thorgeirsson, S. S. (2004). Hepatocyte growth factor/c-met signaling pathway is required for efficient

liver regeneration and repair. *Proceedings of the National Academy of Sciences*, *101*(13), 4477-4482.

Jee, J., Lebow, E. S., Yeh, R., Das, J. P., Namakydoust, A., Paik, P. K., Chaft, J. E., Jayakumaran, G., Rose Brannon, A., Benayed, R., Zehir, A., Donoghue, M., Schultz, N., Chakravarty, D., Kundra, R., Madupuri, R., Murciano-Goroff, Y. R., Tu, H. Y., Xu, C. R., . . . Li, B. T. (2022). Overall survival with circulating tumor DNA-guided therapy in advanced non-small-cell lung cancer. *Nat Med*, *28*(11), 2353-2363.

Jeffers, M., Taylor, G. A., Weidner, K. M., Omura, S., & Vande Woude, G. F. (1997). Degradation of the Met tyrosine kinase receptor by the ubiquitin-proteasome pathway. *Mol Cell Biol*, *17*(2), 799-808.

Jeong, A. L., & Yang, Y. (2013). PP2A function toward mitotic kinases and substrates during the cell cycle. *BMB reports*, *46*(6), 289.

Jiao, Y., Ou, W., Meng, F., Zhou, H., & Wang, A. (2011). Targeting HSP90 in ovarian cancers with multiple receptor tyrosine kinase coactivation. *Mol Cancer*, *10*, 125.

Joffre, C., Barrow, R., Ménard, L., Calleja, V., Hart, I. R., & Kermorgant, S. (2011). A direct role for Met endocytosis in tumorigenesis. *Nat Cell Biol*, *13*(7), 827-837.

Jumper, J., Evans, R., Pritzel, A., Green, T., Figurnov, M., Ronneberger, O., Tunyasuvunakool, K., Bates, R., Žídek, A., & Potapenko, A. (2021). Highly accurate protein structure prediction with AlphaFold. *Nature*, *596*(7873), 583-589.

Jura, N., Endres, N. F., Engel, K., Deindl, S., Das, R., Lamers, M. H., Wemmer, D. E., Zhang, X., & Kuriyan, J. (2009). Mechanism for activation of the EGF receptor catalytic domain by the juxtamembrane segment. *Cell*, *137*(7), 1293-1307.

Kabeche, L., Nguyen, H. D., Buisson, R., & Zou, L. (2018). A mitosis-specific and R loop–driven ATR pathway promotes faithful chromosome segregation. *Science*, *359*(6371), 108-114.

Kaneko, T., Huang, H., Zhao, B., Li, L., Liu, H., Voss, C. K., Wu, C., Schiller, M. R., & Li, S. S.-C. (2010). Loops govern SH2 domain specificity by controlling access to binding pockets. *Science signaling*, *3*(120), ra34-ra34.

Kaneko, T., Joshi, R., Feller, S. M., & Li, S. S. (2012). Phosphotyrosine recognition domains: the typical, the atypical and the versatile. *Cell Communication and Signaling*, *10*(1), 1-20.

Karnitz, L. M., & Zou, L. (2015). Molecular Pathways: Targeting ATR in Cancer TherapyTargeting ATR in Cancer Therapy. *Clinical Cancer Research*, *21*(21), 4780-4785.

Kauma, S. W., Bae-Jump, V., & Walsh, S. W. (1999). Hepatocyte growth factor stimulates trophoblast invasion: a potential mechanism for abnormal placentation in preeclampsia. *The Journal of Clinical Endocrinology & Metabolism*, *84*(11), 4092-4096.

Kermorgant, S., & Parker, P. J. (2008). Receptor trafficking controls weak signal delivery: a strategy used by c-Met for STAT3 nuclear accumulation. *The Journal of cell biology*, *182*(5), 855-863.

Kim, H., Hong, S. H., Kim, J. Y., Kim, I.-C., Park, Y.-W., Lee, S.-J., Song, S.-W., Kim, J. J., Park, G., & Kim, T. M. (2017). Preclinical development of a humanized neutralizing antibody targeting HGF. *Experimental & Molecular Medicine*, *49*(3), e309-e309.

Kim, H. J., Kang, S. K., Kwon, W. S., Kim, T. S., Jeong, I., Jeung, H. C., Kragh, M., Horak, I. D., Chung, H. C., & Rha, S. Y. (2018). Forty-nine gastric cancer cell lines with integrative genomic profiling for development of c-MET inhibitor. *Int J Cancer*, *143*(1), 151-159.

Kinoshita, E., Kinoshita-Kikuta, E., & Koike, T. (2009). Separation and detection of large phosphoproteins using Phos-tag SDS-PAGE. *Nature protocols*, *4*(10), 1513-1521.

Kiyatkin, A., van Alderwerelt van Rosenburgh, I. K., Klein, D. E., & Lemmon, M. A. (2020). Kinetics of receptor tyrosine kinase activation define ERK signaling dynamics. *Science signaling*, *13*(645), eaaz5267.

Knight, J. F., Lesurf, R., Zhao, H., Pinnaduwage, D., Davis, R. R., Saleh, S. M., Zuo, D., Naujokas, M. A., Chughtai, N., & Herschkowitz, J. I. (2013). Met synergizes with p53 loss to induce mammary tumors that possess features of claudin-low breast cancer. *Proceedings of the National Academy of Sciences*, *110*(14), E1301-E1310.

Koch, A., Mancini, A., El Bounkari, O., & Tamura, T. (2005). The SH2-domian-containing inositol 5-phosphatase (SHIP)-2 binds to c-Met directly via tyrosine residue 1356 and involves hepatocyte growth factor (HGF)-induced lamellipodium formation, cell scattering and cell spreading. *Oncogene*, *24*(21), 3436-3447.

Kolatsi-Joannou, M., Moore, R., Winyard, P. J., & Woolf, A. S. (1997). Expression of hepatocyte growth factor/scatter factor and its receptor, MET, suggests roles in human embryonic organogenesis. *Pediatric research*, *41*(5), 657-665.

Konicek, B. W., Capen, A. R., Credille, K. M., Ebert, P. J., Falcon, B. L., Heady, G. L., Patel, B. K., Peek, V. L., Stephens, J. R., & Stewart, J. A. (2018). Merestinib

(LY2801653) inhibits neurotrophic receptor kinase (NTRK) and suppresses growth of NTRK fusion bearing tumors. *Oncotarget*, *9*(17), 13796.

Kovacs, E., Das, R., Wang, Q., Collier, T. S., Cantor, A., Huang, Y., Wong, K., Mirza, A., Barros, T., & Grob, P. (2015). Analysis of the role of the C-terminal tail in the regulation of the epidermal growth factor receptor. *Molecular and cellular biology*, *35*(17), 3083-3102.

Kozlov, G., Perreault, A., Schrag, J. D., Park, M., Cygler, M., Gehring, K., & Ekiel, I. (2004). Insights into function of PSI domains from structure of the Met receptor PSI domain. *Biochemical and biophysical research communications*, *321*(1), 234-240.

Krämer, A., Mailand, N., Lukas, C., Syljuåsen, R. G., Wilkinson, C. J., Nigg, E. A., Bartek, J., & Lukas, J. (2004). Centrosome-associated Chk1 prevents premature activation of cyclin-B–Cdk1 kinase. *Nature cell biology*, *6*(9), 884-891.

Kumar, A., Mazzanti, M., Mistrik, M., Kosar, M., Beznoussenko, G. V., Mironov, A. A., Garre, M., Parazzoli, D., Shivashankar, G., & Scita, G. (2014). ATR mediates a checkpoint at the nuclear envelope in response to mechanical stress. *Cell*, *158*(3), 633-646.

Lai, A. Z., Abella, J. V., & Park, M. (2009). Crosstalk in Met receptor oncogenesis. *Trends Cell Biol*, *19*(10), 542-551.

Lai, A. Z., Cory, S., Zhao, H., Gigoux, M., Monast, A., Guiot, M.-C., Huang, S., Tofigh, A., Thompson, C., & Naujokas, M. (2014). Dynamic reprogramming of signaling upon met inhibition reveals a mechanism of drug resistance in gastric cancer. *Science signaling*, *7*(322), ra38-ra38.

Lai, A. Z., Durrant, M., Zuo, D., Ratcliffe, C. D., & Park, M. (2012). Met kinase-dependent loss of the E3 ligase Cbl in gastric cancer. *J Biol Chem*, *287*(11), 8048-8059.

Lamorte, L., Kamikura, D. M., & Park, M. (2000). A switch from p130Cas/Crk to Gab1/Crk signaling correlates with anchorage independent growth and JNK activation in cells transformed by the Met receptor oncoprotein. *Oncogene*, *19*(52), 5973-5981.

Lee, J.-K., Joo, K. M., Lee, J., Yoon, Y., & Nam, D.-H. (2014). Targeting the epithelial to mesenchymal transition in glioblastoma: the emerging role of MET signaling. *OncoTargets and therapy*, 1933-1944.

Lee, S., Jung, J., Lee, Y. J., Kim, S. K., Kim, J. A., Kim, B. K., Park, K. C., Kwon, B. M., & Han, D. C. (2021). Targeting HSF1 as a Therapeutic Strategy for Multiple Mechanisms of EGFR Inhibitor Resistance in EGFR Mutant Non-Small-Cell Lung Cancer. *Cancers (Basel)*, *13*(12).

Lefebvre, J., Ancot, F., Leroy, C., Muharram, G., Lemière, A., & Tulasne, D. (2012). Met degradation: more than one stone to shoot a receptor down. *Faseb j*, *26*(4), 1387-1399.

Lefebvre, J., Muharram, G., Leroy, C., Kherrouche, Z., Montagne, R., Ichim, G., Tauszig-Delamasure, S., Chotteau-Lelievre, A., Brenner, C., & Mehlen, P. (2013). Caspase-generated fragment of the Met receptor favors apoptosis via the intrinsic pathway independently of its tyrosine kinase activity. *Cell death & disease*, *4*(10), e871-e871.

Lemmon, M. A., & Schlessinger, J. (2010). Cell signaling by receptor tyrosine kinases. *Cell*, *141*(7), 1117-1134.

Lengyel, E., Prechtel, D., Resau, J. H., Gauger, K., Welk, A., Lindemann, K., Salanti, G., Richter, T., Knudsen, B., & Vande Woude, G. F. (2005). C-Met overexpression in node-positive breast cancer identifies patients with poor clinical outcome independent of Her2/neu. *International journal of cancer*, *113*(4), 678-682.

Li, C., Wu, J. J., Hynes, M., Dosch, J., Sarkar, B., Welling, T. H., di Magliano, M. P., & Simeone, D. M. (2011). c-Met is a marker of pancreatic cancer stem cells and therapeutic target. *Gastroenterology*, *141*(6), 2218-2227. e2215.

Li, J., Akbani, R., Zhao, W., Lu, Y., Weinstein, J. N., Mills, G. B., & Liang, H. (2017). Explore, visualize, and analyze functional cancer proteomic data using the cancer proteome atlas. *Cancer research*, *77*(21), e51-e54.

Li, J., Lu, Y., Akbani, R., Ju, Z., Roebuck, P. L., Liu, W., Yang, J.-Y., Broom, B. M., Verhaak, R. G., & Kane, D. W. (2013). TCPA: a resource for cancer functional proteomics data. *Nature methods*, *10*(11), 1046-1047.

Li, W., Xu, H., Xiao, T., Cong, L., Love, M. I., Zhang, F., Irizarry, R. A., Liu, J. S., Brown, M., & Liu, X. S. (2014). MAGeCK enables robust identification of essential genes from genome-scale CRISPR/Cas9 knockout screens. *Genome biology*, *15*(12), 1-12.

Lietha, D., Chirgadze, D. Y., Mulloy, B., Blundell, T. L., & Gherardi, E. (2001). Crystal structures of NK1-heparin complexes reveal the basis for NK1 activity and enable engineering of potent agonists of the MET receptor. *Embo j*, *20*(20), 5543-5555.

Lisabeth, E. M., Falivelli, G., & Pasquale, E. B. (2013). Eph receptor signaling and ephrins. *Cold Spring Harbor perspectives in biology*, *5*(9), a009159.

Liu, B. A., Engelmann, B. W., & Nash, P. D. (2012a). High-throughput analysis of peptide-binding modules. *Proteomics*, *12*(10), 1527-1546.

Liu, B. A., Engelmann, B. W., & Nash, P. D. (2012b). The language of SH2 domain interactions defines phosphotyrosine-mediated signal transduction. *FEBS letters*, *586*(17), 2597-2605.

Liu, H., Chen, X., Focia, P. J., & He, X. (2007). Structural basis for stem cell factor–KIT signaling and activation of class III receptor tyrosine kinases. *The EMBO Journal*, *26*(3), 891-901.

Lock, L. S., Frigault, M. M., Saucier, C., & Park, M. (2003). Grb2-independent recruitment of Gab1 requires the C-terminal lobe and structural integrity of the Met receptor kinase domain. *J Biol Chem*, *278*(32), 30083-30090.

Lokker, N. A., Mark, M. R., Luis, E. A., Bennett, G. L., Robbins, K. A., Baker, J. B., & Godowski, P. J. (1992). Structure-function analysis of hepatocyte growth factor: identification of variants that lack mitogenic activity yet retain high affinity receptor binding. *Embo j*, *11*(7), 2503-2510.

Lu, S., Fang, J., Li, X., Cao, L., Zhou, J., Guo, Q., Liang, Z., Cheng, Y., Jiang, L., & Yang, N. (2020). Phase II study of savolitinib in patients (pts) with pulmonary sarcomatoid carcinoma (PSC) and other types of non-small cell lung cancer (NSCLC) harboring MET exon 14 skipping mutations (METex14+). In: American Society of Clinical Oncology.

Ma, P. C. (2015). MET receptor juxtamembrane exon 14 alternative spliced variant: novel cancer genomic predictive biomarker. *Cancer Discov*, *5*(8), 802-805.

Ma, P. C., Jagadeeswaran, R., Jagadeesh, S., Tretiakova, M. S., Nallasura, V., Fox, E. A., Hansen, M., Schaefer, E., Naoki, K., Lader, A., Richards, W., Sugarbaker, D., Husain, A. N., Christensen, J. G., & Salgia, R. (2005). Functional expression and mutations of c-Met and its therapeutic inhibition with SU11274 and small interfering RNA in non-small cell lung cancer. *Cancer Res*, *65*(4), 1479-1488.

Maguire, W. F., Schmitz, J. C., Scemama, J., Czambel, K., Lin, Y., Green, A. G., Wu, S., Lin, H., Puhalla, S., Rhee, J., Stoller, R., Tawbi, H., Lee, J. J., Wright, J. J., Beumer, J. H., Chu, E., & Appleman, L. J. (2021). Phase 1 study of safety, pharmacokinetics, and pharmacodynamics of tivantinib in combination with bevacizumab in adult patients with advanced solid tumors. *Cancer Chemother Pharmacol*, *88*(4), 643-654.

Maina, F., Casagranda, F., Audero, E., Simeone, A., Comoglio, P. M., Klein, R., & Ponzetto, C. (1996). Uncoupling of Grb2 from the Met receptor in vivo reveals complex roles in muscle development. *Cell*, *87*(3), 531-542.

Maina, F., Hilton, M. C., Ponzetto, C., Davies, A. M., & Klein, R. (1997). Met receptor signaling is required for sensory nerve development and HGF promotes axonal growth and survival of sensory neurons. *Genes & development*, *11*(24), 3341-3350.

Marona, P., Górka, J., Kotlinowski, J., Majka, M., Jura, J., & Miekus, K. (2019). C-Met as a key factor responsible for sustaining undifferentiated phenotype and therapy resistance in renal carcinomas. *Cells*, *8*(3), 272.

Maroun, C. R., Holgado-Madruga, M., Royal, I., Naujokas, M. A., Fournier, T. M., Wong, A. J., & Park, M. (1999). The Gab1 PH domain is required for localization of Gab1

at sites of cell-cell contact and epithelial morphogenesis downstream from the met receptor tyrosine kinase. *Molecular and cellular biology*, *19*(3), 1784-1799.

Maroun, C. R., Naujokas, M. A., Holgado-Madruga, M., Wong, A. J., & Park, M. (2000). The tyrosine phosphatase SHP-2 is required for sustained activation of extracellular signal-regulated kinase and epithelial morphogenesis downstream from the met receptor tyrosine kinase. *Molecular and cellular biology*, *20*(22), 8513-8525.

Maroun, C. R., Naujokas, M. A., & Park, M. (2003). Membrane targeting of Grb2-associated binder-1 (Gab1) scaffolding protein through Src myristoylation sequence substitutes for Gab1 pleckstrin homology domain and switches an epidermal growth factor response to an invasive morphogenic program. *Molecular biology of the cell*, *14*(4), 1691-1708.

Marshall, C. (1995). Specificity of receptor tyrosine kinase signaling: transient versus sustained extracellular signal-regulated kinase activation. *Cell*, *80*(2), 179-185.

Mathieu, L. N., Larkins, E., Akinboro, O., Roy, P., Amatya, A. K., Fiero, M. H., Mishra-Kalyani, P. S., Helms, W. S., Myers, C. E., & Skinner, A. M. (2022). FDA Approval Summary: Capmatinib and Tepotinib for the Treatment of Metastatic NSCLC Harboring MET Exon 14 Skipping Mutations or AlterationsFDA Approval Summary: Capmatinib and Tepotinib. *Clinical Cancer Research*, *28*(2), 249-254.

Matsumoto, K., & Nakamura, T. (1996). Emerging multipotent aspects of hepatocyte growth factor. *J Biochem*, *119*(4), 591-600.

McCurdy, S., Pacal, M., Ahmad, M., & Bremner, R. (2017). A CDK2 activity signature predicts outcome in CDK2-low cancers. *Oncogene*, *36*(18), 2491-2502.

Merchant, M., Ma, X., Maun, H. R., Zheng, Z., Peng, J., Romero, M., Huang, A., Yang, N. Y., Nishimura, M., Greve, J., Santell, L., Zhang, Y. W., Su, Y., Kaufman, D. W., Billeci, K. L., Mai, E., Moffat, B., Lim, A., Duenas, E. T., . . . Yansura, D. G. (2013). Monovalent antibody design and mechanism of action of onartuzumab, a MET antagonist with anti-tumor activity as a therapeutic agent. *Proc Natl Acad Sci U S A*, *110*(32), E2987-2996.

Mikhaylova, O., Stratton, Y., Hall, D., Kellner, E., Ehmer, B., Drew, A. F., Gallo, C. A., Plas, D. R., Biesiada, J., & Meller, J. (2012). VHL-regulated MiR-204 suppresses tumor growth through inhibition of LC3B-mediated autophagy in renal clear cell carcinoma. *Cancer Cell*, *21*(4), 532-546.

Miller, M., Ginalski, K., Lesyng, B., Nakaigawa, N., Schmidt, L., & Zbar, B. (2001). Structural basis of oncogenic activation caused by point mutations in the kinase domain of the MET proto-oncogene: modeling studies. *Proteins*, *44*(1), 32-43.

Min, M., Rong, Y., Tian, C., & Spencer, S. L. (2020). Temporal integration of mitogen history in mother cells controls proliferation of daughter cells. *Science*, *368*(6496), 1261-1265.

Mitra, A. K., Sawada, K., Tiwari, P., Mui, K., Gwin, K., & Lengyel, E. (2011). Ligand-independent activation of c-Met by fibronectin and α(5)β(1)-integrin regulates ovarian cancer invasion and metastasis. *Oncogene*, *30*(13), 1566-1576.

Miyazawa, K., Tsubouchi, H., Naka, D., Takahashi, K., Okigaki, M., Arakaki, N., Nakayama, H., Hirono, S., Sakiyama, O., Takahashi, K., & et al. (1989). Molecular cloning and sequence analysis of cDNA for human hepatocyte growth factor. *Biochem Biophys Res Commun*, *163*(2), 967-973.

Mohapatra, B., Ahmad, G., Nadeau, S., Zutshi, N., An, W., Scheffe, S., Dong, L., Feng, D., Goetz, B., & Arya, P. (2013). Protein tyrosine kinase regulation by ubiquitination: critical roles of Cbl-family ubiquitin ligases. *Biochimica Et Biophysica Acta (BBA)-Molecular Cell Research*, *1833*(1), 122-139.

Mok, T. S. K., Geater, S. L., Su, W.-C., Tan, E.-H., Yang, J. C.-H., Chang, G.-C., Han, M., Komarnitsky, P., Payumo, F., & Garrus, J. E. (2016). A randomized phase 2 study comparing the combination of ficlatuzumab and gefitinib with gefitinib alone in Asian patients with advanced stage pulmonary adenocarcinoma. *Journal of Thoracic Oncology*, *11*(10), 1736-1744.

Mol, C. D., Dougan, D. R., Schneider, T. R., Skene, R. J., Kraus, M. L., Scheibe, D. N., Snell, G. P., Zou, H., Sang, B.-C., & Wilson, K. P. (2004). Structural basis for the autoinhibition and STI-571 inhibition of c-Kit tyrosine kinase. *Journal of Biological Chemistry*, *279*(30), 31655-31663.

Mondino, A., Giordano, S., & Comoglio, P. M. (1991). Defective posttranslational processing activates the tyrosine kinase encoded by the MET proto-oncogene (hepatocyte growth factor receptor). *Molecular and cellular biology*, *11*(12), 6084-6092.

Montagne, R., Berbon, M., Doublet, L., Debreuck, N., Baranzelli, A., Drobecq, H., Leroy, C., Delhem, N., Porte, H., & Copin, M. (2015). Necrosis-and apoptosis-related Met cleavages have divergent functional consequences. *Cell death & disease*, *6*(5), e1769-e1769.

Montagner, A., Yart, A., Dance, M., Perret, B., Salles, J.-P., & Raynal, P. (2005). A novel role for Gab1 and SHP2 in epidermal growth factor-induced Ras activation. *Journal of Biological Chemistry*, *280*(7), 5350-5360.

Montesano, R., Matsumoto, K., Nakamura, T., & Orci, L. (1991). Identification of a fibroblast-derived epithelial morphogen as hepatocyte growth factor. *Cell*, *67*(5), 901-908.

Nagy, P., Claus, J., Jovin, T. M., & Arndt-Jovin, D. J. (2010). Distribution of resting and ligand-bound ErbB1 and ErbB2 receptor tyrosine kinases in living cells using number and brightness analysis. *Proceedings of the National Academy of Sciences*, *107*(38), 16524-16529.

Naka, D., Ishii, T., Yoshiyama, Y., Miyazawa, K., Hara, H., Hishida, T., & Kidamura, N. (1992). Activation of hepatocyte growth factor by proteolytic conversion of a single chain form to a heterodimer. *J Biol Chem*, *267*(28), 20114-20119.

Nakamura, T. (1991). Structure and function of hepatocyte growth factor. *Prog Growth Factor Res*, *3*(1), 67-85.

Nakamura, T., & Mizuno, S. (2010). The discovery of hepatocyte growth factor (HGF) and its significance for cell biology, life sciences and clinical medicine. *Proc Jpn Acad Ser B Phys Biol Sci*, *86*(6), 588-610.

Nakamura, T., Nishizawa, T., Hagiya, M., Seki, T., Shimonishi, M., Sugimura, A., Tashiro, K., & Shimizu, S. (1989). Molecular cloning and expression of human hepatocyte growth factor. *Nature*, *342*(6248), 440-443.

Naldini, L., Vigna, E., Ferracini, R., Longati, P., Gandino, L., Prat, M., & Comoglio, P. M. (1991). The tyrosine kinase encoded by the MET proto-oncogene is activated by autophosphorylation. *Mol Cell Biol*, *11*(4), 1793-1803.

Naldini, L., Weidner, K. M., Vigna, E., Gaudino, G., Bardelli, A., Ponzetto, C., Narsimhan, R. P., Hartmann, G., Zarnegar, R., Michalopoulos, G. K., & et al. (1991). Scatter factor and hepatocyte growth factor are indistinguishable ligands for the MET receptor. *Embo j*, *10*(10), 2867-2878.

Nasa, I., Cressey, L. E., Kruse, T., Hertz, E. P., Gui, J., Graves, L. M., Nilsson, J., & Kettenbach, A. N. (2020). Quantitative kinase and phosphatase profiling reveal that CDK1 phosphorylates PP2Ac to promote mitotic entry. *Science signaling*, *13*(648), eaba7823.

Network, C. G. A. R. (2014). Comprehensive molecular profiling of lung adenocarcinoma. *Nature*, *511*(7511), 543.

Neufeld, G., Sabag, A. D., Rabinovicz, N., & Kessler, O. (2012). Semaphorins in angiogenesis and tumor progression. *Cold Spring Harb Perspect Med*, *2*(1), a006718.

Okano, Y., Mizuno, K., Osada, S., Nakamura, T., & Nozawa, Y. (1993). Tyrosine phosphorylation of phospholipase Cγ in c-met/HGF receptor-stimulated hepatocytes: comparison with HepG2 hepatocarcinoma cells. *Biochemical and biophysical research communications*, *190*(3), 842-848.

Olsen, J. V., Vermeulen, M., Santamaria, A., Kumar, C., Miller, M. L., Jensen, L. J., Gnad, F., Cox, J., Jensen, T. S., & Nigg, E. A. (2010). Quantitative phosphoproteomics

reveals widespread full phosphorylation site occupancy during mitosis. *Science signaling*, *3*(104), ra3-ra3.

Organ, S. L., & Tsao, M. S. (2011). An overview of the c-MET signaling pathway. *Ther Adv Med Oncol*, *3*(1 Suppl), S7-s19.

Orian-Rousseau, V., Chen, L., Sleeman, J. P., Herrlich, P., & Ponta, H. (2002). CD44 is required for two consecutive steps in HGF/c-Met signaling. *Genes Dev*, *16*(23), 3074-3086.

Orian-Rousseau, V., Morrison, H., Matzke, A., Kastilan, T., Pace, G., Herrlich, P., & Ponta, H. (2007). Hepatocyte growth factor-induced Ras activation requires ERM proteins linked to both CD44v6 and F-actin. *Mol Biol Cell*, *18*(1), 76-83.

Ou, S.-H. I. (2011). Crizotinib: a novel and first-in-class multitargeted tyrosine kinase inhibitor for the treatment of anaplastic lymphoma kinase rearranged non-small cell lung cancer and beyond. *Drug design, development and therapy*, 471-485.

Ou, S. H. (2012). Crizotinib: a drug that crystallizes a unique molecular subset of non-small-cell lung cancer. *Expert Rev Anticancer Ther*, *12*(2), 151-162.

Paik, P. K., Drilon, A., Fan, P.-D., Yu, H., Rekhtman, N., Ginsberg, M. S., Borsu, L., Schultz, N., Berger, M. F., & Rudin, C. M. (2015). Response to MET Inhibitors in Patients with Stage IV Lung Adenocarcinomas Harboring MET Mutations Causing Exon 14 SkippingMET Inhibitors in MET Exon 14 Splice Variant Lung Cancer. *Cancer discovery*, *5*(8), 842-849.

Paik, P. K., Drilon, A., Fan, P. D., Yu, H., Rekhtman, N., Ginsberg, M. S., Borsu, L., Schultz, N., Berger, M. F., Rudin, C. M., & Ladanyi, M. (2015). Response to MET

inhibitors in patients with stage IV lung adenocarcinomas harboring MET mutations causing exon 14 skipping. *Cancer Discov*, *5*(8), 842-849.

Paik, P. K., Felip, E., Veillon, R., Sakai, H., Cortot, A. B., Garassino, M. C., Mazieres, J., Viteri, S., Senellart, H., Van Meerbeeck, J., Raskin, J., Reinmuth, N., Conte, P., Kowalski, D., Cho, B. C., Patel, J. D., Horn, L., Griesinger, F., Han, J. Y., . . . Le, X. (2020). Tepotinib in Non-Small-Cell Lung Cancer with MET Exon 14 Skipping Mutations. *N Engl J Med*, *383*(10), 931-943.

Pal, K., Bandyopadhyay, A., Zhou, X. E., Xu, Q., Marciano, D. P., Brunzelle, J. S., Yerrum, S., Griffin, P. R., Vande Woude, G., Melcher, K., & Xu, H. E. (2017). Structural Basis of TPR-Mediated Oligomerization and Activation of Oncogenic Fusion Kinases. *Structure*, *25*(6), 867-877 e863.

Paliouras, G. N., Naujokas, M. A., & Park, M. (2009). Pak4, a novel Gab1 binding partner, modulates cell migration and invasion by the Met receptor. *Mol Cell Biol*, *29*(11), 3018-3032.

Parachoniak, C. A., Luo, Y., Abella, J. V., Keen, J. H., & Park, M. (2011). GGA3 functions as a switch to promote Met receptor recycling, essential for sustained ERK and cell migration. *Dev Cell*, *20*(6), 751-763.

Park, M., Dean, M., Kaul, K., Braun, M. J., Gonda, M. A., & Vande Woude, G. (1987). Sequence of MET protooncogene cDNA has features characteristic of the tyrosine kinase family of growth-factor receptors. *Proc Natl Acad Sci U S A*, *84*(18), 6379-6383.

Patnaik, A., Weiss, G., Papadopoulos, K., Hofmeister, C. C., Tibes, R., Tolcher, A., Isaacs, R., Jac, J., Han, M., & Payumo, F. (2014). Phase I ficlatuzumab monotherapy or

with erlotinib for refractory advanced solid tumours and multiple myeloma. *British journal of cancer*, *111*(2), 272-280.

Peek, M., Moran, P., Mendoza, N., Wickramasinghe, D., & Kirchhofer, D. (2002). Unusual proteolytic activation of pro-hepatocyte growth factor by plasma kallikrein and coagulation factor XIa. *J Biol Chem*, *277*(49), 47804-47809.

Peinado, H., Alečković, M., Lavotshkin, S., Matei, I., Costa-Silva, B., Moreno-Bueno, G., Hergueta-Redondo, M., Williams, C., García-Santos, G., & Ghajar, C. M. (2012). Melanoma exosomes educate bone marrow progenitor cells toward a pro-metastatic phenotype through MET. *Nature Medicine*, *18*(6), 883-891.

Pellegrini, L., Burke, D. F., von Delft, F., Mulloy, B., & Blundell, T. L. (2000). Crystal structure of fibroblast growth factor receptor ectodomain bound to ligand and heparin. *Nature*, *407*(6807), 1029-1034.

Pennacchietti, S., Michieli, P., Galluzzo, M., Mazzone, M., Giordano, S., & Comoglio, P. M. (2003). Hypoxia promotes invasive growth by transcriptional activation of the met protooncogene. *Cancer Cell*, *3*(4), 347-361.

Peschard, P., Fournier, T. M., Lamorte, L., Naujokas, M. A., Band, H., Langdon, W. Y., & Park, M. (2001). Mutation of the c-Cbl TKB domain binding site on the Met receptor tyrosine kinase converts it into a transforming protein. *Molecular cell*, *8*(5), 995-1004.

Peschard, P., Ishiyama, N., Lin, T., Lipkowitz, S., & Park, M. (2004). A conserved DpYR motif in the juxtamembrane domain of the Met receptor family forms an atypical c-Cbl/Cbl-b tyrosine kinase binding domain binding site required for suppression of oncogenic activation. *Journal of Biological Chemistry*, *279*(28), 29565-29571.

Peschard, P., Ishiyama, N., Lin, T., Lipkowitz, S., & Park, M. (2004). A conserved DpYR motif in the juxtamembrane domain of the Met receptor family forms an atypical c-Cbl/Cbl-b tyrosine kinase binding domain binding site required for suppression of oncogenic activation. *J Biol Chem*, *279*(28), 29565-29571.

Peschard, P., & Park, M. (2003). Escape from Cbl-mediated downregulation: a recurrent theme for oncogenic deregulation of receptor tyrosine kinases. *Cancer Cell*, *3*(6), 519-523.

Peschard, P., & Park, M. (2007). From Tpr-Met to Met, tumorigenesis and tubes. *Oncogene*, *26*(9), 1276-1285.

Petschnigg, J., Groisman, B., Kotlyar, M., Taipale, M., Zheng, Y., Kurat, C. F., Sayad, A., Sierra, J. R., Usaj, M. M., & Snider, J. (2014). The mammalian-membrane two-hybrid assay (MaMTH) for probing membrane-protein interactions in human cells. *Nature methods*, *11*(5), 585-592.

Pines, G., Huang, P. H., Zwang, Y., White, F. M., & Yarden, Y. (2010). EGFRvIV: a previously uncharacterized oncogenic mutant reveals a kinase autoinhibitory mechanism. *Oncogene*, *29*(43), 5850-5860.

Polo, S., & Di Fiore, P. P. (2006). Endocytosis conducts the cell signaling orchestra. *Cell*, *124*(5), 897-900.

Ponzetto, C., Bardelli, A., Maina, F., Longati, P., Panayotou, G., Dhand, R., Waterfield, M. D., & Comoglio, P. M. (1993). A novel recognition motif for phosphatidylinositol 3-kinase binding mediates its association with the hepatocyte growth factor/scatter factor receptor. *Molecular and cellular biology*, *13*(8), 4600-4608.

Ponzetto, C., Zhen, Z., Audero, E., Maina, F., Bardelli, A., Basile, M. L., Giordano, S., Narsimhan, R., & Comoglio, P. (1996). Specific uncoupling of GRB2 from the Met receptor: differential effects on transformation and motility. *Journal of Biological Chemistry*, *271*(24), 14119-14123.

Powell, E. M., Mars, W. M., & Levitt, P. (2001). Hepatocyte growth factor/scatter factor is a motogen for interneurons migrating from the ventral to dorsal telencephalon. *Neuron*, *30*(1), 79-89.

Pryor, P. R., & Luzio, J. P. (2009). Delivery of endocytosed membrane proteins to the lysosome. *Biochimica Et Biophysica Acta (BBA)-Molecular Cell Research*, *1793*(4), 615-624.

Qian, L.-W., Mizumoto, K., Maehara, N., Ohuchida, K., Inadome, N., Saimura, M., Nagai, E., Matsumoto, K., Nakamura, T., & Tanaka, M. (2003). Co-cultivation of pancreatic cancer cells with orthotopic tumor-derived fibroblasts: fibroblasts stimulate tumor cell invasion via HGF secretion whereas cancer cells exert a minor regulative effect on fibroblasts HGF production. *Cancer letters*, *190*(1), 105-112.

Recio, J. A., & Merlino, G. (2002). Hepatocyte growth factor/scatter factor activates proliferation in melanoma cells through p38 MAPK, ATF-2 and cyclin D1. *Oncogene*, *21*(7), 1000-1008.

Reid, J. F., Sokolova, V., Zoni, E., Lampis, A., Pizzamiglio, S., Bertan, C., Zanutto, S., Perrone, F., Camerini, T., & Gallino, G. (2012). miRNA Profiling in Colorectal Cancer Highlights miR-1 Involvement in MET-Dependent ProliferationmiRNA Profiling in Colorectal Cancer. *Molecular Cancer Research*, *10*(4), 504-515.

Rickert, K. W., Patel, S. B., Allison, T. J., Byrne, N. J., Darke, P. L., Ford, R. E., Guerin, D. J., Hall, D. L., Kornienko, M., Lu, J., Munshi, S. K., Reid, J. C., Shipman, J. M., Stanton, E. F., Wilson, K. J., Young, J. R., Soisson, S. M., & Lumb, K. J. (2011). Structural basis for selective small molecule kinase inhibition of activated c-Met. *J Biol Chem*, *286*(13), 11218-11225.

Rodrigues, G. A., Park, M., & Schlessinger, J. (1997). Activation of the JNK pathway is essential for transformation by the Met oncogene. *The EMBO Journal*, *16*(10), 2634-2645.

Rosen, L. S., Goldman, J. W., Algazi, A. P., Turner, P. K., Moser, B., Hu, T., Wang, X. A., Tuttle, J., Wacheck, V., Wooldridge, J. E., & Banck, M. (2017). A First-in-Human Phase I Study of a Bivalent MET Antibody, Emibetuzumab (LY2875358), as Monotherapy and in Combination with Erlotinib in Advanced Cancer. *Clin Cancer Res*, *23*(8), 1910-1919.

Royal, I., & Park, M. (1995). Hepatocyte growth factor-induced scatter of Madin-Darby canine kidney cells requires phosphatidylinositol 3-kinase. *Journal of Biological Chemistry*, *270*(46), 27780-27787.

Rubin, J. S., Day, R. M., Breckenridge, D., Atabey, N., Taylor, W. G., Stahl, S. J., Wingfield, P. T., Kaufman, J. D., Schwall, R., & Bottaro, D. P. (2001). Dissociation of heparan sulfate and receptor binding domains of hepatocyte growth factor reveals that heparan sulfate-c-met interaction facilitates signaling. *J Biol Chem*, *276*(35), 32977-32983.

Sachs, M., Brohmann, H., Zechner, D., Müller, T., Hülsken, J., Walther, I., Schaeper, U., Birchmeier, C., & Birchmeier, W. (2000). Essential role of Gab1 for signaling by the c-Met receptor in vivo. *The Journal of cell biology*, *150*(6), 1375-1384.

Sadiq, A. A., & Salgia, R. (2013). MET as a possible target for non–small-cell lung cancer. *Journal of clinical oncology*, *31*(8), 1089.

Saffarian, S., Li, Y., Elson, E. L., & Pike, L. J. (2007). Oligomerization of the EGF receptor investigated by live cell fluorescence intensity distribution analysis. *Biophysical journal*, *93*(3), 1021-1031.

Saldivar, J. C., Hamperl, S., Bocek, M. J., Chung, M., Bass, T. E., Cisneros-Soberanis, F., Samejima, K., Xie, L., Paulson, J. R., & Earnshaw, W. C. (2018). An intrinsic S/G2 checkpoint enforced by ATR. *Science*, *361*(6404), 806-810.

Sangwan, V., Abella, J., Lai, A., Bertos, N., Stuible, M., Tremblay, M. L., & Park, M. (2011). Protein-tyrosine phosphatase 1B modulates early endosome fusion and trafficking of Met and epidermal growth factor receptors. *J Biol Chem*, *286*(52), 45000-45013.

Sangwan, V., Paliouras, G. N., Abella, J. V., Dubé, N., Monast, A., Tremblay, M. L., & Park, M. (2008). Regulation of the Met receptor-tyrosine kinase by the protein-tyrosine phosphatase 1B and T-cell phosphatase. *Journal of Biological Chemistry*, *283*(49), 34374-34383.

Santharam, M. A., Shukla, A., Ihsan, A. U., Cloutier, M., Levesque, D., Ramanathan, S., Boisvert, F. M., & Ilangumaran, S. (2021). SILAC proteomics implicates SOCS1 in modulating cellular macromolecular complexes and the ubiquitin conjugating enzyme UBE2D involved in MET receptor tyrosine kinase downregulation. *Biochimie*, *182*, 185-196.

Sasaki, T., Knyazev, P. G., Clout, N. J., Cheburkin, Y., Göhring, W., Ullrich, A., Timpl, R., & Hohenester, E. (2006). Structural basis for Gas6–Axl signalling. *The EMBO Journal*, *25*(1), 80-87.

Sawada, K., Radjabi, A. R., Shinomiya, N., Kistner, E., Kenny, H., Becker, A. R., Turkyilmaz, M. A., Salgia, R., Yamada, S. D., & Vande Woude, G. F. (2007). c-Met overexpression is a prognostic factor in ovarian cancer and an effective target for inhibition of peritoneal dissemination and invasion. *Cancer research*, *67*(4), 1670-1679.

Scagliotti, G., Moro-Sibilot, D., Kollmeier, J., Favaretto, A., Cho, E. K., Grosch, H., Kimmich, M., Girard, N., Tsai, C.-M., & Hsia, T.-C. (2020). A randomized-controlled phase 2 study of the MET antibody emibetuzumab in combination with erlotinib as first-line treatment for EGFR mutation–positive NSCLC patients. *Journal of Thoracic Oncology*, *15*(1), 80-90.

Schaeper, U., Gehring, N. H., Fuchs, K. P., Sachs, M., Kempkes, B., & Birchmeier, W. (2000). Coupling of Gab1 to c-Met, Grb2, and Shp2 mediates biological responses. *The Journal of cell biology*, *149*(7), 1419-1432.

Schiering, N., Knapp, S., Marconi, M., Flocco, M. M., Cui, J., Perego, R., Rusconi, L., & Cristiani, C. (2003). Crystal structure of the tyrosine kinase domain of the hepatocyte growth factor receptor c-Met and its complex with the microbial alkaloid K-252a. *Proc Natl Acad Sci U S A*, *100*(22), 12654-12659.

Schlee, S., Carmillo, P., & Whitty, A. (2006). Quantitative analysis of the activation mechanism of the multicomponent growth-factor receptor Ret. *Nature chemical biology*, *2*(11), 636-644.

Schlessinger, J. (2000). Cell signaling by receptor tyrosine kinases. *Cell*, *103*(2), 211-225.

Schmidt, L., Duh, F.-M., Chen, F., Kishida, T., Glenn, G., Choyke, P., Scherer, S. W., Zhuang, Z., Lubensky, I., & Dean, M. (1997). Germline and somatic mutations in the tyrosine kinase domain of the MET proto-oncogene in papillary renal carcinomas. *Nature genetics*, *16*(1), 68-73.

Schneidman-Duhovny, D., Hammel, M., Tainer, J. A., & Sali, A. (2016). FoXS, FoXSDock and MultiFoXS: Single-state and multi-state structural modeling of proteins and their complexes based on SAXS profiles. *Nucleic acids research*, *44*(W1), W424-W429.

Schulze, W. X., Deng, L., & Mann, M. (2005). Phosphotyrosine interactome of the ErbB-receptor kinase family. *Molecular systems biology*, *1*(1), 2005.0008.

Schwall, R. H., Chang, L. Y., Godowski, P. J., Kahn, D. W., Hillan, K. J., Bauer, K. D., & Zioncheck, T. F. (1996). Heparin induces dimerization and confers proliferative activity onto the hepatocyte growth factor antagonists NK1 and NK2. *J Cell Biol*, *133*(3), 709-718.

Scott, A. J., Arcaroli, J. J., Bagby, S. M., Yahn, R., Huber, K. M., Serkova, N. J., Nguyen, A., Kim, J., Thorburn, A., Vogel, J., Quackenbush, K. S., Capasso, A., Schreiber, A., Blatchford, P., Klauck, P. J., Pitts, T. M., Eckhardt, S. G., & Messersmith, W. A. (2018). Cabozantinib Exhibits Potent Antitumor Activity in Colorectal Cancer Patient-Derived Tumor Xenograft Models via Autophagy and Signaling Mechanisms. *Mol Cancer Ther*, *17*(10), 2112-2122.

Seiden-Long, I., Navab, R., Shih, W., Li, M., Chow, J., Zhu, C. Q., Radulovich, N., Saucier, C., & Tsao, M.-S. (2008). Gab1 but not Grb2 mediates tumor progression in Met overexpressing colorectal cancer cells. *Carcinogenesis*, *29*(3), 647-655.

Sequist, L. V., Han, J.-Y., Ahn, M.-J., Cho, B. C., Yu, H., Kim, S.-W., Yang, J. C.-H., Lee, J. S., Su, W.-C., & Kowalski, D. (2020). Osimertinib plus savolitinib in patients with EGFR mutation-positive, MET-amplified, non-small-cell lung cancer after progression on EGFR tyrosine kinase inhibitors: interim results from a multicentre, open-label, phase 1b study. *The Lancet Oncology*, *21*(3), 373-386.

Shaw, A. T., Kim, T. M., Crinò, L., Gridelli, C., Kiura, K., Liu, G., Novello, S., Bearz, A., Gautschi, O., & Mok, T. (2017). Ceritinib versus chemotherapy in patients with ALK-rearranged non-small-cell lung cancer previously given chemotherapy and crizotinib (ASCEND-5): a randomised, controlled, open-label, phase 3 trial. *The Lancet Oncology*, *18*(7), 874-886.

Sigismund, S., Woelk, T., Puri, C., Maspero, E., Tacchetti, C., Transidico, P., Di Fiore, P. P., & Polo, S. (2005). Clathrin-independent endocytosis of ubiquitinated cargos. *Proceedings of the National Academy of Sciences*, *102*(8), 2760-2765.

Simpson, J. E., & Gammoh, N. (2020). The impact of autophagy during the development and survival of glioblastoma. *Open Biology*, *10*(9), 200184.

Soria, J.-C., Jang, S. J., Khuri, F. R., Hassan, K., Liu, D., Hong, W. K., & Mao, L. (2000). Overexpression of cyclin B1 in early-stage non-small cell lung cancer and its clinical implication. *Cancer research*, *60*(15), 4000-4004.

Spencer, S. L., Cappell, S. D., Tsai, F.-C., Overton, K. W., Wang, C. L., & Meyer, T. (2013). The proliferation-quiescence decision is controlled by a bifurcation in CDK2 activity at mitotic exit. *Cell*, *155*(2), 369-383.

Spina, A., De Pasquale, V., Cerulo, G., Cocchiaro, P., Della Morte, R., Avallone, L., & Pavone, L. M. (2015). HGF/c-MET axis in tumor microenvironment and metastasis formation. *Biomedicines*, *3*(1), 71-88.

Stamos, J., Lazarus, R. A., Yao, X., Kirchhofer, D., & Wiesmann, C. (2004). Crystal structure of the HGF beta-chain in complex with the Sema domain of the Met receptor. *Embo j*, *23*(12), 2325-2335.

Stauber, D. J., DiGabriele, A. D., & Hendrickson, W. A. (2000). Structural interactions of fibroblast growth factor receptor with its ligands. *Proceedings of the National Academy of Sciences*, *97*(1), 49-54.

Steinig, A. G., Li, A. H., Wang, J., Chen, X., Dong, H., Ferraro, C., Jin, M., Kadalbajoo, M., Kleinberg, A., Stolz, K. M., Tavares-Greco, P. A., Wang, T., Albertella, M. R., Peng, Y., Crew, L., Kahler, J., Kan, J., Schulz, R., Cooke, A., . . . Mulvihill, M. J. (2013). Novel 6-aminofuro[3,2-c]pyridines as potent, orally efficacious inhibitors of cMET and RON kinases. *Bioorg Med Chem Lett*, *23*(15), 4381-4387.

Stella, G. M., Benvenuti, S., Gentile, A., & Comoglio, P. M. (2017). MET activation and physical dynamics of the metastatic process: the paradigm of cancers of unknown primary origin. *EBioMedicine*, *24*, 34-42.

Stoker, M., Gherardi, E., Perryman, M., & Gray, J. (1987). Scatter factor is a fibroblast-derived modulator of epithelial cell mobility. *Nature*, *327*(6119), 239-242.

Su, W., Gutmann, D. H., Perry, A., Abounader, R., Laterra, J., & Sherman, L. S. (2004). CD44-independent hepatocyte growth factor/c-Met autocrine loop promotes malignant peripheral nerve sheath tumor cell invasion in vitro. *Glia*, *45*(3), 297-306.

Sulpice, E., Ding, S., Muscatelli-Groux, B., Bergé, M., Han, Z. C., Plouet, J., Tobelem, G., & Merkulova-Rainon, T. (2009). Cross-talk between the VEGF-A and HGF signalling pathways in endothelial cells. *Biology of the Cell*, *101*(9), 525-539.

Suzawa, K., Offin, M., Lu, D., Kurzatkowski, C., Vojnic, M., Smith, R. S., Sabari, J. K., Tai, H., Mattar, M., & Khodos, I. (2019). Activation of KRAS Mediates Resistance to Targeted Therapy in MET Exon 14–mutant Non–small Cell Lung CancerKRAS Mutation in MET exon14 NSCLC. *Clinical Cancer Research*, *25*(4), 1248-1260.

Suzawa, K., Offin, M., Schoenfeld, A. J., Plodkowski, A. J., Odintsov, I., Lu, D., Lockwood, W. W., Arcila, M. E., Rudin, C. M., & Drilon, A. (2019). Acquired MET exon 14 alteration drives secondary resistance to epidermal growth factor receptor tyrosine kinase inhibitor in EGFR-mutated lung cancer. *JCO precision oncology*, *3*.

Tanaka, N., Kyuuma, M., & Sugamura, K. (2008). Endosomal sorting complex required for transport proteins in cancer pathogenesis, vesicular transport, and non-endosomal functions. *Cancer science*, *99*(7), 1293-1303.

Tang, J., Erikson, R. L., & Liu, X. (2006). Checkpoint kinase 1 (Chk1) is required for mitotic progression through negative regulation of polo-like kinase 1 (Plk1). *Proceedings of the National Academy of Sciences*, *103*(32), 11964-11969.

Tashiro, K., Hagiya, M., Nishizawa, T., Seki, T., Shimonishi, M., Shimizu, S., & Nakamura, T. (1990). Deduced primary structure of rat hepatocyte growth factor and

expression of the mRNA in rat tissues. *Proc Natl Acad Sci U S A*, *87*(8), 3200-3204.

Tesfay, L., Schulz, V. V., Frank, S. B., Lamb, L. E., & Miranti, C. K. (2016). Receptor tyrosine kinase Met promotes cell survival via kinase-independent maintenance of integrin α3β1. *Mol Biol Cell*, *27*(15), 2493-2504.

Tiedt, R., Degenkolbe, E., Furet, P., Appleton, B. A., Wagner, S., Schoepfer, J., Buck, E., Ruddy, D. A., Monahan, J. E., Jones, M. D., Blank, J., Haasen, D., Drueckes, P., Wartmann, M., McCarthy, C., Sellers, W. R., & Hofmann, F. (2011). A drug resistance screen using a selective MET inhibitor reveals a spectrum of mutations that partially overlap with activating mutations found in cancer patients. *Cancer Res*, *71*(15), 5255-5264.

Till, J. H., Becerra, M., Watty, A., Lu, Y., Ma, Y., Neubert, T. A., Burden, S. J., & Hubbard, S. R. (2002). Crystal structure of the MuSK tyrosine kinase: insights into receptor autoregulation. *Structure*, *10*(9), 1187-1196.

Toettcher, J. E., Weiner, O. D., & Lim, W. A. (2013). Using optogenetics to interrogate the dynamic control of signal transmission by the Ras/Erk module. *Cell*, *155*(6), 1422-1434.

Tolbert, W. D., Daugherty-Holtrop, J., Gherardi, E., Vande Woude, G., & Xu, H. E. (2010). Structural basis for agonism and antagonism of hepatocyte growth factor. *Proc Natl Acad Sci U S A*, *107*(30), 13264-13269.

Topel, H., Bağırsakçı, E., Yılmaz, Y., Güneş, A., Bağcı, G., Çömez, D., Kahraman, E., Korhan, P., & Atabey, N. (2021). High glucose induced c-Met activation promotes

aggressive phenotype and regulates expression of glucose metabolism genes in HCC cells. *Sci Rep*, *11*(1), 11376.

Trüb, T., Choi, W. E., Wolf, G., Ottinger, E., Chen, Y., Weiss, M., & Shoelson, S. E. (1995). Specificity of the PTB domain of Shc for β turn-forming pentapeptide motifs amino-terminal to phosphotyrosine. *Journal of Biological Chemistry*, *270*(31), 18205-18208.

Tuck, A. B., Park, M., Sterns, E. E., Boag, A., & Elliott, B. E. (1996). Coexpression of hepatocyte growth factor and receptor (Met) in human breast carcinoma. *The American journal of pathology*, *148*(1), 225.

Tulasne, D., Deheuninck, J., Lourenco, F. C., Lamballe, F., Ji, Z., Leroy, C., Puchois, E., Moumen, A., Maina, F., & Mehlen, P. (2004). Proapoptotic function of the MET tyrosine kinase receptor through caspase cleavage. *Molecular and cellular biology*, *24*(23), 10328-10339.

Uchikawa, E., Chen, Z., Xiao, G.-Y., Zhang, X., & Bai, X.-c. (2021). Structural basis of the activation of c-MET receptor. *Nature Communications*, *12*(1).

Uchikawa, E., Chen, Z., Xiao, G. Y., Zhang, X., & Bai, X. C. (2021). Structural basis of the activation of c-MET receptor. *Nat Commun*, *12*(1), 4074.

Ueno, M., Lee, L. K., Chhabra, A., Kim, Y. J., Sasidharan, R., Van Handel, B., Wang, Y., Kamata, M., Kamran, P., & Sereti, K.-I. (2013). c-Met-dependent multipotent labyrinth trophoblast progenitors establish placental exchange interface. *Developmental cell*, *27*(4), 373-386.

Umeki, K., Shiota, G., & Kawasaki, H. (1999). Clinical significance of c-met oncogene alterations in human colorectal cancer. *Oncology*, *56*(4), 314-321.

Van Cutsem, E., Karaszewska, B., Kang, Y.-K., Chung, H. C., Shankaran, V., Siena, S., Go, N. F., Yang, H., Schupp, M., & Cunningham, D. (2019). A Multicenter Phase II Study of AMG 337 in Patients with MET-Amplified Gastric/Gastroesophageal Junction/Esophageal Adenocarcinoma and Other MET-Amplified Solid TumorsAMG 337 Phase II Study in MET-Amplified Tumors. *Clinical Cancer Research*, *25*(8), 2414-2423.

Virzì, A. R., Gentile, A., Benvenuti, S., & Comoglio, P. M. (2018). Reviving oncogenic addiction to MET bypassed by BRAF (G469A) mutation. *Proceedings of the National Academy of Sciences*, *115*(40), 10058-10063.

Volz, Y., Koschut, D., Matzke-Ogi, A., Dietz, M. S., Karathanasis, C., Richert, L., Wagner, M. G., Mély, Y., Heilemann, M., Niemann, H. H., & Orian-Rousseau, V. (2015). Direct binding of hepatocyte growth factor and vascular endothelial growth factor to CD44v6. *Biosci Rep*, *35*(4).

Wagner, M. J., Stacey, M. M., Liu, B. A., & Pawson, T. (2013). Molecular mechanisms of SH2-and PTB-domain-containing proteins in receptor tyrosine kinase signaling. *Cold Spring Harbor perspectives in biology*, *5*(12), a008987.

Wang, W., Marimuthu, A., Tsai, J., Kumar, A., Krupka, H. I., Zhang, C., Powell, B., Suzuki, Y., Nguyen, H., Tabrizizad, M., Luu, C., & West, B. L. (2006). Structural characterization of autoinhibited c-Met kinase produced by coexpression in bacteria with phosphatase. *Proc Natl Acad Sci U S A*, *103*(10), 3563-3568.

Wang, Y., Pennock, S. D., Chen, X., Kazlauskas, A., & Wang, Z. (2004). Platelet-derived growth factor receptor-mediated signal transduction from endosomes. *Journal of Biological Chemistry*, *279*(9), 8038-8046.

Wee, P., Shi, H., Jiang, J., Wang, Y., & Wang, Z. (2015). EGF stimulates the activation of EGF receptors and the selective activation of major signaling pathways during mitosis. *Cellular signalling*, *27*(3), 638-651.

Weidner, K. M., Behrens, J., Vandekerckhove, J., & Birchmeier, W. (1990). Scatter factor: molecular characteristics and effect on the invasiveness of epithelial cells. *J Cell Biol*, *111*(5 Pt 1), 2097-2108.

Weidner, K. M., Di Cesare, S., Sachs, M., Brinkmann, V., Behrens, J., & Birchmeier, W. (1996). Interaction between Gab1 and the c-Met receptor tyrosine kinase is responsible for epithelial morphogenesis. *Nature*, *384*(6605), 173-176.

Wiesmann, C., Fuh, G., Christinger, H. W., Eigenbrot, C., Wells, J. A., & de Vos, A. M. (1997). Crystal structure at 1.7 Å resolution of VEGF in complex with domain 2 of the Flt-1 receptor. *Cell*, *91*(5), 695-704.

Wolf, J., Seto, T., Han, J.-Y., Reguart, N., Garon, E. B., Groen, H. J., Tan, D. S., Hida, T., de Jonge, M., & Orlov, S. V. (2020). Capmatinib in MET exon 14–mutated or MET-amplified non–small-cell lung cancer. *New England Journal of Medicine*, *383*(10), 944-957.

Wolf, J., Seto, T., Han, J. Y., Reguart, N., Garon, E. B., Groen, H. J. M., Tan, D. S. W., Hida, T., de Jonge, M., Orlov, S. V., Smit, E. F., Souquet, P. J., Vansteenkiste, J., Hochmair, M., Felip, E., Nishio, M., Thomas, M., Ohashi, K., Toyozawa, R., . . . Investigators, G. m.-. (2020). Capmatinib in MET Exon 14-Mutated or MET-Amplified Non-Small-Cell Lung Cancer. *N Engl J Med*, *383*(10), 944-957.

Wu, Y., Yao, X., Zhu, M., Qian, H., Jiang, L., Lan, T., Wu, M., Pang, J., & Chen, Y. (2016). PKG II reverses HGF-triggered cellular activities by phosphorylating serine 985 of c-Met in gastric cancer cells. *Oncotarget*, *7*(23), 34190-34200.

Wybenga-Groot, L. E., Baskin, B., Ong, S. H., Tong, J., Pawson, T., & Sicheri, F. (2001). Structural basis for autoinhibition of the Ephb2 receptor tyrosine kinase by the unphosphorylated juxtamembrane region. *Cell*, *106*(6), 745-757.

Xin, X., Yang, S., Ingle, G., Zlot, C., Rangell, L., Kowalski, J., Schwall, R., Ferrara, N., & Gerritsen, M. E. (2001). Hepatocyte growth factor enhances vascular endothelial growth factor-induced angiogenesis in vitro and in vivo. *The American journal of pathology*, *158*(3), 1111-1120.

Xu, L., Nilsson, M. B., Saintigny, P., Cascone, T., Herynk, M. H., Du, Z., Nikolinakos, P. G., Yang, Y., Prudkin, L., Liu, D., Lee, J. J., Johnson, F. M., Wong, K. K., Girard, L., Gazdar, A. F., Minna, J. D., Kurie, J. M., Wistuba, II, & Heymach, J. V. (2010). Epidermal growth factor receptor regulates MET levels and invasiveness through hypoxia-inducible factor-1alpha in non-small cell lung cancer cells. *Oncogene*, *29*(18), 2616-2627.

Yakes, F. M., Chen, J., Tan, J., Yamaguchi, K., Shi, Y., Yu, P., Qian, F., Chu, F., Bentzien, F., Cancilla, B., Orf, J., You, A., Laird, A. D., Engst, S., Lee, L., Lesch, J., Chou, Y.-C., & Joly, A. H. (2011). Cabozantinib (XL184), a Novel MET and VEGFR2 Inhibitor, Simultaneously Suppresses Metastasis, Angiogenesis, and Tumor Growth. *Molecular Cancer Therapeutics*, *10*(12), 2298-2308.

Yallowitz, A., Ghaleb, A., Garcia, L., Alexandrova, E. M., & Marchenko, N. (2018). Heat shock factor 1 confers resistance to lapatinib in ERBB2-positive breast cancer cells. *Cell Death Dis*, *9*(6), 621.

Yang, X.-M., Vogan, K., Gros, P., & Park, M. (1996). Expression of the met receptor tyrosine kinase in muscle progenitor cells in somites and limbs is absent in Splotch mice. *Development*, *122*(7), 2163-2171.

Yao, Z., Aboualizadeh, F., Kroll, J., Akula, I., Snider, J., Lyakisheva, A., Tang, P., Kotlyar, M., Jurisica, I., & Boxem, M. (2020). Split Intein-Mediated Protein Ligation for detecting protein-protein interactions and their inhibition. *Nature Communications*, *11*(1), 2440.

Zeng, L.-F., Zhang, R.-Y., Bai, Y., Wu, L., Gunawan, A. M., & Zhang, Z.-Y. (2014). Hydroxyindole carboxylic acid-based inhibitors for receptor-type protein tyrosine protein phosphatase beta. *Antioxidants & Redox Signaling*, *20*(14), 2130-2140.

Zhang, X., Gureasko, J., Shen, K., Cole, P. A., & Kuriyan, J. (2006). An allosteric mechanism for activation of the kinase domain of epidermal growth factor receptor. *Cell*, *125*(6), 1137-1149.

Zhang, Y., Xia, M., Jin, K., Wang, S., Wei, H., Fan, C., Wu, Y., Li, X., Li, X., & Li, G. (2018). Function of the c-Met receptor tyrosine kinase in carcinogenesis and associated therapeutic opportunities. *Molecular cancer*, *17*(1), 1-14.

Zhang, Y.-W., Wang, L.-M., Jove, R., & Vande Woude, G. F. (2002). Requirement of Stat3 signaling for HGF/SF-Met mediated tumorigenesis. *Oncogene*, *21*(2), 217-226.

Zhang, Y. W., & Vande Woude, G. F. (2003). HGF/SF-met signaling in the control of branching morphogenesis and invasion. *Journal of cellular biochemistry*, *88*(2), 408-417.

Zhu, H., Naujokas, M. A., Fixman, E. D., Torossian, K., & Park, M. (1994). Tyrosine 1356 in the carboxyl-terminal tail of the HGF/SF receptor is essential for the transduction of signals for cell motility and morphogenesis. *Journal of Biological Chemistry*, *269*(47), 29943-29948.

Zhu, H., Naujokas, M. A., & Park, M. (1994). Receptor chimeras indicate that the met tyrosine kinase mediates the motility and morphogenic responses of hepatocyte growth/scatter factor. *Cell Growth and Differentiation-Publication American Association for Cancer Research*, *5*(4), 359-366.

Zhu, M., Doshi, S., Gisleskog, P. O., Oliner, K. S., Ruixo, J. J. P., Loh, E., & Zhang, Y. (2014). Population pharmacokinetics of rilotumumab, a fully human monoclonal antibody against hepatocyte growth factor, in cancer patients. *Journal of Pharmaceutical Sciences*, *103*(1), 328-336.

Zimmer, Y., Vaseva, A. V., Medová, M., Streit, B., Blank-Liss, W., Greiner, R. H., Schiering, N., & Aebersold, D. M. (2010). Differential inhibition sensitivities of MET mutants to the small molecule inhibitor SU11274. *Cancer letters*, *289*(2), 228-236.